Protein Releasing Microspheres for an *In Vitro* Intimal Hyperplasia Model

A Major Qualifying Project Report:

Submitted to the Faculty

of the

WORCESTER POLYTECHNIC INSTITUTE

In partial fulfillment of the requirements for the

Degree of Bachelor of Science

By

Mateo Frare **Joshua Manning**
Teniola Oguntolu **Arth Sharma**

Date Submitted:
April 25, 2019

Table of Contents

Acknowledgements

The team would like to thank the following WPI faculty and graduate students who have helped with the development of this design project:

- **Project Advisors:** Marsha W. Rolle Ph.D, Catherine F. Whittington Ph.D
- **Biomedical Engineering Department Faculty:** Sakthikumar Ambady Ph.D, Jeannine Coburn Ph.D, Lisa Wall
- **Biology/Biotechnology Department Faculty:** Tanja Dominko Ph.D, Louis Roberts Ph.D, JoAnn Whitefleet-Smith Ph.D
- **Other Faculty:** Nancy Burnham Ph.D, Destin Heilman Ph.D, Satya Shivkumar Ph.D
- **Graduate Students:** Chiara Bollati, Jonian Grosha, Kimberly Ornell, Dalia M. Shendi

The team would especially like to acknowledge Dr. Marsha W. Rolle and Dr. Catherine Whittington for all of the support and guidance they have provided in terms of experimental planning and execution as well as with presentation of deliverables. The team would like to recognize Lisa Wall for her aid in acquiring supplies and acclimating the team to the labspace. Additionally, the team would like to thank Dr. Jeannine Coburn for supplying the team with silk and providing guidance with its fabrication, to Dr. Sakthikumar Ambady for providing the team with rat smooth muscle cells for experimental use, to Dr. Nancy Burnham for allowing the team to utilize the scanning electron microscope, and to Dr. Louis Roberts for assistance with the spectrophotometer and fluorescent plate reader.

Authorship

Abstract: Mateo Frare

1. Introduction: Arth Sharma, Josh Manning

2.1 Pathology: Arth Sharma

2.1.1 Clinical Need: Arth Sharma

2.2 Current Testing Models: Arth Sharma

2.3 Investigated Solutions: Josh Manning

2.3.1 Gene Altering: Josh Manning

2.3.2 Microspheres for Growth Factor Delivery: Josh Manning

2.4 Microsphere Fabrication: Mateo Frare

2.5 Potential Biomaterials for Microsphere Fabrication: Mateo Frare

2.5.1 Gelatin: Mateo Frare

2.5.2 Silk: Teniola Oguntolu

2.5.3 Chitosan: Mateo Frare

2.5.4 Polyanhydrides: Mateo Frare

2.5.5 PLGA: Arth Sharma

2.5.6 Hydroxyapatite: Mateo Frare

3.1 Initial Client Statement: Teniola Oguntolu

3.2 Objectives: Teniola Oguntolu

3.2.1 Comparison of Objectives: Teniola Oguntolu

3.3 Constraints: Teniola Oguntolu

3.4 Functions: Teniola Oguntolu

3.5 Standards: Josh Manning

3.6 Revised Client Statement: Teniola Oguntolu, Mateo Frare

4.1 Design Selection: Arth Sharma

4.2 Alternative Designs: Arth Sharma

4.2.1 Gelatin Microspheres: Joshua Manning

4.2.2 Chitosan Microspheres: Mateo Frare

4.2.3 Silk Microspheres: Teniola Oguntolu

4.2.4 PLGA Microspheres: Arth Sharma

5.1 Flow of Methodology: Joshua Manning

5.2 Phase I Testing: Joshua Manning

5.2.1 MTT Assay: Joshua Manning

5.2.2 Scanning Electron Microscopy: Arth Sharma

5.2.3 Phase I Conclusions: Arth Sharma

5.3 Phase II Testing: Joshua Manning

5.3.1 Encapsulation Efficiency: Mateo Frare

5.3.2 Activity and Release Assay: Mateo Frare

5.3.3 Phase II Conclusions: Mateo Frare

6.1 Summary of Final Design: Arth Sharma

6.1.1 Economics: Teniola Oguntolu

6.1.2 Environmental Impact: Teniola Oguntolu

6.1.3 Societal Influence: Teniola Oguntolu

6.1.4 Political Ramifications: Teniola Oguntolu

6.1.5 Ethical Concerns: Teniola Oguntolu

6.1.6 Health and Safety Issues: Teniola Oguntolu

6.1.7 Manufacturability: Teniola Oguntolu

6.1.8 Sustainability: Teniola Oguntolu

7. Discussion: Mateo Frare

8. Conclusion & Recommendations: Teniola Oguntolu, Joshua Manning

Abstract

Intimal hyperplasia (IH) is a prevalent vascular disease characterized by lesion formation on blood vessels, usually through cell growth at the site of an injury. Creating a tissue engineered blood vessel (TEBV) with intimal hyperplasia would serve as an *in vitro* disease model which would enhance and expedite drug testing. Though such an *in vitro* model has yet to be engineered, it may be achieved by incorporating growth factor-releasing microspheres into a localized region of the TEBV. The team was tasked with designing microspheres that can release growth factor to stimulate the formation of a lesion by localized cell proliferation in the established blood vessel model. Four materials (gelatin, chitosan, PLGA, and silk) were selected as options for the microsphere design. Each material was fabricated and tested to determine compliance with established design objectives and constraints, and silk was ultimately chosen as the superior material for use in the TEBV intimal hyperplasia model. In conducting an MTT assay to ensure the materials were biocompatible with smooth muscle cells, silk, like the other materials, induced only a slight reduction in cellular metabolic activity. Additionally, silk showed the most consistent size distribution characterized by scanning electron microscopy. Microspheres were tested for encapsulation efficiency of lysozyme, an analog protein, by running a lysozyme activity assay on a dissolved sample of loaded microspheres. Silk showed a greater encapsulation efficiency than the other tested material, chitosan. Also, results from the release assay suggest active lysozyme is released from silk microspheres in media suspension over the course of seven days, showing silk's potential to release active protein. It is suggested that continued encapsulation and release testing be done on new microsphere batches loaded with growth factor and that overall functionality of the microspheres be assessed once incorporated into the TEBV to analyze the potential of the design for the intended application.

Table of Figures

Table of Tables

1. Introduction

After surgical modification or damage to a blood vessel, smooth muscle cells (SMCs) comprising the muscular layer of the impacted blood vessel walls often grow inward and close the vessel. This phenomenon, known as intimal hyperplasia (IH), precludes normal blood flow due to the formation of a lesion which heightens the risk of a patient sustaining a blood clot and impedes the passage of blood to the affected organs. Endothelial cells (ECs) lining the vessel interior may initiate this increase in SMC proliferation due to improper stimuli, such as abnormal blood flow patterns imposing larger wall stresses than metabolically necessary (Zhang et al., 2018). This impeded blood flow can reduce the supply of oxygen delivered to tissues which commonly results in tissue necrosis (Mylonaki et al., 2016). IH commonly arises in blood vessel corrective procedures, wherein attempts to widen the vessel fail over time and the vessel narrows once more, a condition known as restenosis. Among common blood vessel interventions, as many as 50 percent of angioplasties fail due to intimal hyperplasia and restenosis (Glagov, 1994; Collins et al., 2012).

Currently, few FDA approved drugs exist for treatment of IH progression, mainly due to an inadequate understanding of the mechanism of the condition (Mylonaki et al, 2016). To remedy this shortage of clinical treatments, studies of potential drug delivery options are ongoing. Current *in vivo* models, however, have mainly utilized non-human models, such as rats, wherein vessels are artificially narrowed through atherosclerosis, the abnormal accumulation of cholesterol within the animal's vasculature (Hui, 2010). Additionally, rat vessels exhibit different flow patterns and histology than those in humans, making them a poor model for mirroring human IH (Hui, 2010). To better emulate IH in humans, blood vessels composed of human-sourced cells are needed, as they can better recapitulate the characteristics of human blood vessels seen *in vivo*.

In vitro disease or organ models are valuable in drug testing, because they do not face the same ethical issues as using *in vivo* models and still provide a biological structure that accurately simulates *in vivo* capabilities. Tissue-engineered blood vessels (TEBVs), in addition to serving as an accurate model of *in vivo* vasculature, can also provide greater control of morphology as an *in vitro* model of IH. Though not yet successfully established, a TEBV that models vascular diseases has been highly sought throughout the field of tissue engineering in the hopes of enhancing and expediting drug testing. Synthesizing TEBVs *in vitro*, has been accomplished a variety of different techniques, including three-dimensional (3D) bioprinting and self-assembly of 3D tissue rings. However, at this point uniform TEBVs, modeling healthy blood vessels, have been engineered, though only to serve as possible vessel replacements (Dahl et al., 2011; Hibino et al., 2010; Strobel et al., 2017).

Specifically, an accurate, reproducible, *in vitro* IH model is needed. The lack of standardization of IH in current, non-human blood vessel models in different studies arises from the varying methods for creating IH. The formed lesion produces an IH model whose parameters, such as vessel diameter and cell counts, vary depending on the manufacturing process utilized (Hui, 2010). To remedy this lack of reproducibility, drug delivery devices, such as microspheres, can be explored. These microspheres can be derived from various techniques and can provide for localized dispersal of a loaded substance. For example, microspheres can be embedded in TEBV to disperse a drug molecule (Alagusundaram et al.,

2009). Microspheres can be made with standardized protocols which can be altered to vary drug loading capacity and rate of degradation. With a variety of biocompatible materials of which to construct these vehicles, scalable amounts of a lesion-forming biologic can be loaded within. Biologics consist of a variety of organic substances such as artificial hormones, growth factors, and enzymes that can actively impact cellular biochemistry in its intended area of the body (Lochhead, 2012). For the stimulation of localized cell proliferation to model a lesion within the blood vessel, platelet-derived growth factor-BB (PDGF-BB) can be used to promote abnormal accumulation of SMCs into a vessel lumen (Hui, 2010; Collins et al., 2012). Microspheres loaded with vascular growth factors can be integrated into an *in vitro* TEBV to trigger IH by releasing its load over time to vessel SMCs (Strobel et al., 2017). The Rolle Lab at Worcester Polytechnic Institute currently utilizes a scaffold-free system that has been engineered to allow for the creation of TEBVs from SMCs differentiated from primary human smooth muscle cells. SMCs are seeded into ring-shaped agarose wells, in which the cells self-assemble into 3D toroids following an incubation period of 3 days. The toroid rings are then placed on top of each other to allow for toroid fusion into a 3D tissue tube (Strobel et al., 2018).

Previous research from the Rolle lab has indicated that gelatin microspheres have the ability to be incorporated within toroids of the TEBV (Strobel et al., 2018). During the TEBV fabrication process, gelatin microspheres were co-seeded into the agarose wells with the SMCs. Toroid fusion was still seen after the 3 day incubation period with the addition of the gelatin microspheres, and no difference in TEBV formation was seen during this new fabrication technique. The study found that gelatin microspheres could be incorporated into focal regions of the TEBV successfully. Therefore, it was suggested in future studies that microspheres could be loaded with growth factors for inducing *in vitro* disease models (Strobel et al. 2018).

In this project, the team aimed to create microspheres capable of releasing growth factor, that can be used to stimulate cell proliferation and IH lesion formation in a TEBV. Successful creation of the IH model can be accomplished by culturing PDGF-BB-loaded microspheres with SMCs during the formation of a few toroids. These toroids containing microspheres can then be fused within normal TEBV rings, creating a vessel with microspheres embedded at a specific region. This region will begin to emulate a lesion as the localized microspheres release PDGF-BB and the nearby cells are induced to proliferate (Strobel et al., 2018). Determining the best design for creating the growth-factor releasing microspheres is an important step in accomplishing this goal. An overall map of our project is shown in Figure 1.

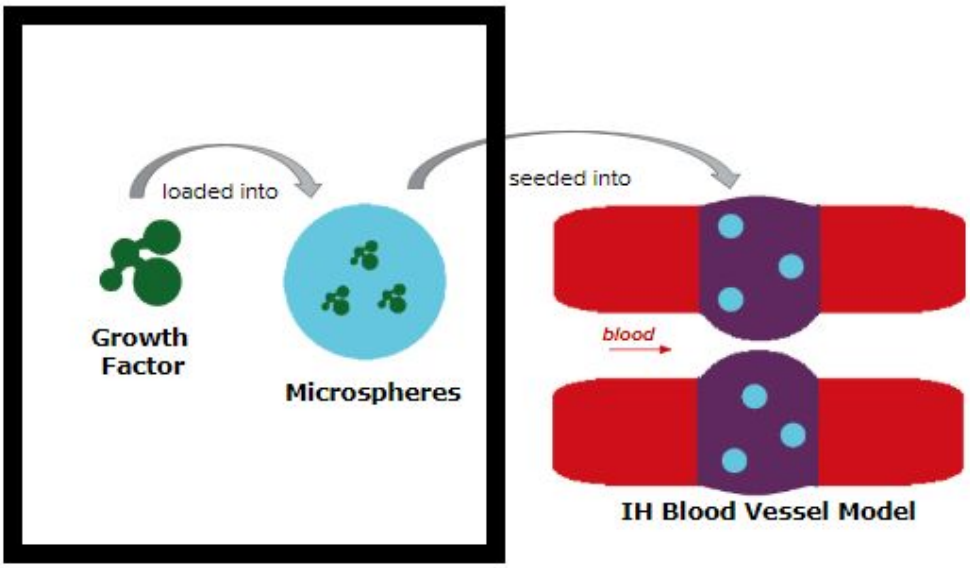

Figure 1: *Project plan schematic. This study focuses on the portion framed by the black box. The team sought to develop microspheres capable of releasing growth factor to cause IH.*

In subsequent studies, the team found that gelatin microspheres degrade too quickly to allow for sustained PDGF release and IH lesion formation, so the focus of the team's project was to explore alternative microsphere materials.

2. Literature Review

2.1 Pathology

IH arises as proliferative lesions form within arteries and veins (Collins et al., 2012). Both blood vessel types are composed of an exterior layer of structural collagen and compliant elastin. The dichotomy of these two opposite proteins confers varying resilience to a blood vessel in the tunica externa. Moving inwards, SMCs occupy the tunica media layer to control vessel dilation and contraction (Figure 2). Adjacent to the tunica media is the tunica intima, wherein simple squamous ECs interface with blood cells and proteins (Galante et al., 2007; Collins et al., 2012)

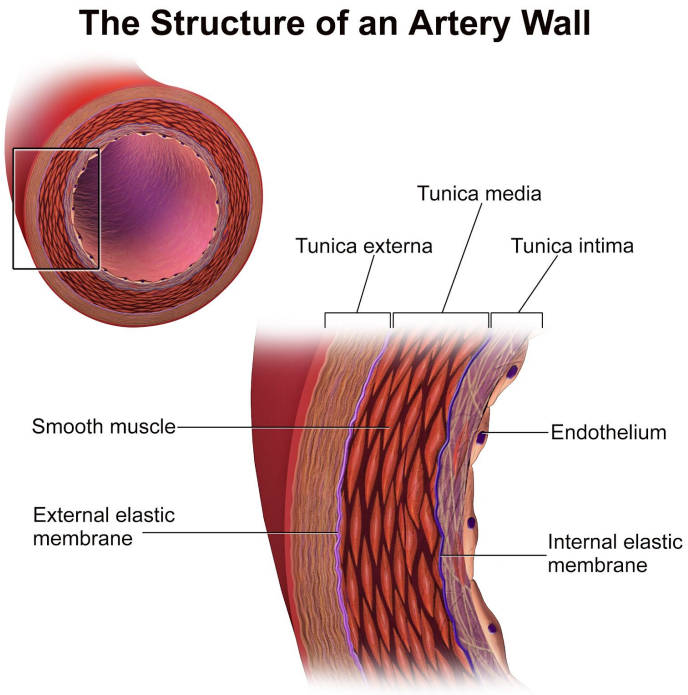

Figure 2: *Arterial Wall Anatomy (Blausen, 2014).*

In healthy patients, the tunica intima provides a sleek, non-thrombogenic surface upon which blood can flow, exhibiting a shear stress on this layer of about 15 dyne/cm² (Collins et al., 2012; Glagov, 1994). Wall thickness may vary based on the stress exhibited. If this stress is increased abnormally above this shear stress value, the endothelial layer may sustain injury and excrete cytokines and oxidative species that can dilate the vessel and encourage SMC proliferation (Yau et al., 2015; Zhang et al., 2018). In tandem, platelets may come into contact with the collagen layer beneath and, compounded with a thrombogenic protein called tissue factor produced by the tunica intima and tunica media layers, clot at the site of damage on the vessel wall (Yau et al., 2015). Upon its binding, in addition to interactions of other blood clotting factors, PDGF-BB is released by granules within the platelets (Yau et al., 2015).

PDGF-BB is a molecule found within vascular systems which serves as a mitogen for connective tissue cells (Heldin & Westermark, 1999). Specifically, PDGF-BB has been shown to play a significant role in inducing the phenotypic change in SMCs from the mature contractile state to the proliferative state associated with IH lesions (Zhao et al., 2011). PDGF-BB is present during embryonic development of the SMCs, allowing for the proliferation and growth of tissue vessels within the embryo. Following the increase of transforming growth factor-beta (TGF-β) expression within the system, expression of PDGF-BB decreases significantly, and PDGF-BB expression only increases during wound healing of the vascular tissue due to the need of increased proliferation of the injured cells (Heldin & Westermark, 1999). Under physiological conditions, SMCs remain in a stable, contractile state. However, overexpression of PDGF-BB within mature vascular tissues in a normal healthy state promotes

de-differentiation of SMCs into their proliferative state, leading to abnormal over-proliferation of the SMCs and the formation of lesions characteristic of IH *in vivo* (Huang et al., 2002; Collins et al., 2012).

To treat this pathology, an *in vitro* model that mimics the stages of IH is needed. Before going into clinical trials, the FDA mandates that the efficacy and utility of potential therapeutic in question be demonstrated in lab experiments in Step 1 of their approval process (Carpenter, 2002). Therefore a robust system that is conducive to measuring a drug's therapeutic efficacy, must be created. For IH, an *in vitro* blood vessel system with defined lesions, induced by PDGF-BB, could serve as this model.

2.1.1 Clinical Need

Currently, no viable methods outside of surgery can fully treat or prevent IH. In both native and grafted vessels, IH can arise from various molecular pathways and macroscopic factors, such as vessel injury and interaction with implanted polymer materials. Removing diseased portions of vessels or inserting stents can cause further injury to adjacent sites in the vessel, which can cause a recurrence of IH. Indeed, up to 60% of vessel transplants experience IH (Collins et al., 2012). Moreover, current medications can only alleviate symptoms of IH, rather than treating the condition itself. Specifically, anticoagulants like warfarin can act to prevent blood clots within IH-impacted vessels but require long-term usage and can cause internal bleeding (Collins et al., 2012). Anti-inflammatory drugs can lower the expression of cytokines that cause IH, but may require continuous administration (e.g., injection) and only target specific cytokines, leaving other molecular signals unchecked (Collins et al., 2012). Therefore, given the current lack of cure for IH, further research into the pathology of the disease is needed for a permanent remedy to the condition.

2.2 Current Testing Models

Modern models for simulating IH have involved artificial induction of IH within rodents for *in vivo* studies. Specifically, for *in vivo* studies, the development of atherosceloritic plaque inside blood vessels by suturing vessels with polymers like polypropylene (PPE) is one method to induce IH (Hui, 2010; Mylonaki et al., 2016). For this method, the vascular endothelial layer is injured by introduction of the PPE surface by cutting the vessel and sewing it to the polymer. By damaging the vessel wall, the SMCs becomes exposed within the vessel and multiply inwards (Mylonaki et al., 2016). Moreover, the plastic graft can increase the presence of cytokines that can trigger vessel SMCs to undergo mitosis. These diseased vessels then need to be prepared for study by injecting the vessels with vehicles loaded with vessel-dilating or blood-thinning medications. After adding tested drug, the studied vessel can be analyzed by various methods, including histological cross-sections, live cell staining, ELISA for SMC biomarkers, and microscopy (Mylonaki et al., 2016; Collins et al., 2012). A limitation with using *in vivo* models is the lack of identical vasculature and blood composition between different tested animals, adding variability to results collected from the animal study (Hui, 2010).

An *ex vivo* technique involves removing IH-injured vessels from a cadaver or other species and preserving it in formalin and paraffin wax for vascular disease studies (Cizek et al., 2007). Though the preserved vessels retain their structure and morphology, in formaldehyde, proteins within vascular cells will be fused by covalent bonds, blocking their active sites and rendering them nonfunctional (Venuti et

al., 2004). Proteins within vascular SMCs must retain their natural structure for SMCs to thrive and not die, so they can progress into IH (Mylonaki et al., 2016). Therefore, to study the development of IH for drug screening within a living system, cells cannot be preserved in formaldehyde and paraffin.

An additional shortcoming common to both types of models is a lack of reproducibility and ease of access. Intact vessels from cadavers and animals may be in short-supply, require special licensing and handling to utilize, and entail extraneous variables arising from the whole model organism that can skew analysis of a potential IH therapy (Cizek et al., 2007). Moreover, as current methods utilize vessels from natural sources, their composition cannot be specifically controlled, the results from analysis of one blood vessel cannot be extrapolated accurately to describe other vessels, especially to human vessels if the vessel is derived from another species, such as a rat. A human model is thus needed for a more streamlined, controlled approach, wherein vessels can be specifically tailored and created on-demand.

2.3 Investigated Solutions

There are currently multiple solutions which have been discussed that would allow for the formation of proliferative lesions within blood vessels (Hui, 2010; Mylonaki et al., 2016; Strobel et al., 2018). However, there is still a need for an improved system to induce proliferation of SMCs within a TEBV to address aforementioned shortcomings in current *in vivo* and *ex vivo* models. Two popular solutions presented include genetic alteration of vessel SMCs and delivery of growth factors within the tissue rings through drug delivery systems such as microspheres. Growth factor delivery, specifically PDGF-BB and TGF-β, have been linked with characteristics of IH (Strobel et al., 2016). In both of the investigated solutions presented, one of the growth factors has played a significant role in the anticipated formation of intimal hyperplasia lesions.

2.3.1 Gene Altering

One potential strategy to create IH lesions *in vitro* is through genetic alteration of the SMCs. Specifically, the ability to inhibit TGF-β signaling within SMCs could prove to play a role in inducing a diseased state within vascular tissues. TGF-β consists of a family of cytokines that regulate cellular functions including growth, adhesion, migration, apoptosis, and differentiation (Guo & Chen, 2012). It has been hypothesized that TGF-β also plays a significant role in vascular development and SMC differentiation (Perrella et al., 1998). One of the main contributors to many cardiovascular disorders, including IH, is the abnormal differentiation of SMCs from their proliferative embryonic state to their contractile mature state (Guo & Chen, 2012). It has been shown that the TGF-β signaling pathway is one of the main causes of this SMC differentiation.

During angiogenesis, or the production of new blood vessels, SMCs maintain a proliferative state to allow for the growth and formation of these new vascular tissues within the body. This process continues until the tissues exhibit the desired complex system seen within mature systems (Guo & Chen, 2012). At this point, TGF-β binds to specific type I and type II kinase receptors present on the SMCs. This activates TGF-β within the SMCs, and results in differentiation of the SMCs present within the

system (Perrella et al., 1998). The differentiation of the SMCs slows the proliferative state and instead induces the normal mature contractile state (Guo & Chen, 2012).

There have been multiple *in vivo* experiments performed in mice to determine whether genetic alterations of TGF-β alleles or the removal of receptors in SMCs could decrease TGF-β expression within the vascular system (Grainger et al., 1998; Guo & Chen, 2012). Both studies have shown a correlation between decreased TGF-β expression and allele deletion or kinase receptor removal. Furthermore, decreased TGF-β expression has also been correlated with fewer levels of differentiation markers within the SMCs, increasing proliferation capacity within the system (Grainger et al., 1998; Guo & Chen, 2012). This diminished capacity for cellular differentiation leads to the continued proliferation of the SMCs within the blood vessel, which causes the formation of IH within patients. While pilot studies have shown promise with genetic alterations of SMCs, the cost needed to perform these experiments pose limitations. On average, experimental setup can cost as much as $2,000 per experiment (NIH n.d.). Therefore, a less expensive alternative should be explored.

2.3.2 Microspheres for Growth Factor Delivery

A second investigated solution to create the characteristic lesions of IH is through the release of growth factors to induce SMC proliferation. This process can be completed through the use of biomaterial based microspheres integrated within SMC toroids. The microspheres can encapsulate and release growth factor through either surface degradation or diffusion. Microspheres are known for their ability to easily diffuse within a variety of solvents and substances depending on the material they are comprised from. Through varying fabrication techniques, microspheres can be synthesized from various materials, including polymers, glasses, and ceramics. Due to this high variety of fabrication techniques, microspheres can be selected and tailored to improve functionality within their specific applications (Hossain et al., 2015).

There is a vast assortment of applications for microspheres both in the field of biomedicine and in other commercial applications. These applications can include separation of molecules and medical imaging (Ma et al., 2005; Upputuri & Pramanik, 2017). Microspheres are also commonly used as a scaffold for cells within biological systems. Because the spheres can be synthesized to have a porous architecture, they can be used for seeding cells in a mechanism allowing for the transfer of nutrients (Dastidar et al., 2018). Polycaprolactone and titanium dioxide composite microspheres, for example, have shown to be osteoconductive, possessing pores found to adequately support the ingrowth of bone tissue (Khoshroo et al., 2017).

Drug delivery systems are potentially the most widely-utilized applications of microspheres. Microspheres with intended drug delivery applications are typically loaded with some chemical or molecule drug prior to implementation within the body. The release of this drug typically occurs by some form of diffusion through the matrix or by microsphere degradation (Fredenberg et al., 2011). Drug-releasing microspheres are used in many ways and in different organ systems. Microspheres wielding a neuro-protection drug, for one, can be injected into the eye, for nerve maintenance of patients with eye or vision conditions such as glaucoma (Bravo-Osuna et al., 2018). Drug-eluting microspheres can also be used for occlusion of blood vessels that supply nutrients to liver tumors, a process known as

chemoembolization (Fuchs et al., 2017). Pulmonary drug delivery is another common microsphere function, for which the microscopic inhalants bind to lung tissue prior to bloodstream re-absorbance (Deshmukh & Sangawar, 2016).

2.4 Microsphere Fabrication

Microspheres can be synthesized through multiple techniques (Table I). Most microsphere fabrication techniques exploit the phenomenon of emulsion, though some others use more complex microfluidic systems for a more precise, monodisperse end product (Geczy et al., 2018). The simplest emulsion techniques are known as single emulsions where a solution of the dissolved matrix material is added to a solution of very low affinity. For instance, if the matrix material is dispersed in water, the solution could be added to a hydrophobic substance, such as oil. The solutions are then disrupted through stirring, forming small orbs of the matrix solution. A drug can be incorporated into the microspheres either directly into the aqueous matrix solution prior to the emulsion or after the microspheres have been formed and isolated from the emulsion. If the drug and matrix material have opposing affinities to water, this emulsion process is repeated, resulting in a double emulsion (McCall & Sirianni, 2013).

Another similar microsphere fabrication technique, known as the polymerization technique, involves dispersing droplets of monomers of matrix material into a different solution. When heat is applied during fabrication, the monomers begin to polymerize. This process often involves incorporation of crosslinkers, stabilizers and a reaction catalyst (Alagusundaram, 2009; Wang et al., 2006). Though this is typically a fast fabrication process, the incorporation of many reagents can increase sensitivity to reaction conditions (Dastidar et al., 2018).

Spray-drying is another common fabrication method used in laboratory settings. For this technique, the drug and matrix material are dissolved in some volatile solvent, which quickly evaporates upon heating. After evaporation of this solvent, the matrix and drug form mist droplets which can be isolated from the air with cyclone separating equipment. This fabrication is most appropriate for applications involved with pathogens (Alagusundaram, 2009). Unfortunately, with this process, controlling microsphere attributes, such as pore-size, is very difficult and this technique cannot be used with heat-sensitive materials (Dastidar et al., 2018).

The phase-separating method for microsphere fabrication begins with a solution of dissolved drug and dispersed droplets of the matrix material. A substance of very low affinity to the solvent is then added to the solution, triggering the incorporation of the drug into the matrix droplets in the form of a visible liquid-to-solid phase change (Alagusundaram, 2009; Guo et al., 2015). This process can be used to form unique microsphere structures such as, core-shell copolymer formations (Guo et al., 2015). In this process, however, uniform droplet-drug dispersion is difficult to achieve and there is high sensitivity to reaction conditions (Dastidar et al., 2018).

Table I: *Common Microsphere Fabrication Techniques*

Fabrication Technique	Basic Principle
Single Emulsion	Add aqueous matrix solution to hydrophobic solution; Stir to form particles
Double Emulsion	Add aqueous drug solution to hyrophobic matrix solution; Add combined solution to aqueous solution; stir to form particles
Polymerization	Add matrix material to solution; Heat solution to induce polymerization of matrix material into particles
Spray Drying	Dissolve matrix material in volatile solvent; Heat solution to evaporate into particles
Phase Separation	Add drops of matrix material into drug solution; Introduce reagent to drive drug into matrix droplets to form loaded particles

2.5 Potential Biomaterials for Microsphere Fabrication

The material of which microspheres are synthesized usually depends on the intended application. Though microspheres can be fabricated from a variety of material types, those used in the medical field are most commonly made of ceramics, glasses, and polymers (Table II). Materials from each of these classifications were considered for the growth factor delivery system and are later described in greater detail.

Table II: *Biomaterials Commonly Used for Microspheres*

	Glasses & Ceramics	Synthetic Biomaterials	Natural Biomaterials
Advantages	● Often bioactive and can form strong bonds with biological tissues (Rahaman et al., 2011) ● Often osteoconductive, promoting bone growth (Rahaman et al., 2011) ● Antimicrobial and wound-repair properties (Kawashita, 2005; Rahaman et al., 2011)	● Degradation profiles can be easily tailored (Sinha & Trehan, 2003) ● Can be altered to exhibit controlled drug release (Sinha & Trehan, 2003)	● Products of degradation are typically biocompatible (Del Gaudio et al., 2017)
Disadvantages	● Usually very brittle which increases risk of fracture-related complications (Rahaman et al., 2011)	● Degradation can yield harmful products (Sinha & Trehan, 2003) ● Usually hydrophobic, making encapsulation of hydrophilic drugs difficult (Sinha & Trehan, 2003)	● Degradation often occurs very quickly unless the materials are altered (Del Gaudio et al., 2017) ● Cross-linking agents used to slow degradation often have some toxicity (Del Gaudio et al., 2017)
Examples of Microsphere Applications	● Porous glass microspheres to serve as chromatography beads (Conzone & Day, 2009) ● Ceramic microspheres that release radiation-emitting isotopes for cancer therapy (Day & Ehrhardt, 1988)	● Hydrolyzable microspheres for controlled drug release with degradation tailored to application via processing alterations (Anderson & Shive, 1997) ● Embolization microspheres for blocking blood flow to tumors (Saralidze et al., 2010)	● Gelatin microspheres for delivering anticancer agents to the stomach (Hashida et al., 1977) ● Targeted drug delivery using polymers that degrade in specific body regions such as chitosan that degrades in response to a colon bacteria (Lorenzo-Lamosa et al., 1977)
Common Materials	● Silicon dioxide, Aluminum oxide, Iron oxide, Hydroxyapatite, Yttrium oxide, & Yttrium phosphate (Kawashita, 2005)	● Polyesters, such as polylactic acid (PLA) and poly(lactic co-glycolic) acid (PLGA) (Anderson & Shive, 1997)	● Gelatin, Albumin, Starch, Silk, & Chitosan (Alagusundaram, 2009)

2.5.1 Gelatin

Collagen, one of the most abundant proteins in the human body, found in the extracellular matrix of most mammalian cells, has a hierarchical structure in nature (Fratzl, 2003). Hydrolyzing or denaturing the triple helix of collagen fibers results in gelatin, one of the most commonly used biological materials in many biomedical applications, including microspheres (Benjakul & Kittiphattanabawon, 2018). Gelatin is a promising biomaterial in that it is non-toxic, biocompatible and biodegradable, like collagen (Table II) (Wang et al., 2016a). Most of the characteristics of gelatin, however, vary greatly depending on extraction method, the degree of denaturation, electrolyte content, and other processing parameters (Olsen et al.,

2003). Overall, gelatin is quite weak in terms of its mechanical strength, and it is quickly hydrolyzed and broken down in most biological systems. To increase its strength and resistance to degradation, gelatin is often chemically altered with crosslinking agents (Ratanavaraporn et al., 2010). The majority of these crosslinking agents, such as glutaraldehyde, are cytotoxic (Poursamar et al., 2016). Other non-toxic, less-studied crosslinkers, such as mammalian derived transglutaminase, have however, shown potential for gelatin stability enhancement applications (Yang et al., 2018). A major advantage of gelatin is its low cost in comparison to many other microsphere scaffold materials.

Gelatin is often used as a drug carrying biomaterial as it is capable of binding to a variety of organic molecules including nucleic acids, sugars and proteins. For example, based on its isoelectric point, which is determined by method of denaturation, gelatin can bind to growth factors of an affinitive charge (Young et al., 2005). Additionally, gelatin is bioresorbable which allows for the drug release via bulk degradation due to common physiological reactions such as hydrolysis. If an encapsulated protein or drug does not release via diffusion, active hydrolysis and proteolytic activity will expose it as the gelatin degrades (Young et al., 2005). Crosslinked gelatin has thus shown a capability of carrying growth factors through static charge and releasing them upon degradation (Yamamoto et al., 2001). A water-in-oil emulsion technique is typically performed to fabricate gelatin microspheres which are later submerged in a solution containing the crosslinking agent (Tabata et al., 1999). Size is a difficult parameter to control with gelatin microspheres due to the inability to produce consistent polymer sizes after collagen is denatured (Saddler & Horsey, 1987). The release profile of drug from a gelatin microsphere varies greatly in accordance with its molecular make-up and fabrication specifications. Gelatin's drug elution profile depends on the crosslinking agent used, as crosslinkers are often found to yield a more-controlled release (Yang et al., 2018, Cortesi et al., 1998). Despite the amount of cross-linking, however, most gelatin microspheres lose a great deal of drug during burst release (Iwanaga et al., 2003). Alterations such as adding methacrylic anhydrides to gelatin can also result in a more sustained drug release with exposure to collagenase enzymes (Nguyen et al., 2015).

Table III: *Pros and Cons of Gelatin for use in Microspheres*

Gelatin	
Pros	Cons
Non-toxic and biocompatible	Physical and chemical characteristics vary based on extraction method
Biodegradable characteristics	High potential for burst release
Can increase strength and resistance to degradation through crosslinking	Majority of crosslinking agents are cytotoxic
Inexpensive	Difficult to control microsphere size
Commonly used biomaterial for drug carrying and drug release	

2.5.2 Silk

Silk is a natural protein fiber that is cultivated from the *Bombyx mori* silkworm. The thread of silk that is produced is composed of a structural fibroin protein and is coated by the protective sericin protein. During the manufacturing process of silk fibers, sericin is removed through a degumming process as a waste product (Mondal 2007). The remaining silk fibroin material can be used in a wide variety of applications because of its unique structure and advantageous properties, (Table IV). During the silk-spinning process, silk fibroin self-assembles into crystalline β-sheet structures through the incorporation of physical crosslinking (Hu et al., 2006) which allows the silk fiber to possess beneficial mechanical properties including high strength, toughness, and elasticity. Other unique properties of silk fibroin include biocompatibility, biodegradability, and a high stability because of its structure. Due to the advantageous attributes of silk fibroin, it has been investigated for use in both medical and clinical applications. Additionally, silk fibroin produces a very low antigenic response within the body and allows for cell adhesion (Wang et al., 2007). Some of the applications for this polymer include enzyme immobilization, surgical sutures, tissue engineering scaffolds, and drug delivery systems.

In drug delivery applications, silk fibroin can be used to fabricate microspheres for the encapsulation and controlled release of proteins. There are various methods for the preparation of silk fibroin microspheres, such as a water-in-oil emulsion to encase proteins (Srihanam et al., 2011). For the fabrication of our silk microspheres, we will be following a procedure using silk/PVA blend films (Wang X. et al., 2010). By air-drying the blended solution, dissolving the film in water, and removing any

residual PVA through centrifugation, water-insoluble silk microspheres can be obtained. Also, silk fibroin microspheres have the capability to be loaded with growth factors to be used for delivery applications. (Wenk et al., 2009). Additionally, the material's crystalline beta-sheet structure allows for controllable drug release. (Lammel et al., 2010).

Table IV: *Pros and Cons of Silk for use in Microspheres*

Silk	
Pros	Cons
Non-toxic	Relatively expensive
Promotes cell growth and proliferation	Wide distribution of microsphere sizes
Low antigenic response	Degradation behavior is dependent on silk processing
Can be loaded with growth factors	
Biocompatible	
Relatively slow degradation; zero order release	
Biodegradable	
High drug loading capacity and stability	
Minimal electrical conductivity	

2.5.3 Chitosan

Like gelatin, chitosan is a natural biomaterial that is derived from a highly-structured fibrillar natural material found in a variety of organisms. Chitosan, a polyelectrolytic polysaccharide that is produced from the deacetylation of chitin, is commonly acquired from the shells of crustaceans (Hudson & Jenkins, 2001). Chitosan possesses many intrinsic properties that bode well for its use in biomedical applications (Table V). For example, chitosan is highly soluble and thus, can be used in a variety of structures including gels, films, and fibers (Ridaudo, 2006). Also, chitosan is biocompatible and inert, thus posing little risk of immune rejection upon implantation within the body (Hao et al., 2010). Furthermore, chitosan has been shown to have wound-healing attributes and its oligosaccharide degradation products have been found to facilitate proliferation, especially among nerve cells (Kim et al., 2008, Zhao et al., 2017). However, due to its hydrophilic nature and its sensitivity to pH change, chitosan

is not very stable in comparison to other biomaterials (Ridaudo, 2006). To increase its stability, chitosan can be crosslinked with a variety of agents such as genipin and vanillic aldehyde (Kawadkar & Chauhan, 2012; Zhai et al., 2018). Because of its unique properties, chitosan is used in a variety of applications with fields ranging from agriculture to medicine (Hudson & Jenkins, 2001).

Many of the biomedical applications of chitosan involve drug delivery, especially with drugs for regenerating tissue within the nervous system (Wang et al., 2016 b, Zhao et al., 2017). Chitosan has high affinity to many proteins, which makes it a good protein-drug carrier (Hao et al., 2010). Additionally, chitosan is bioresorbable which allows for the release of drug via bulk degradation usually due to hydrolysis and enzymatic activity and a variety of modifications can be performed to adjust its rate of degradation (Di Martino et al., 2005). For fabrication, chitosan microspheres are commonly created through the emulsification technique, for which various parameters, such as stirring speed, can be altered to change resulting properties (He et al., 2016). For example, chitosan microsphere drug-release properties can be controlled by altering particle degradation through surface modifications such as acetylation of amino groups (Zhou et al., 2014). Additionally, increased crosslinking of chitosan microspheres has been associated with prolonged release profiles (Zeng et al., 2011). The fragments of chitosan, formed upon degradation, and platelet derived growth factor, have even been shown to work in conjunction with one another to promote cell proliferation. Chitosan particles loaded with PDGF-BB, for example, were observed to stimulate a significant increase in cell count and viability of human gingival fibroblasts in comparison to treatment groups with exposure to chitosan and PDGF-BB alone (Silva et al., 2013).

Table V: *Pros and Cons of Chitosan for use in Microspheres*

Chitosan	
Pros	Cons
Biocompatible	Not very stable
Zero foreign body response	Often requires a cross-linking agent
High affinity to most protein	Sensitive to environmental conditions
Non-toxic degradation products	Usually exhibits burst release
Chitosan oligosaccharides promote cell proliferation	
Degradation profile can be controlled by manipulating fabrication	

2.5.4 Polyanhydrides

Polyanhydrides are a class of synthetic polymer used in many biomedical applications, possessing a variety of the advantageous and disadvantageous properties (Table VI). For one, polyanhydrides can be sterilized quite easily via gamma radiation and are considered safe for use within a variety of biological systems. Further, the degradation products of polyanhydrides are entirely eliminated from the body within a few months, as they are often composed natural body constituents, and some serve as easily processed-metabolites (Kumar et al., 2002). Though these by-products are acidic, they generally do not lower surrounding pH to the same degree as other degradable polymers like polyesters (Gopferich & Langer, 1993).

Polyanhydrides have a variety of properties that make them suitable for advanced drug delivery applications. For instance, polyanhydrides are capable of carrying and stabilizing a variety of protein drug types such as antibodies and growth factors (Ghadi et al., 2017; Delgado-Rivera et al., 2013). Polyanhydride microspheres are commonly fabricated by either hot-melt encapsulation, spray drying, or double emulsion solvent removal, though there are ultrasonic stream disturbance techniques that can be employed with the proper equipment. (Kumar et al., 2002; Berkland, 2004). Polyanhydrides, unlike other polyesters and most biomolecules, undergo surface degradation, yielding predictable drug-release profile that approach zero-order release (Gopferich, 1996). This unique release profile comes from a combination of two characteristics: its hydrophobicity and its abundance of hydrolysable anhydride bonds on the material surface (Uhrich et al., 1999). These highly favorable drug release characteristics, in accompaniment with localization and targeting, makes polyanhydrides very suitable for applications involving highly toxic drugs, such as those used in cancer treatment (Jain et al., 2005). Fabrication and engineering design can have an influence on the release profile of a drug. For instance, the distribution and release of drug from polyanhydride microspheres have been observed to vary in size of the protein it was carrying (Berkland, 2004). Polyanhydrides in general, release drugs steadily over long durations compared to other polymers, and these release durations can be extended via copolymerization. For example, microspheres composed of poly sebacic anhydride, one of the most common microsphere poly anhydrides, was shown to be able to release bovine serum albumin in a controlled fashion over the span of close to two weeks in sodium dodecyl sulfate aqueous solution; this release duration was seen to increase when copolymerized with poly(1,6-bis-*p*-carboxyphenoxy) hexane (Determan et al., 2004).

Table VI: *Pros and Cons of Polyanhydrides for use in Microspheres*

Polyanhydrides	
Pros	Cons
Zero-order drug release	Fast degradation time (less than a week)
FDA approved for drug delivery processes	Needs caustic chemicals to prepare microspheres (e.g., dichloromethane)
Biodegradable	Relatively expensive
Breakdown products non-harmful to host	
A plethora of variants, each with unique properties	
Supports immune response (adjuvant)	

2.5.5 Poly(lactic-co-glycolic acid) (PLGA)

PLGA is a polyester with many advantages for use as a biomaterial (Table VII). Comprised of alternating copolymeric chains of PLA and polyglycolic acid (PGA) monomers, water hydrolysis of the esteric bond is the common means of breaking apart chains (Danhier et al., 2016). As a bulk degrading copolymer, PLGA is liable to break suddenly by water entry into its matrix. However, by varying the ratio of PGA monomers to PLA monomers, different rates of sustained drug release may be attained. Rate of drug release also depends on the thickness of the hydration layer surrounding the polymer (Makadia et al., 2011). The former monomer, lacking one methyl group which the latter contains, is relatively polar, so occupying polymeric chains with its presence may increase water solvation and hydrolysis. For example, an 85:15 PLA to PGA ratio, has been shown to have a lower burst release compared to a 50:50 ratio copolymer (Han et al., 2016). Moreover, lyophilized powder reagents of varying molecular weights adds extra control of degradation rate, where heavier chains degrade slower and exhibit less burst release (Makadia et al., 2011).

Depending on the fabrication technique utilized, a narrow or wide size distribution can be attained. A variety of techniques exist to produce PLGA microspheres, including microfluidics, coaxial tri-capillary electrospraying, and emulsion techniques (Han et al., 2016). Usually, oil-in-water and water-in-oil-in-water emulsions do not involve complex reagents dichloromethane, which is used as a solvent, and other machinery (Han et al., 2016). In terms of these emulsion techniques, the former tends to produce a narrow distribution of microspheres and involve less reagent than the latter (Han et al., 2016). However, other variants of emulsion techniques can be used to improve the encapsulation

efficiency of biologics over these more traditional emulsion methods (Han et al., 2016; Yuan et al., 2013). Having a size profile that can be varied from nanoscale to microscale, PLGA microspheres can be easily incorporated into vasculature without affecting native tissue architecture. However, microsphere diameters must be less than 200μm to avoid an immune response *in vivo* (Yi et al., 2008; Han et al., 2016). As a scaffold material for blood vessels, it does not interfere with normal blood vessel function until it degrades into acidic products, which can, in turn, inhibit SMC function and potentially affect the function of PDGF-BB, if pH drops much below the 7.4 pH at which PDGF-BB works optimally (Yi et al., 2008). In terms of cost, manufacturers provide an assortment of powdered forms of the polymer. Though more expensive than gelatin, large catalogs of options compensate for this shortcoming.

Table VII: *Pros and Cons of PLGA for use in Microspheres*

PLGA	
Pros	Cons
Customizable degradation rates and reactivities based on component monomer units and identities	Burst release may cause premature release of loaded drug
FDA approved for drug delivery processes	Requires caustic chemicals to prepare microspheres (e.g., dichloromethane)
Biodegradable	
Breakdown products non-harmful to host	
Sustained release of loaded drugs	
Does not interfere with SMC proliferation/growth	
No immunogenic response	

2.5.6 Hydroxyapatite

Synthetic hydroxyapatite is a ceramic biomaterial used in many applications such as bone scaffolding, bone filling, and implant coating. Among other properties (Table VIII), hydroxyapatite is strong and wear resistant but does not possess much toughness due to its brittle nature. Hydroxyapatite is biocompatible and bioactive, which allows it to bind to biological tissues such as bone. In addition to orthopedic applications, hydroxyapatite is used in drug delivery (Szczes et al., 2017).

Hydroxyapatite drug delivery systems often take advantage of microsphere carriers. Hydroxyapatite microspheres are typically hollow or mesoporous and are thus capable of carrying large amounts of drug (Szczes et al., 2017). Though co-precipitation and microwave radiating techniques are sometimes used in their fabrication, hydroxyapatite microspheres are commonly synthesized via a simple hydrothermal process entailing a dropwise, stirred emulsion that is later autoclave prior to particle retrieval (Lin et al., 2011; Qi et al., 2015). Unfortunately, in order to control microsphere conformation with this method of fabrication, acidic modifiers, such as citric acid, must be incorporated, which could affect biocompatibility (Qi et al., 2015).

The uniques degradation behavior of hydroxyapatite results in many favorable drug-release attributes. Standard, synthetic hydroxyapatite is incapable of much resorption and thus must be altered chemically, through the addition of ions such as magnesium or strontium, to increase degradation (Xiao et al., 2016). Though it cannot degrade quickly in most biological systems, hydroxyapatite is porous which allows for diffusive release of a loaded drug. Hydroxyapatite microspheres have been shown to exhibit sustained release of a variety of drugs, such as hemoglobin or vancomycin, lasting over the course of several days (Qi et al., 2012; Long et al., 2013).

Table VIII: *Pros and Cons of Hydroxyapatite for use in Microspheres*

Hydroxyapatite	
Pros	Cons
Biocompatible	Poor degradability; occurs very slowly
Capable of cell adhesion	Poor mechanical properties
Supports binding of MSCs	Requires caustic chemicals to prepare microspheres (e.g., dichloromethane)
Relatively non-toxic	Exhibits burst release
Minimal electrical conductivity	Low surface area
Zero foreign body response	Low drug loading capacity

3. Project Strategy

3.1 Initial Client Statement

The initial client statement provided by our client, Dr. Marsha Rolle is stated as follows:

"To develop a controlled release microsphere that can encapsulate and release PDGF-BB at a specified dose and duration, integrate within self-assembled human cell rings, maximize encapsulation efficiency by minimizing growth factor waste, and has the capability of being reproduced at different scales."

The initial client statement was then further expanded and revised to incorporate the determined constraints, objectives, and functions.

3.2 Objectives

After review of the client statement and constraints, a list of principle objectives were identified and compiled to address the most critical aspects for the design:

- Controlled PDGF-BB release
- Efficient PDGF-BB encapsulation
- Consistent microsphere size distribution
- Significant microsphere yield via fabrication method
- Cost of materials

Controlled PDGF-BB release: The purpose of this objective is to measure the amount of PDGF-BB being released into the system. The microsphere should begin releasing growth factor at a minimum of 10 days after initial combination within the tissue ring. The release profile should provide a constant and controlled release to allow for ring fusion and to minimize waste of growth factor. The microsphere should release approximately 50-100 ng/mL of PDGF-BB to the SMC tissue ring over a 1-2 week duration.

Efficient PDGF-BB encapsulation: The purpose of this objective is to verify that the microsphere possesses a high encapsulation efficiency to minimize growth factor or protein waste.

Consistent microsphere size distribution: To ensure precision and repeatability, another important objective is for the microsphere to have a maintained size distribution. The fabrication process of the microspheres should allow for consistent diameter measurements and uniform properties.

High microsphere fabrication yield. In order to determine which material is the most effective for our system, the material's fabrication method should allow for easy replication and should result in a high microsphere yield.

Inexpensive microsphere design. The total cost for our system and the components used to

maintain its function should not exceed the $900 budget for the project.

3.2.1 Comparison of Objectives

After meeting with the client and conducting a literature review, the objectives were evaluated and prioritized in terms of importance by developing a pairwise comparison chart. The pairwise comparison chart was used to establish new design objectives.

Table IX: *Pairwise Comparison for the Evaluation of Objectives*

	Release	Encapsulation	Size Distribution	Fabrication Ease	Cost	Total	Rank
Release	X	1	1	1	1	4	**1**
Encapsulation	0	X	1	1	1	3	**2**
Size Distribution	0	0	X	0	0	0	**5**
Fabrication Ease	0	0	1	X	0	1	**4**
Cost	0	0	1	1	X	2	**3**

In order to determine their significance relative to one another, each objective was compared and contrasted against one another using the pairwise comparison chart (Table IX). In this chart, a value of 1 or 0 signifies that an objective has greater or lesser priority to the one it is being compared to, respectively. Objectives were evaluated based on their overall priority in achieving the project goals and satisfying the needs presented in the client statement. Through this method, the three most important criteria for our design were the release and encapsulation of protein. Thus, during the design process, these three objectives became our areas of focus.

3.3 Constraints

In order to successfully design our system, a list of constraints were identified and developed to satisfy the previously stated needs of our client. If the system did not meet each of these constraints, then the project would have been determined a failure. Each constraint necessary for the success of our system is listed as follows:

The microsphere must retain PDGF-BB activity. While PDGF-BB is loaded within the microsphere and during its release into the tissue ring, through either diffusion or surface degradation, the material must not inhibit the function or disrupt the activity of PDGF-BB.

The microsphere must be biocompatible with SMCs. The initial microsphere material and any additional byproducts produced through diffusion or degradation must be biocompatible with the SMCs. The system should also be non-toxic to ensure cell viability.

The selected material must have the capability to be sterilized. The selected biomaterial chosen for the design process must be capable of being sterilized to prevent contamination.

3.4 Functions

After evaluation of the objectives and constraints, a list of functions were created to define each action the drug delivery system must perform in order to meet each of the design requirements. The principle functions and the means to test them are as follows:

Table X: *Functions and Means of Design Requirements*

Function	Mean 1	Mean 2
Release duration for 10-14 days	Selection of biomaterial with the most suitable properties	Method of microparticle fabrication
Measure cell viability	Cytotoxicity assay & Live/Dead staining	Observing cell viability via microscopy
Measure sustained release of PDGF-BB	Quantifying the material's encapsulation efficiency of lysozyme	Quantifying amount of lysozyme released over time using a release assay
Minimize burst release of PDGF-BB	Increasing strength and resistance of polymer through cross-linking.	Adjustment of fabrication protocol for individual material
Material sterilization to prevent contamination	Sterilization via autoclave to kill off microorganisms	UV Sterilization to prevent spread and growth of microorganisms
Maintain cells at physiological conditions	Ensuring cell growth with specialized cell culture medium (10% FBS, 1% Penicillin Streptomycin, 1% Glutamax)	Incubation of cells in optimal growth conditions (37℃, 5% CO_2, 20% O_2)

As seen in Table X, the first function that this design should have is a release profile for a duration of 10-14 days. The means to how this function will be obtained is through the selection of the biomaterial with the most optimal properties and its fabrication method to ensure prolonged release of the PDGF-BB to induce cell proliferation. The next function for our design is to measure the sustained release of the growth factor in the system. The means for this function is through the use of encapsulation and release assays, which will allow our project team to both measure and observe the release profile. To prevent waste factor from being a significant issue, a function was determined to minimize the burst release of PDGF-BB. The means to attain this function was based on the fabrication method for the biomaterial of interest, which could be accomplished through the addition of cross-linking for certain materials, or a combination of multiple materials within one microsphere. Another important function is to prevent contamination from occurring in our system. To achieve this, all relevant equipment will be UV sterilized before and after use. Lastly, in order to ensure cell survival in the system, a determined function was for the system to maintain cells at their physiological conditions. The means to attain this function will be standard cell culture procedure which will be conducted throughout the experiment. For incubation, the cells will be maintained at a temperature of 37℃, a CO_2 level of 5-10%, and an oxygen level that is approximately 20%.

3.5 Standards

In order for the creation of a safe and reliable product, there are multiple industry standards which will need to be met. Standards set forth by both the International Standards Organization (ISO) and the American Society for Testing and Materials (ASTM) will need to be met for our project to be successful.

The first industry standard that needs to be met for our project is ISO 10993-5:2009 which tests for *in vitro* cytotoxicity, and encompasses our objective to produce microspheres which are biocompatible within the TEBV. This test ensures that the integrated microsphere surface, or byproducts released through diffusion or degradation, will not kill nor harm the cells in unintended ways due to toxicity from these agents. Additionally, the second standard ASTM F2739-16 also encompasses our objective to produce biocompatible microspheres. This standard tests the quantification of cell viability within biomaterial scaffolds, which will also indicate that the microspheres are not harmful to the cells in contact. The third standard is ISO 11737-2:2009, which involves tests on the sterilization ability of medical devices. This ensures that the microsphere materials have the ability to be sterilized through an accepted procedure before being added to the TEBV, and will not cause any unwarranted harm to the cells. The fourth standard which relates to our project is ASTM F3142-16, which standardizes the evaluation of biomolecule release from a tissue engineered medical product. This correlates with one of our primary objectives detailing a controlled release of PDGF-BB from the microsphere into the TEBV. This is focused primarily on the elimination of an initial burst release of growth factor from the microsphere.

3.6 Revised Client Statement

Following further revisions and an improved understanding of the project's constraints and objectives, the initial client statement was improved upon. The resulting client statement reads as follows:

Design and fabricate a microsphere drug delivery system to facilitate or promote proliferation within a tissue engineered SMC ring, such as to mimic a lesion of intimal hyperplasia. PDGF-BB should be encapsulated efficiently within the microspheres and have a controlled release from the microspheres to the surrounding SMCs. The microsphere design should have a 10-14 day release profile. Incorporation of the microspheres should not alter the integrity or conformation of the tissue ring. Effective fabrication and implementation of the microspheres should be reproducible.

4. Design Process

4.1 Design Selection

As the team has elected to use microspheres in the design of an *in vitro* IH model, different materials were compared to our baseline material of gelatin on how well each meets outlined objectives and constraints. Gelatin was selected as the baseline material because the Rolle lab has incorporated gelatin microspheres within TEBVs in the past (Strobel et al., 2017). The lowest ranked materials were then eliminated from further experimentation to conserve time and funds and narrow the team's focus.

Due to the limitation presented by the project budget and the expense of PDGF-BB cost, a cheaper analog protein was required for microsphere loading. For this purpose, the protein lysozyme was used. Lysozyme presents a similar weight and structure compared to PDGF-BB. Additionally, protein activity could be verified during release through the use of lysozyme specific enzyme assays.

Each material was characterized through review of studies detailing each material's physical properties, cost, fabrication method, and chemical structure. Before consideration of how well each material meets the team's objectives, each material was evaluated on whether it addressed all of our design constraints:

- The microspheres must retain protein activity.
- The microspheres must be biocompatible with SMCs.
- The microspheres must have the capability of being sterilized.

All materials that were determined to have met all design constraints were then compared based on how well each material met our design objectives. Table XI shows the decision matrix comparing each material.

Table XI: *Decision matrix of microsphere materials*

	Gelatin	PLGA	Polyanhydrides	Hydroxyapatite	Chitosan	Silk
Release of PDGF (6)	0	1	1	0	0	0
Encapsulation of PDGF (5)	0	0	0	0	0	0
Size Distribution (1)	0	1	1	0	0	1
Fabrication Ease (2)	0	-1	-1	-1	0	1
Integration (4)	0	1	0	1	0	1
Proliferation (7)	0	0	0	0	1	0
Cost (3)	0	-1	-1	-1	-1	-1
Total	0	2	0	-1	0	2
Weighted Total	0	6	2	-1	4	4
Rank	N/A	1	3	4	2*	2*

The leftmost column lists ordered microsphere characteristics in which each material was compared on how well they perform in a specific category, compared to the baseline material of gelatin. A rank of 1 denotes superior performance to baseline, a -1 shows inferior performance, and a 0 signifies no gain or loss over using the baseline material. Shown in parentheses, each weighted value was assigned based on how important that category is for attaining the overall goals of our design, as determined by Table XI. The lower the weight value, the less imperative that the objective must be met.

Assigned the lowest weight value of 1, size distribution of fabricated microspheres is deemed least critical as microspheres are seeded into TEBV cultures as the SMCs proliferate and form the component blood vessel tissue rings (Strobel et al., 2017). As the client seeks a reproducible process that can make consistently sized microspheres, to enhance the standardization of the IH drug testing model, the microspheres must have a narrow size distribution to ensure accurate dispensing of loaded drugs, such as PDGF-BB, into the cell culture. If microspheres varied in size greatly, there will be unequal loading and unloading of drug particles from microspheres to different regions of the vessel and negatively impact

the specific targeting of an IH lesion (Strobel et al., 2017). However, microspheres will vary in size from batch to batch with team fabrication protocols, so this objective is an ideal goal, and not very attainable in our design, and thus not important. Among the materials selected, PLGA, polyanhydrides, and silk were found to have more consistent size ranges after their respective fabrication processes than the current process the client uses for gelatin microspheres (Berkland, 2004; Han et al., 2016; Strobel et al., 2017; Wang X. et al., 2010) .

Fabrication ease and cost, which also have lower weight values, concern the production process of turning each material into microspheres. Ultimately, the team wants to ascertain a cost effective process that can be scaled-up as desired. As such, a fabrication protocol that uses the most inexpensive reagents and equipment would prove ideal for achieving this goal, but falls under the importance granted for size distribution. For the production of PLGA, polyanhydride, and hydroxyapatite microspheres, it was found that production was more lengthy and costly for each material compared to the baseline, whereas silk microspheres had a shorter production time and less expensive reagents used to make microspheres (Berkland, 2004; Han et al., 2016; Strobel et al., 2017; Wang X. et al., 2010; Xiao et al., 2016) .

Integration of the microsphere, which has a mid-range weighted value, is defined as how well it can fit into TEBV rings without impacting tissue structure and growth, based on microsphere size alone. Between 20 μm and 40 μm is an ideal range. As the final IH testing design seeks to model *in vivo* blood vessels for accurate drug testing, to best emulate blood vessel structure, TEBV structure must be similar to the natural equivalent. Consequently, microspheres should not impede proper blood vessel formation and affect vessel properties, such as contractility (Strobel et al., 2017). Small microspheres are therefore favorable, and the smaller the microspheres that can be attained, the better the blood vessel structure can be maintained. However, as integration/size of the microsphere is a broad category, with a range of permissible sizes, more flexibility in this category allows for differently sized microspheres.

With the next two categories of higher importance, materials were compared based on the encapsulation and release abilities of PDGF-BB. For the first category, the materials were compared based on whether each could entrap the growth factor or a similarly sized protein. Every material in the above matrix could support encapsulation of PDGF-BB or a protein of similar weight, such as the surrogate protein lysozyme. In terms of the release profile of the loaded protein, the microsphere should begin the sustained release of 50-100 ng/mL of PDGF-BB at minimum 10 days after fusion within a SMC ring, up to 2 weeks. As the time span of release is over days, there is room for materials to exhibit slightly different release profiles and rates within that time, but any candidate material should remain close to the aforementioned ranges. Moreover, having a high initial burst release of the protein can prove toxic to the TEBV tissue (Huang & Brazel, 2001). Compared to gelatin, PLGA and polyanhydrides support more sustained release into the surrounding tissue.

The most important category is whether a material can facilitate proliferation of SMCs within the TEBV culture and formation of the IH lesion. Though PDGF-BB will trigger IH formation, the ability of the microsphere material itself to support proliferation of cells could prove an asset for the our design, which is why this category is ranked highest. The stimulation of IH within a TEBV is the ultimate goal of this project, so any contribution from the microsphere material in this regard is a worthwhile feature of a

prospective microsphere material. Among all materials, only chitosan has demonstrated the ability to encourage cellular proliferation (Kim et al., 2008).

After evaluation of each material, the first and second ranked materials were selected for experimental study as this project's duration of 1 academic year and limited budget of $900 prevents study of all materials. PLGA shows most promise in meeting design objectives whereas silk and chitosan show equal rank in meeting objectives. Thus, all three materials will be used in addition to the baseline, gelatin. Polyanhydride and hydroxyapatite were excluded from our experiments as a result of their lower ranking, with fabrication cost and fabrication ease of each material the largest reasons for their rejection. As this project is concerned with developing microspheres capable of releasing growth factor, these materials' low rankings would impede this main goal.

4.2 Alternative Designs

With the selection of PLGA, silk, chitosan, and gelatin as our experimental microsphere materials. The team first worked to optimize the production of each material. Microspheres of each material were fabricated from protocols that combined design steps from other published fabrication methods and adaptations due to available equipment.

4.2.1 Gelatin Microspheres

Fabrication

Gelatin microspheres were fabricated using a water-in-oil emulsion technique (Figure 3). The procedure followed an adapted protocol outlined in Tabata et al. 1999. Genipin was used as a crosslinking agent to strengthen the microspheres and offer more resistance to their degradation. The gelatin microspheres were first formed through the emulsion technique, followed by genipin crosslinking and loading of the microspheres with lysozyme as our test protein. The stepwise protocol for experimentation can be found in Appendix B. In summary, a solution consisting of 11.1% (w/v) gelatin in deionized water was added dropwise to 250 mL of olive oil. Following the dropwise addition, the mixture was stirred at 45℃ for 10 minutes. The temperature was then lowered to 20℃ and stirred for thirty additional minutes. The mixture was stirred at 800 rpm using a stir plate and stir bar. One hundres mL of chilled acetone was added to the solution and stirred for another hour. An additional 100 mL of chilled acetone was added to the solution and stirring continued for another 5 minutes. Microspheres were then filtered out of the water, oil, and acetone solution through the use of a Buchner funnel and filter paper. The microspheres were washed with acetone and air dried before proceeding with crosslinking. The dried microspheres were added to an aqueous solution of 5 mL 1% genipin in deionized water at varying times to promote different crosslinking percentages. For the initial trials, the time remained constant at 12 hours, before the microspheres were then collected, washed with deionized water and stored at 4℃. Microspheres that were used for experimental testing were UV sterilized for 10 min before being loaded with lysozyme. The sterile microspheres were soaked in a solution of 80 ng/μL lysozyme and phosphate buffered saline (PBS). The solution was vortexed and kept at 4℃ for 15 hours.

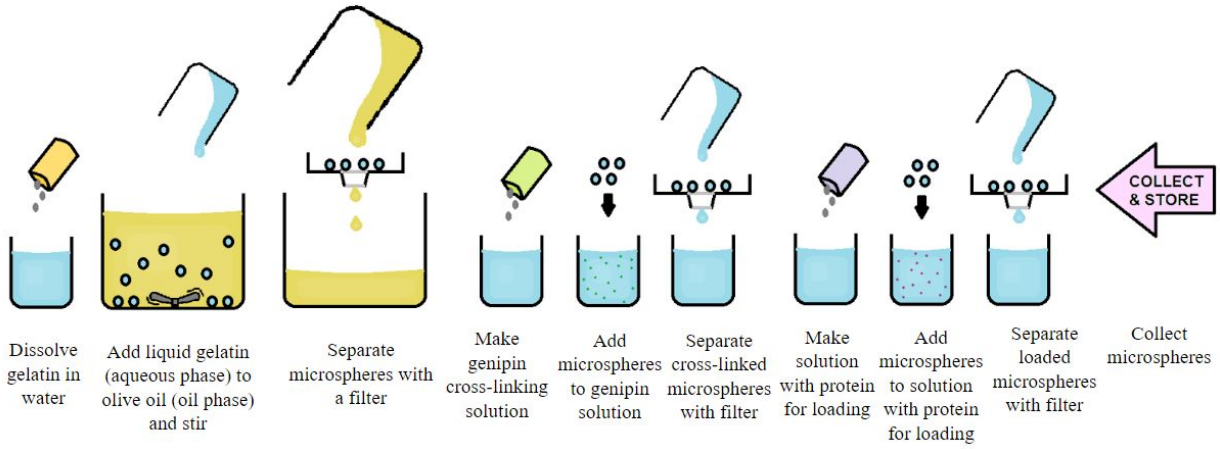

Figure 3: *Schematic of gelatin microsphere fabrication process*

Observations

Following fabrication of the microspheres, it was determined that alterations were necessary to increase the efficiency and reproducibility of the protocol. The most apparent limitation when performing this procedure was the large range of microsphere sizes. After filtration, by just viewing the microspheres with a naked eye, large differences in size range between the individual microspheres formed were observed. In an effort to limit this range, a homogenizer was used in place of stirring in an effort to decrease the overall size of the fabricated microspheres. The resulting microspheres also experienced severe clumping during filtration, with a large aggregate of microspheres being formed within the middle of the plate. The aggregation could be caused by the large size of the microspheres, and therefore could be eliminated through use of the homogenizer.

In addition, a second limitation of the referenced protocol was the time to complete the fabrication process. Using this procedure, the fabrication took at least two days to complete due to the crosslinking and loading of the microspheres. Also, the large volumes of materials being used increased the amount of time needed to filter the microspheres. Due to the viscosity of the oil presented within the emulsion, the length of time needed for complete filtration through the filter paper and Buchner funnel was at least an additional hour. The procedure was altered by lowering the starting volume used for the fabrication process. Instead of 250 mL, only 100 mL of olive oil was used going forward, with less gelatin and genipin being used as well.

A third limitation to the aforementioned protocol was found during the air drying step. After the washing step was completed, the gelatin microspheres were air dried overnight in order to evaporate off any remaining liquid from the surfaces of the microspheres. However, after air drying the microspheres had shrunk and looked as if they had denatured overnight.

The referenced protocol was altered based on the limitations presented above. In addition to using smaller volumes of materials for fabrication, a homogenizer was incorporated into the stirring steps in an effort to limit the large size and large size distribution of the gelatin microspheres. For the final ten

minutes of the stirring step, the mixture was taken off of the plate and instead homogenized at 14,000 rpm for ten minutes.

Figure 4: *Gelatin microspheres observed macroscopically following the use of the homogenizer*

In an effort to limit the time taken to fabricate the microspheres, the washing step was changed as well. Instead of using a Buchner funnel and filter paper, the oil and microsphere mixture was centrifuged at 7,000 rpm for five minutes or until a gelatin microsphere pellet formed. The oil was then aspirated from the conical tube, and acetone was added back into the conical tube. This procedure was repeated until all the oil had been aspirated out of the gelatin mixture.

4.2.2 Chitosan Microspheres

Fabrication

Chitosan microspheres were fabricated using a water-in-oil emulsion technique (Figure 5). Genipin was used as a crosslinking agent. Similar to the gelatin microspheres, the chitosan microspheres were loaded with lysozyme, though for the chitosan fabrication procedure, the lysozyme was added to the aqueous chitosan solution prior to emulsion.

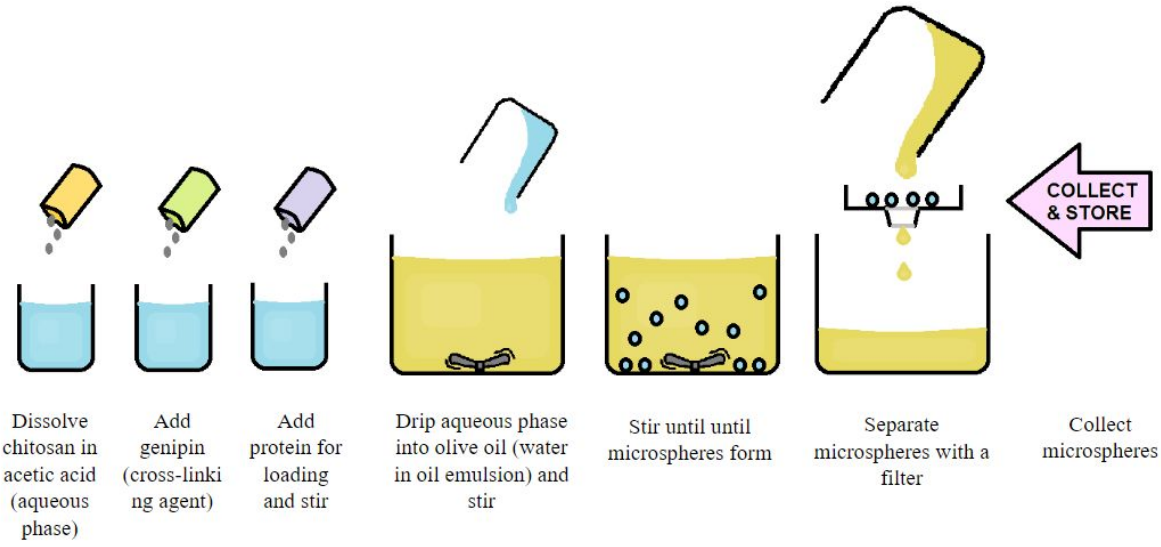

Figure 5: *Schematic of chitosan microsphere fabrication process*

The procedure was adapted from a previously outlined protocol (Appendix C) (Karnchanajindanun et al., 2011). Generally, dehydrated chitosan was dissolved in 2% acetic acid to make a 0.5% (w/v) aqueous solution. Genipin was added to the solution, resulting in a 20:1 chitosan-to-genipin ratio. After gentle stirring to allow for cross linking, the lysozyme is added and dispersed into the solution. The aqueous phase is added dropwise to a large volume (approximately 150 mL) of olive oil and agitated with a homogenizer at 1,100 rpm for an hour in order to form microspheres (Figure 5). The emulsion is then transferred to tubes and centrifuged to separate excess oil from the chitosan, which forms a pellet at the bottom of the tube. The remainder of the liquid is removed via filtration followed by a rinse with isopropyl alcohol. The microspheres were stored in 4°C and UV sterilized prior to use with cells.

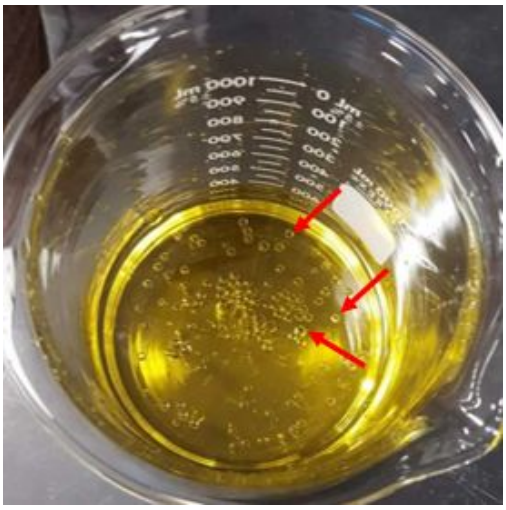

Figure 6: *Droplets of chitosan-genipin solution in oil prior to stirring. Red arrows point to aqueous chitosan-genipin droplets within the oil.*

Observations

The procedure was altered after initial attempts, to try to improve the efficiency of the protocol. The most apparent drawback of the fabrication of chitosan microspheres is the duration of the process. In addition to a six-hour cross-linking period, the high viscosity of the oil makes the use of a Buchner funnel for filtration quite tedious. The olive oil emulsion volume was therefore reduced by half and centrifugation was performed to remove most of the oil prior to the filtration step. After drying onto filter paper over the funnel, the chitosan spheres clumped together forming flakes. The observed clumping was not however as severe as that observed with the gelatin microspheres.

4.2.3 Silk Microspheres

Fabrication

The team prepared silk microspheres by adapting a silk/PVA blend film procedure (Figure 7) (Wang X. et al., 2010). The full stepwise protocol can be found in Appendix D. In this process, solutions of silk and PVA were mixed together at a 1:4 ratio in a glass beaker. The blend solution was transferred to a 35 mm petri dish and stirred at 150 rpm for 2 hours at room temperature. Afterward, the blend solution was left in a fume hood to dry overnight and form a dried film. To dissolve the blend film, 10 mL of Milli-Q water was added to the petri dish and shaken gently for 10 minutes at room temperature. The mixture was transferred to a centrifuge tube and centrifuged at 4,000 rpm for 20 minutes, and the supernatant was then carefully removed. This process was repeated twice. The adhered pellet was suspended in 2 mL of Milli-Q water. A vortex device was used to disperse the clustered silk microspheres for 15 seconds. For storage, the suspended microspheres were placed at 4℃.

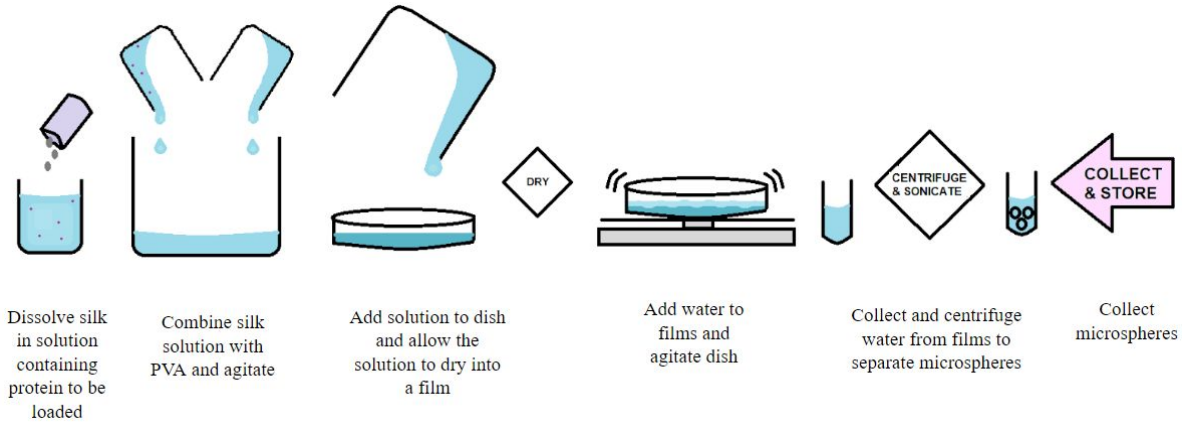

Figure 7:*Schematic of silk microsphere fabrication process*

Observations

Several adjustments were made to the silk microsphere fabrication protocol in order to improve the efficiency of the technique and consistency of the results. One limitation in this procedure was the dispersion of the microspheres. To produce the actual particles after centrifugation, a vortex was used for the disruption of the clustered microspheres. Vortexing had caused the silk/PVA mixture to appear cloudy in its suspension which allowed for the determination of the presence of microspheres (Figure 8).

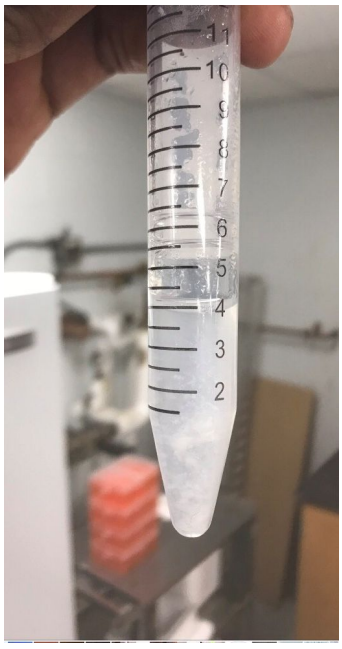

Figure 8: *Dispersed silk microspheres in suspensio*n

The vortexing time for the silk/PVA mixture was therefore reduced from the 15 seconds stated in the protocol. Another limitation was the filtration of the silk microspheres. Initially, the silk microspheres were filtered using a Buchner funnel and filter paper for observation via microscopy. However, the microspheres would adhere to the fibers of the filter paper which made it difficult for observation. To address this issue, the suspended silk solution was vortexed and then transferred to a petri dish to obtain phase contrast images (Figure 9).

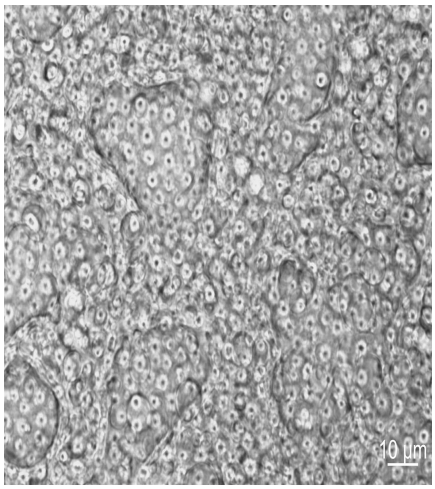

Figure 9: *Phase Contrast image of Silk Microspheres (40x)*

In this image, a nearly uniform silk microsphere particle distribution can be observed. This image demonstrates that this fabrication procedure is capable of generating microspheres with a relatively consistent size distribution.

4.2.4 PLGA Microspheres

Fabrication

PLGA microspheres were made by a water-in-oil-in-water emulsion protocol synthesized from different studies (He et al., 2011; Koda et al., 2017; Nafissi et al., 2011; Li et al., 2014). The full stepwise protocol can be found in Appendix E. All steps were performed in a fume hood, except for the centrifugation step (Figure 10). First, a lysozyme solution was prepared and mixed with a PLGA solution to make a 10% oil solution. The resulting mixture was then sonicated with the Misosonix Sonicator XL2000 for 30 seconds. This mixture was then added to a 300 mL 10°C 1.0% (w/v) PVA bath and homogenized at ~11,250 rpm for about 30 seconds. The solution was then spun at 500 rpm for 3 hours at room temperature. The microspheres were collected by filtering the 300 mL PVA solution through 60 mm filter paper and washing with isopropanol three times, and prior to centrifugation at 5000 rpm for 30 minutes. As freeze-drying could not be performed immediately, for temporary storage, the sample was stored at -20℃.

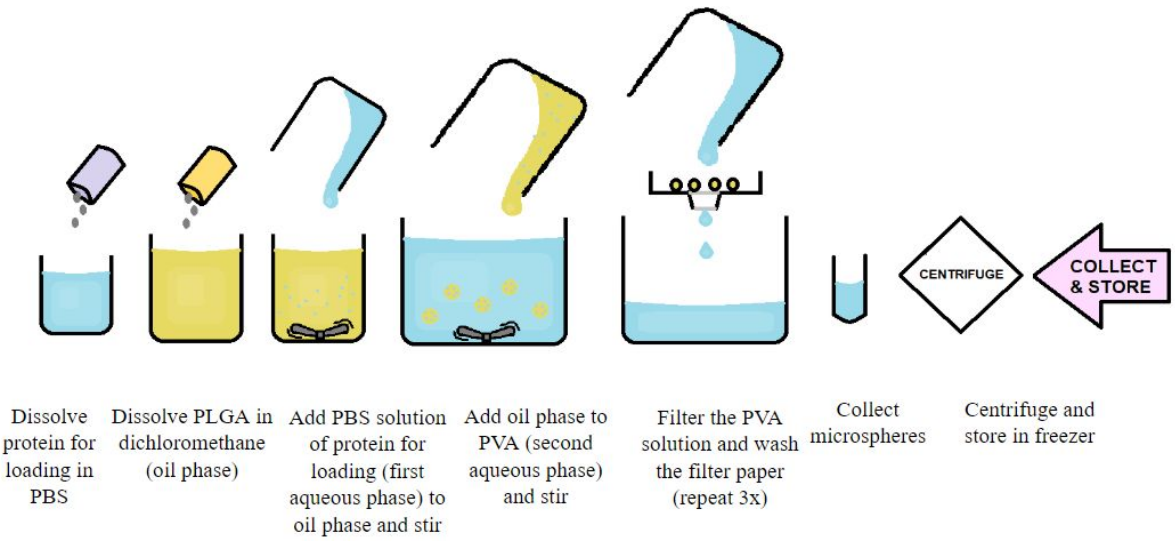

Figure 10: *Schematic of PLGA microsphere fabrication process*

Observations

The original PLGA microsphere protocol was altered to enhance yield and accommodate available equipment. The homogenizer used for the protocol seemed to generate heat when ran for about 1 minute, so the homogenization time was lessened to 30 seconds. Moreover, as the microspheres were suspended in a 300 mL PVA solution, centrifugation proved difficult, so the bath was filtered through 60 mm filter paper three times with a isopropyl alcohol wash instead. The resulting volume of sample collected was 7 mL, which was centrifuged for 30 minutes at 5000 rpm to see if centrifugation could work. A white pellet was collected. About 2 mL of the sample was pipetted into a petri dish and observed under a phase contrast microscope (Figure 11) .

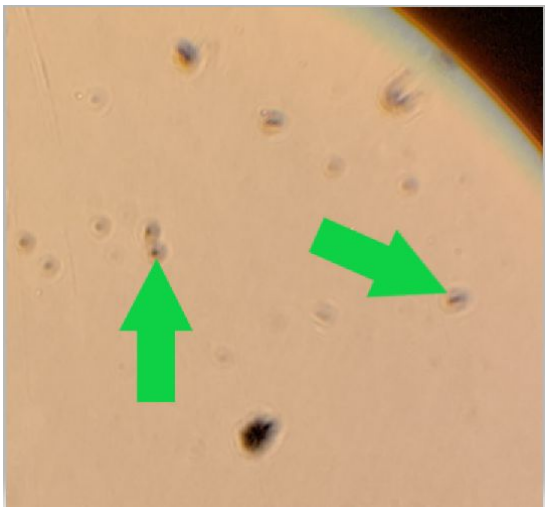

Figure 11: *PLGA microspheres in isopropanol (20x). The green arrows point to clumps of dried microspheres.*

PLGA microspheres can be discerned as individual clear specks, but most appear clumped together in black masses of individual microspheres (Figure 11). Moreover, when observing the microspheres under the microscope, as the plate was tilted, PLGA microsphere clumps could be collected onto the plate.

5. Design Verification

5.1 Flow of Methodology

Following the fabrication of the four alternative microsphere types, it was necessary to establish and run multiple experiments in an effort to alter and eliminate the alternative designs until an exceptional final microsphere design has been reached. The final microsphere design must incorporate all design objectives, functions, means, and constraints in order to establish a safe and reproducible microsphere which meets our design goals. Therefore, a methodology flowchart was established to organize the experiments run throughout the entirety of the project (Figure 12).

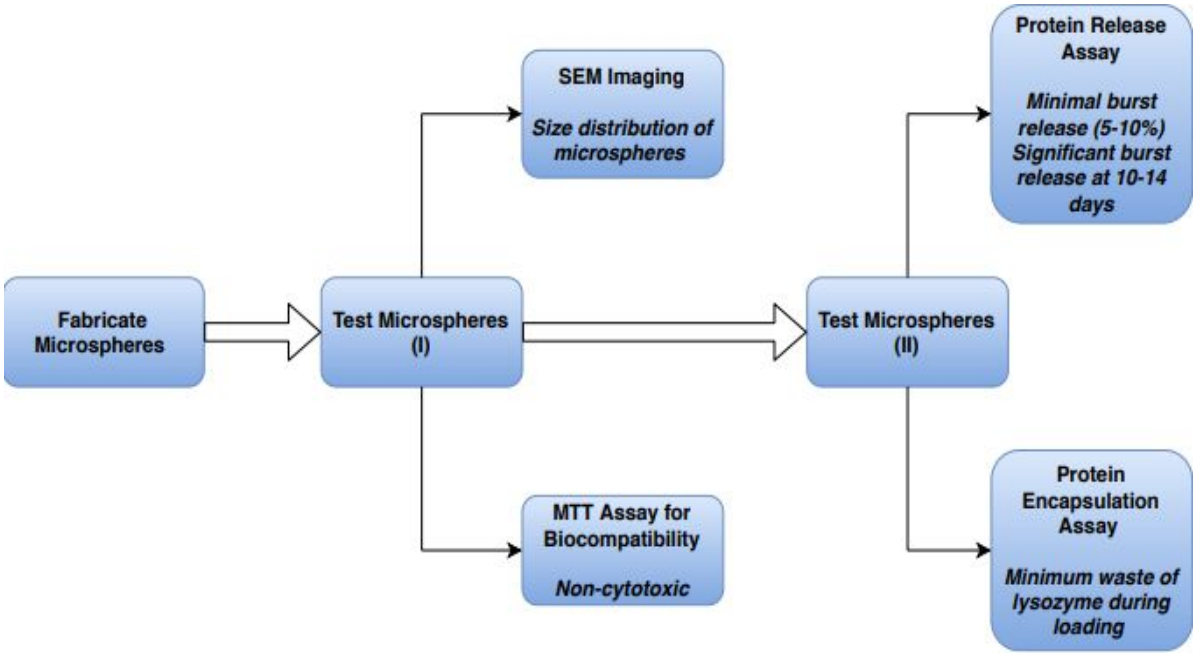

Figure 12: *Methodology flowchart of alternative design testing*

Experimental testing was broken down into two separate phases: Test Microspheres (I) and Test Microspheres (II). The reasoning for the distinction between these experiments was based on the ease of the procedures, as well as the duration of each experiment. Phase I consisted of microscopy testing using Scanning Electron Microscopy (SEM), and a MTT assay to investigate biocompatibility. Phase I testing could be performed without protein loading included in the fabrication process, since these experiments investigated physical properties of the microsphere material solely.

Microspheres were first imaged through the use of an SEM to determine microsphere shape, structure and mean size and distribution. For the purposes of our goal, the microspheres would need to maintain a reproducible size range between 20 and 40 μm to be considered successful. Biocompatibility testing was conducted to ensure that none of the material designs present a cytotoxic risk to the cells during implantation and degradation. The results of the Phase I tests were used to eliminate some of the alternative design materials.

Phase II testing of the microspheres consisted of both a protein encapsulation assay and a release assay. These assays were separated from the previous Phase I methods because incorporation of a protein was required for both experimentation and integration with the selected design materials. Additionally, it was desirable to eliminate potential microsphere designs to minimize waste of the protein and other associated reagents. The encapsulation efficiency of the four microspheres was tested to determine which design is most the successful for entrapping a loaded protein. This is important as a required amount of 50-100 ng/mL PDGF-BB will need to be released to the tissue rings to stimulate proliferation of the SMCs. The protein release assay allowed for the analysis of each microsphere release profile. It is important that the microspheres do not elicit a burst release, meaning they should not release a large percentage of their loaded protein at early points in the experiments. Ideally, the microspheres would not

begin releasing growth factor until 7 days after incorporation within the SMC toroid rings. Additionally, the activity of the releasing protein will also need to be measured during the duration of the release. It is necessary that none of the materials decrease the activity or effectiveness of the cytokine during its release into the SMC environment.

5.2 Phase I Testing

5.2.1 MTT Assay

Biocompatibility of the four chosen materials was assessed through the use of the MTT assay. The MTT assay is used to measure metabolic activity of the SMCs as a metric of cellular proliferation. For this experiment, we measured the metabolic activity of six different experimental groups to determine biocompatibility. Conditioned media from gelatin, chitosan, silk, and PLGA were added to individual wells containing 50,000 SMCs. Additionally, a positive control group with only the 50,000 cells and a negative control group with no cells were included. The 50,000 cells were chosen following the completion of a standard curve, with cell densities ranging from 5,000 to 150,000 cells/mL. The assay allowed for the comparison of metabolic activity between isolated *in vitro* cells and cells in contact with microspheres. The protocol for the MTT assay was adapted from the *Cayman Chemical MTT Cell Proliferation Assay Kit Booklet* (Appendix F). The absorbance readings used for data analysis were measured using a spectrophotometer plate reader at 570 nm.

The six experimental groups were set up through seeding 50,000 cells/mL in 100 µL of normal rSMC media and incubated for one hour at 37℃ and 5% CO_2. Microsphere conditioned media was prepared by adding 3 mg of the respective microspheres in 1 mL of SMC media. The media was incubated at 37℃ and 5% CO_2 for one hour as well. Normal SMC media was aspirated from four sets of wells within the 96 well plate, and 100 µL of the microsphere-conditioned media was added to the respective experimental groups in the 96 well plate. This allowed for the cells to adhere to the bottom of the plate prior to the addition of the microsphere media. Following the addition of reagents, the conditions were measured using a spectrophotometer at 570 nm (Figure 13).

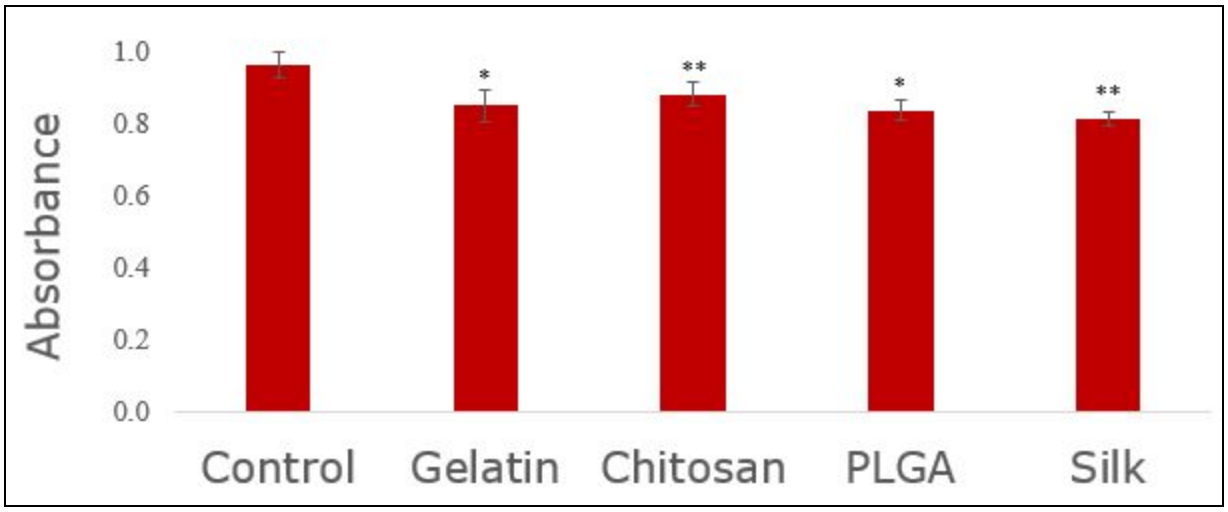

Figure 13: *MTT assay for quantifying metabolic activity and biocompatibility of gelatin, chitosan, PLGA, and silk microspheres. Error bars represent standard deviation with N=3 and n=9. * denotes statistically significant decrease in metabolic activity between the microsphere material and the positive control group ($p<0.05$). ** denotes a statistically significant difference between the microsphere material and the control group, as well as a significant difference between those two types of materials ($p<0.05$).*

The average absorbance levels were calculated for each microsphere condition to allow for statistical comparison between the experimental groups and the control. Statistical analysis was performed through a Single Factor ANOVA and post hoc Tukey-Kramer test for significance.

The Single Factor ANOVA suggested that there was a significant difference across the experimental groups. Therefore, the Tukey-Kramer post hoc test for significance was performed to clarify which experimental groups showed significant difference from the rest. The test showed that all microsphere conditions had a significant decrease when compared back to the baseline control. Additionally, chitosan had a significantly greater mean absorbance level when compared to silk. While the statistical tests did show a significant decrease in absorbance levels across all microsphere samples, the MTT assay still showed that a large amount of cells did stay metabolically active when exposed to each microsphere material. The presence of metabolic activity across each sample was expected since each material used is classified as biocompatible according to the literature.

5.2.2 Scanning Electron Microscopy

SEM was used to characterize the sizes and surfaces of the microspheres. This microscopy method was selected because SEM allows for great resolution, depth, and a 3D perspective of materials. These qualities would allow us to characterize the microspheres not only by size but also by conformation and surface morphology. Each material was suspended in water and stirred or vortexed. Then, 100 μL of each material solution was transferred directly to conductive tape on a mounted SEM slide for analysis

after overnight drying of the solvent from each mount (Figure 14). Average diameters of viewed microspheres of each material in each sample were also measured (Table XII).

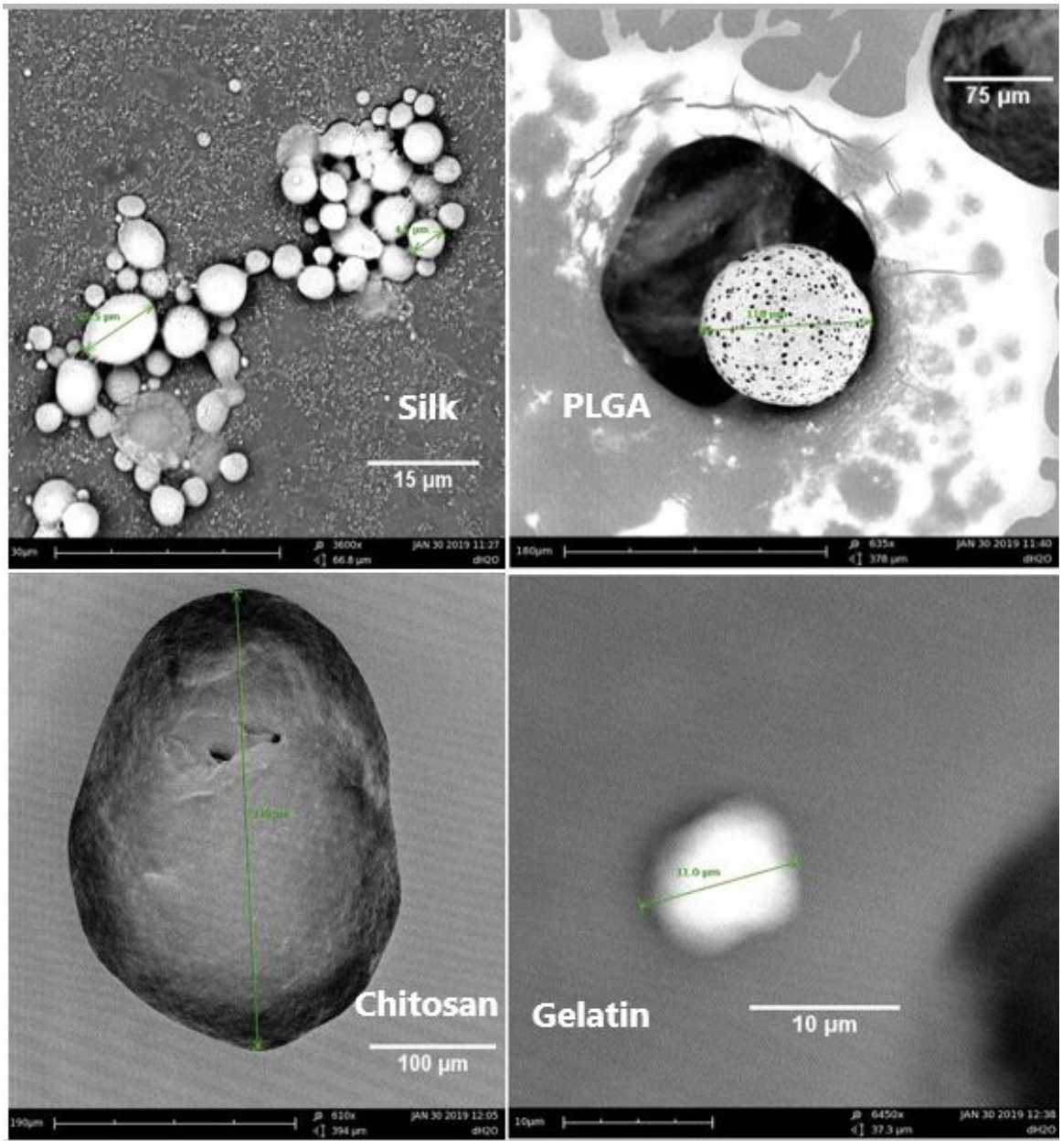

Figure 14: *SEM images of prepared silk microspheres at 3600x, chitosan microsphere at 610x, PLGA microsphere at 635x, gelatin microsphere at 6450x.*

Table XII: *Average (Avg) diameter of observable microspheres in SEM images with standard deviation (stdev). All lengths are in μm.*

Microsphere Type	Silk	Chitosan	Gelatin	PLGA
Microspheres Counted	79	4	1	3
Avg Dia±SD (μm)	3.97±1.95	290.03±49.35	11.0±0.00	108.81±19.69

From these images and measurements, the general size and structure of the four microsphere types can be compared. Among all the microspheres observed, silk gave the greatest abundance of viewable microspheres during image collection, with a sample size of 79 microspheres. Moreover, gelatin and PLGA appeared to be the largest in size with average diameters of 290.03 μm and 108.81 μm, respectively. The one sphere-like structure observed from gelatin had a diameter of about 11 μm. Silk microspheres were generally the smallest with an average diameter of 3.97 μm but had a range of diameters from 1μm to 10μm (Figure 15).

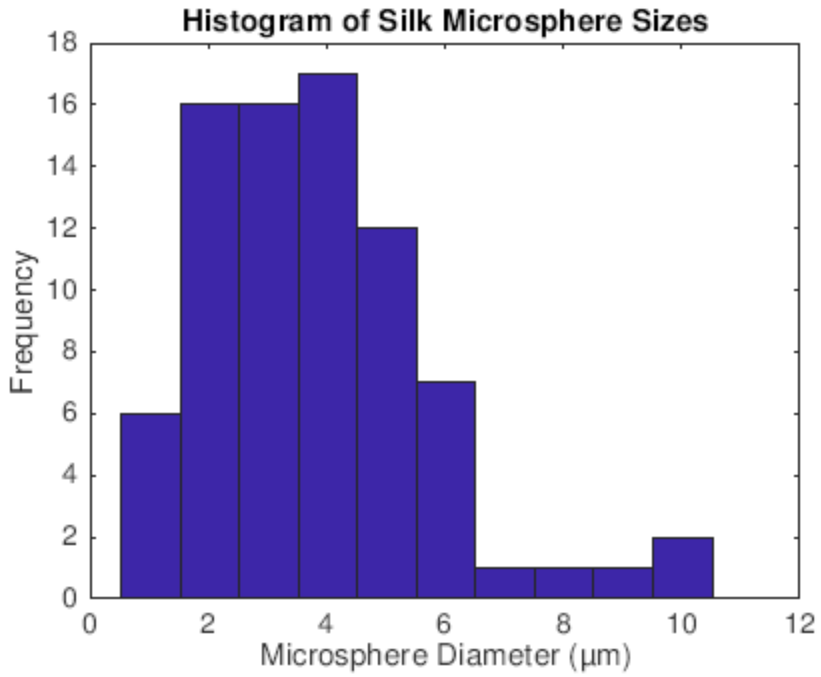

Figure 15: *Histogram of measured silk microsphere diameters.*

Though silk reported the lowest standard deviation, its higher sample size could have lowered that value. This is in contrast to the higher standard deviation values reported for the other materials due to the other microspheres having smaller sample sizes. Gelatin produced virtually no microspheres that could be viewed, aside from a single microsphere that could be found from the SEM scope. This scarcity of microspheres brings to question whether the observed gelatin particle is a microsphere or some other

impurity, as there were no other spheres for comparison. Chitosan particles were clearly present but were not as visibly spherical as silk and PLGA, but rather appearing oblong in conformation. PLGA, among all the materials, shows the most spherical structure, with pores indicating where water was incorporated into the spheres during fabrication. Silk gave a range of globular shapes, generally quite spherical with a smooth surface appearance. Additional SEM images of samples can be found in Appendix G.

5.2.3 Phase I Conclusions

Based on the SEM imaging of microspheres and consideration of fabrication time and ease, gelatin and PLGA were eliminated, even though all materials proved to be biocompatible. In addition, the fabrication processes for gelatin and PLGA were not ideal production factors, so they were not subjected to Phase II testing.

During SEM observations, gelatin microspheres were difficult to detect. Therefore, to standardize SEM preparation, the same specimen mounting protocol was followed for all materials, with gelatin proving most difficult to break apart into individual microspheres. During all fabrication runs with the material, the dissolution of gelatin from a clumped state proved impossible without mechanically breaking it apart. Observing this lack of macroscopic and microscopic indications of gelatin microspheres, the material appears to have the lowest yield of microspheres among the four chosen materials.

However, overall, there is little SEM-based confirmation of successful microsphere formation of gelatin microspheres, which directly counters the team objectives of finding an easily fabricated material that can yield microspheres. For these reasons, gelatin was eliminated from further experiments. In contrast, PLGA did yield microspheres that were observable in SEM. The microspheres had the most visibly spherical shape among all material types, but were further outside the ideal size range of 20-40 μm compared to gelatin.

However, while SEM images confirmed successful production of PLGA microspheres, fabrication proved challenging with the material in terms of equipment required and ease of handling. A sonicator and fume hood are required for the production of PLGA microspheres, in addition to the homogenizer and centrifuge the gelatin, chitosan, and silk protocols require. The higher cost of the polymer itself, compared to gelatin and chitosan, negatively impacts the financial accessibility of PLGA compared to the other materials. Also, the purchased supply of PLGA was exhausted and continued testing became less feasible from a cost perspective due to budget restrictions. Additionally, the requirement of dichloromethane, a known carcinogen, to make PLGA microspheres adds a health risk to the experimenter and necessitates that the entire fabrication run be performed in a fume hood. In contrast, the other materials do not use carcinogenic reagents and can be performed on the lab bench safely. Once made, to truly ensure no dichloromethane remains in the PLGA microsphere sample before cell testing, the particles must be analyzed by chromatography or other spectroscopic methods, which places further economic and time burdens on the lab. Furthermore, the material's acute sensitivity to any moisture necessitates an almost anhydrous environment be maintained for the material's fabrication, which can be challenging, as the humidity level of the lab cannot be feasibly controlled at all times. In contrast, the other materials are comprised of biopolymers that primarily degrade through enzymatic and metabolic

reactions, making them more durable to ambient moisture. Given these deviations from the team's objectives, PLGA was eliminated from further testing.

An ideal design would have a simple, reliable fabrication process that achieves consistent results. Thus far, the silk microspheres fabrication process has proven to be simple relative to the other materials and has yielded physically consistent particles, making silk the most promising candidate for achieving the objectives of the study. Though chitosan has much larger and fewer microspheres compared to silk, as observed in SEM, the material's relative ease of production compared to PLGA and gelatin makes it another possible candidate to satisfy the requirements of this project. Microsphere capable of encapsulating a large proportion of the total loaded protein, and can release the protein in a controlled, prolonged fashion are additional facets of the design that must be tested in Phase II to further assess the aptitude of silk and chitosan microspheres for achieving the design goal.

5.3 Phase II Testing

5.3.1 Encapsulation Assay

Encapsulation efficiency was assessed to determine the percentage of lysozyme that the matrix material is able to encapsulate relative to the amount added to the particles during the loading process. The procedure used to determine encapsulation efficiency consisted of two stages: dissolving the microspheres to release any loaded protein and quantifying the loaded protein. Because different materials dissolve efficiently in different solvents, both of the remaining microspheres have a unique protocol for freeing encapsulated protein for quantification (Table XIII). Appendix G provides more detail regarding preparation for encapsulation quantification. During the preparation steps, neither silk nor chitosan appeared to completely dissolve in solution with their recommended solvent, but broke into smaller, less opaque pieces. The chitosan particles were especially difficult to dissolve, likely as a result of crosslinking during fabrication.

Table XIII: *Solvents used to Dissolve Microspheres for Measuring Encapsulation Efficiency*

Microsphere Material	Method of Dissolving	Source Adapted from
Chitosan	- Dissolve in acetic acid (2% w/v), vortex for 20 minutes, add NaOH and 10X PBS to raise pH	Zeng et al., 2011
Silk	- Dissolve in DI water, vortex for 2 minutes,	Wen et al., 2011

Prior to dissolving the materials that were to be tested for encapsulation, the entire loaded microsphere batches were weighed using an analytical balance. Over the entire course of experimentation, a total of 4 and 5 batches were weighed for chitosan and silk, respectively. The chitosan protocol incorporated a combined material mass of 52 mg (chitosan, genipin and lysozyme) and yielded an average of 24.7 mg of microspheres (~48% yield of materials used in fabrication). The silk protocol, which incorporated 255 mg of material (silk, PVA, and lysozyme), yielded an average of 167.0 mg of

microspheres (~74.2% yield of materials used in fabrication). It should be noted that both silk and chitosan each had one batch with a yield greater than the mass of material incorporated during fabrication, which is, even under ideal fabrication conditions, impossible to achieve. One possible explanation for this, is that the microspheres were not completely dried prior to weighing, thus erroneously increasing the measured mass.

A known mass, approximately 3mg, was extracted from each of the loaded batches of each material and dissolved according to the tabulated protocols. A small volume of each dissolved sample was tested with the an EnzChek™ Lysozyme Assay (full protocol in Appendix H) to quantify the proportion of the encapsulated, active lysozyme. Since the concentration of lysozyme in the assay test wells was known, the total mass of lysozyme in the entire loaded batch could be calculated. This quantified lysozyme mass encapsulated within the particles was then used to calculate encapsulation efficiency (EE) with the following formula.

$$EE = \frac{quantified\ lysozyme}{lysozyme\ initially\ loaded} \times 100\%$$

Multiple iterations of encapsulation testing were performed to optimize the preparatory protocol and experimental setup of the assay (progression of encapsulation assay trials with experimental alterations shown in Appendix K). For this experiment, dissolved samples (~2 mg) for both microsphere materials as well as a stock solution of lysozyme (50 µg/mL), which served as a standard, were diluted 1:10 and 1:4, respectively, in reaction buffer and plated in triplicate. A serial dilution was performed on each of the triplicate standards, resulting in seven 1:2 dilutions sourced from the original plated dilution. The assay also included blank wells, containing only reaction buffer and substrate (no lysozyme nor microsphere solution), and negative and positive control solvent wells. Negative control solvent wells contained only the solvent diluted 1:10 in buffer whereas the positive control solvent wells contained solvent diluted 1:10 in a lysozyme buffer mixture. The final lysozyme concentration for the negative and positive control solvent wells were 0µg/mL and 5µg/mL, respectively.

The final trial for testing encapsulation incorporated several experimental alterations such as (1.) incorporating negative and positive controls for each microsphere solvent, (2.) diluting experimental samples so that fluorescent readings fell within the range of accuracy of the plate reader, and (3.) adding NaOH base to the acetic acid-chitosan solution to raise the solvent pH and reduce lysozyme denaturation. The standard curve acquired for this trial demonstrated a linear relationship between lysozyme concentration and absorbance, as expected. The raw data for the standards, however, plateaued at an absorbance of approximately 700,000, indicating enzyme saturation beyond the upper limit of the plate reader. Because of this, the two greatest lysozyme concentrations were excluded when making the standard curve (Figure 16A).

Using the linear mathematical relationship from the standards to calculate concentration of lysozyme in the dissolved microsphere samples, and scaling up to calculate the mass of lysozyme present in the entirety of the fabricated batches, the encapsulation efficiencies for each material was calculated. The encapsulation efficiency of silk (12.72%) was greater than that of chitosan (0.02%). Silk, however, had a greater standard deviation for encapsulation among the triplicate wells (Figure 16B).

The positive controls for both material solvents yielded increased lysozyme concentration in comparison to the respective dissolved microsphere samples and negative controls. The positive controls for chitosan and silk, which had been plated with a lysozyme concentration of 2.5 μg/mL, yielded absorbances corresponding to concentrations of 1.77μg/mL and 1.93μg/mL, respectively. This attenuation in readings occurred due to enzyme oversaturation from plating at too large a concentration, above that of the greatest value used to establish a standard curve. Silk's encapsulation efficiency was shown to be significantly greater than that of chitosan (Figure 16B). Silk microspheres exhibited significantly greater active lysozyme encapsulation than chitosan microspheres and blank samples ($p<0.05$). (Figure 16C). The trend of increased encapsulation for silk in comparison to chitosan corroborates results from previous trial assays.

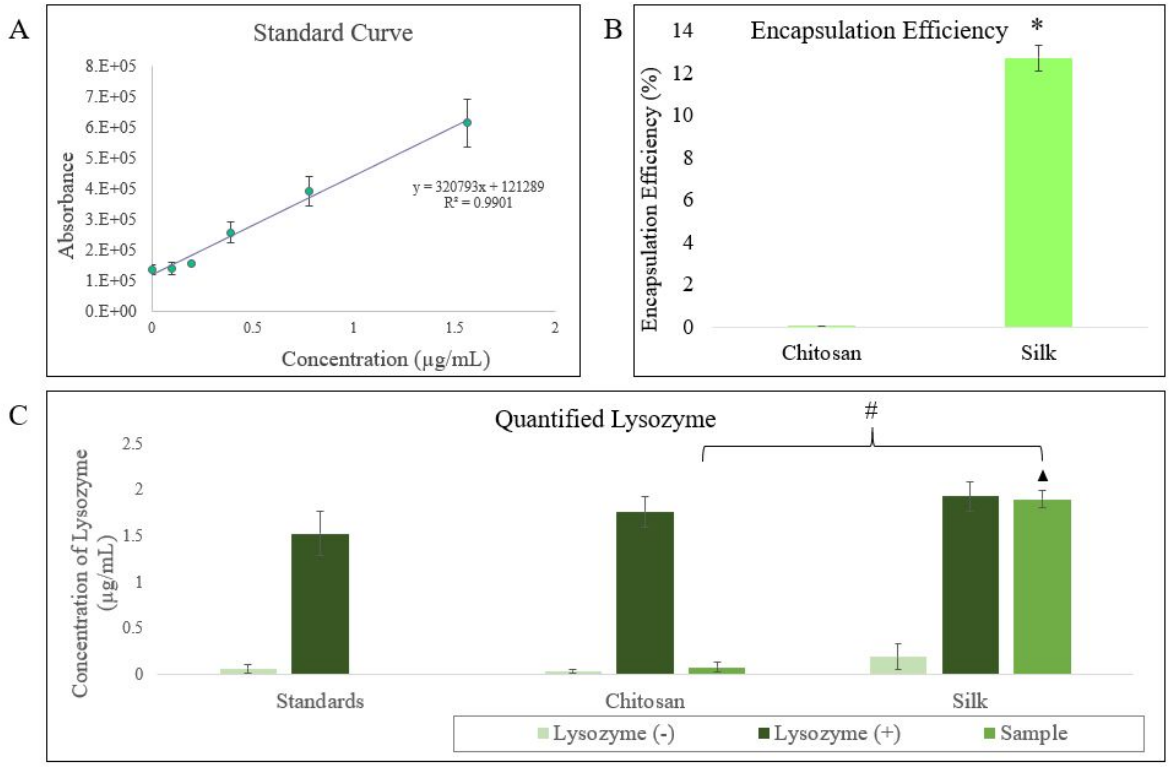

Figure 16: *Lysozyme activity assay for quantifying encapsulation efficiency of chitosan and silk microspheres. Error bars display standard deviation, with n=3. (A) Standard curve graphing the mathematical relationship between measured absorbance and active lysozyme concentration. (B) Calculated encapsulation efficiency of each microsphere material. * denotes statistically significant according to an unpaired t-test assuming unequal variance across chitosan and silk (α=0.05). (C) Mean concentration of active lysozyme calculated for each experimental and control group. Lysozyme (-) groups contain no enzyme with acetic acid solvent, deionized water solvent, and no solvent for chitosan, silk, and standards respectively. Lysozyme (+) group are identical to the lysozyme (-) groups but with lysozyme added at 2.5µg/mL. # denotes statistically significant according to a t-test assuming unequal variance across chitosan and silk (α=0.05). ▲ denotes statistically significant according to a t-test assuming unequal variance across silk and the blank negative control (α=0.05).*

5.3.2 Release Assay

A release assay was performed based on the principle of quantifying the protein present within the supernatant of a solution in which the loaded microspheres are suspended. Similar to the calculation of encapsulation efficiency, the lysozyme released by the microspheres was quantified using the EnzChek™ Lysozyme Assay kit to test supernatant samples of a suspension containing microspheres at various time points. This test was designed to provide insight on two important characteristics of the microsphere degradation behavior. First, the test showed the amount of lysozyme released over an extended duration

of time. Second, because the assay only quantifies the lysozyme that interacts with its substrate, the test confirmed protein activity after sustained release from the microspheres.

To conduct the release assay, a known mass of lysozyme-loaded microspheres was added to complete SMC media. Based on a previously outlined protocol, a small sample of the culture media was immediately extracted from the suspension before use in the assay, as a sample corresponding to time zero (Zeng et al., 2011). To collect subsequent supernatant samples, the solution was centrifuged at 1,500 rpm for 10 minutes before the sample was extracted. The removed supernatant was replaced with fresh media to ensure a consistent suspension volume. Samples were taken at various time points after the initial incorporation of the microspheres, and afterwards immediately stored at -20°C. Between sample collections, the suspension was incubated at 37°C (Appendix M).

First, a release assay was conducted on media-suspended microsphere samples from which samples were collected and frozen at several time points up to 15 days after microsphere incorporation; however, due to a misstep during fabrication, lysozyme was mistakenly added to the silk solution after microsphere formation which is in disagreement with the established protocol which recommends the lysozyme be added to the silk prior to blending with PVA. Because of this the silk microspheres used in the batch were not loaded properly with protein (corroborating raw encapsulation and release data displayed in Appendices K and M respectively). Therefore, it was necessary to repeat the assay with properly loaded microspheres. Due to a time constraint, an abbreviated, 7-day release assay was conducted (Figure 17). A greater quantity of lysozyme was released from the silk microspheres than from the chitosan microspheres, likely due to the fact that the tested silk batch was loaded according to protocol and contained more encapsulated lysozyme to release. The data was displayed as total mass released from the particles. Though this assay only lasted a week in duration, which is shorter than the target duration of release for the microspheres, both chitosan and silk microspheres still seemed to hit a plateau in terms of total lysozyme released. Because the samples were diluted 1:5 prior to reading in the fluorescent plate reader, calculated absorbances did not approach values of oversaturation, eliminating oversaturation as a possible explanation for the plateaus observed. Thus, the plateaus of accumulated release likely occurred due to all of the encapsulated drug releasing from the chitosan early on in suspension. Additionally, chitosan microspheres releasing less active lysozyme than silk, and plateauing at a lower value (~30mg released for chitosan versus ~144mg released for silk), further supports that chitosan had less lysozyme encapsulation and is less capable of releasing active protein.

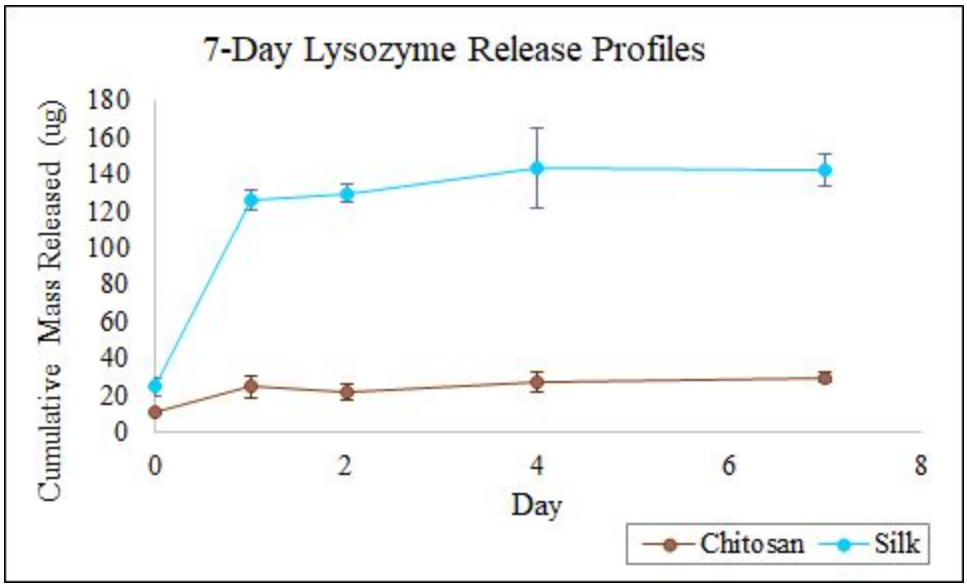

Figure 17: *Total cumulative lysozyme released from 3mg batches of SMC culture media over 1-week. Error bars reflect standard deviations of triplicate samples taken within each timepoint.*

Because the IH blood vessel model application favors microspheres with a sustained release of protein spanning to 10 days after microsphere incorporation, an 11-day experiment was conducted. Two concurrent suspensions for each material were included in the experiment resulting in two experiments with identical setup. Release profiles were obtained according to previously detailed protocols (Figure 18). Both concurrent trials showed similar results, though visual distinction of the profiles for the second trial is obstructed by large error bars demonstrated in the chitosan microsphere suspension. As observed with the 7-day experiment, silk presented a substantial amount of active lysozyme released, plateauing at approximately 60 µg for both suspensions, whereas chitosan showed very little active lysozyme release, plateauing at about 2 µg and 5 µg for suspensions 1 and 2. Again, the plateaus occur early in the time frame at about day 3 which suggests that nearly all of the encapsulated protein is released early in the tested time frame before day 10, which is far sooner than ideal for their intended application.

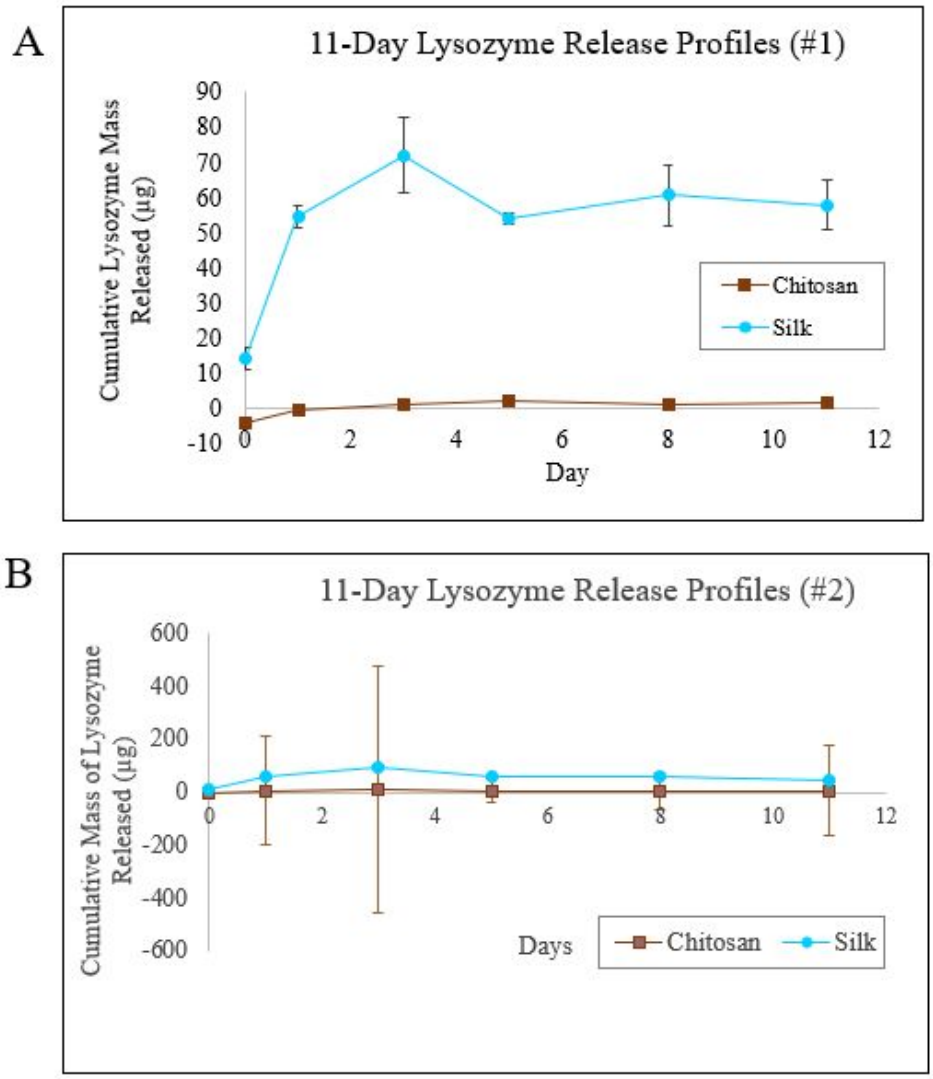

Figure 18: *Total cumulative lysozyme released from 3 mg batches of SMC culture media over 11 days. Error bars reflect standard deviations of triplicate treatments taken within each timepoint. (A) Release profiles from first replicate set of microsphere suspension. (B) Release profiles from second replicate set of microsphere suspension.*

5.2.3 Phase II Conclusions

After completing the methodology of Phase II, chitosan was eliminated, leaving silk as the best candidate material for microspheres with the intended design goal of the client. Chitosan was eliminated principally on the basis of microsphere yield and encapsulation efficiency, as well as review of shortcomings discovered from the results of Phase I and other previously known material characteristics.

Chitosan presented a lower microsphere yield percentage relative to starting fabrication material. As stated in one of the design objectives, for the sake of saving on supplies and reducing the likelihood of having to fabricate microsphere batches more often, it is important that the proposed design has a high yield. Though there was no statistical difference among the yield percentages calculated among the three loaded batches fabricated, this was likely due to the small sample size and the reduced weight of one of the silk batches due to improper loading. This low calculated yield confirmed observations from SEM, for which only a few microspheres where visible on the mount.

In addition to a low yield, chitosan also presented lower encapsulation efficiency of protein. One of the team's design objectives was established to favor microspheres capable of holding large amounts of protein. This is important to the viability of our suggested design because, PDGF-BB, the protein that will eventually be encapsulated into the microspheres for use in the IH model, is very expensive. Using microspheres with a high potential for encapsulating protein is one way to minimize waste of the growth factor. Overall, silk presented a trend of increased encapsulation efficiency compared to chitosan.

Though the release assays presented few conclusive findings regarding which microsphere offered a more sustained release up to ten days in suspension, the findings did provide more insight on retention of protein activity. The release assays performed showed that a substantial amount of active protein is released from the silk microspheres, as opposed to the chitosan microspheres for which this could not be confirmed. Whether the chitosan microspheres presented little lysozyme release due to inactivation of the protein or lack of protein encapsulation, the silk microspheres presented a more promising release profile.

In addition to the results gathered form Phase II, the team reassessed silk and chitosan for findings from Phase I methodology and other known characteristics. Chitosan presented more problems during fabrication than silk. Unlike silk, which did not require the use of an oil phase, chitosan droplets were emulsified in olive oil during particle fabrication. This oil was difficult to remove and required a series of centrifugation, decanting, washing and filtering steps which made the process tedious. In addition, after drying the chitosan particle onto filter paper, the particles appeared to clump together forming macroscopic flaky pieces which were difficult to dissolve. Difficulties that occurred throughout the fabrication process for chitosan microspheres shows that chitosan is less capable of meeting the design objective of easy fabrication.

Ultimately, compared to silk microspheres, chitosan proved less compliant with team design objectives seeking efficient PDGF-BB encapsulation, and simplistic fabrication while maintaining a high yield. For these reasons, silk was chosen as the best candidate for releasing PDGF-BB into tissue rings for an *in vitro* IH blood vessel model.

6. Final Design Validation

Silk microspheres were produced using silk fibroin solution, PVA, and ultrapure water. The material's preparation was completed at room temperature. Before production, a model protein was added

into the fibroin solution and mixed thoroughly. Once prepared, the material can be stored at 4℃ as a microsphere solution before incorporation of the microspheres into the TEBV ring molds to integrate within SMCs of the tissue rings.

6.1 Economics

There is an economic opportunity that exists for the development of a new, effective method to treat IH in the current market. The design and development of a microsphere capable of the sustained release and local delivery of PDGF-BB to fabricated tissue rings could be beneficial for both research and therapeutic purposes. The utilization of an inexpensive *in vitro* IH model can reduce the need for animal testing and have significant economic impact on healthcare costs. The success of designing a PDGF-loaded microsphere capable of producing IH lesions could be used as an *in vitro* model for the testing of therapies in development.

6.2 Environmental Impact

The production and operation of a PDGF-loaded microsphere would have a minimal impact on the environment. By using silk as the biomaterial in our final design, there would be no expected adverse effects to the surrounding environment. Silk is a natural, non-toxic, biodegradable polymer that is FDA approved. Therefore, by using this material in our final design, the microsphere will be considered environmentally friendly and safe for clinical practice.

6.3 Societal Influence

The successful development and production of a controlled-release microsphere could have many benefits in society. As previously mentioned, the purpose of this design is to model human IH initiation and progression for the testing of approved and experimental therapies. Using our model for the testing of IH would also help with the understanding of the physiologic response to vascular tissue injury. Additionally, it could have potential benefits for the aid and treatment of patients who are affected by vascular bypass, angioplasty, and stent failures, and thus could have a positive impact on improving the quality of life in society.

6.4 Political Ramifications

Currently in the United States, there is an ever increasing demand for improved healthcare. Areas such as stem cell research and regenerative medicine have received more attention in the medical field because of the potential benefits and capabilities that they inspire. There is also a growing need to combat cardiovascular disease, since this specific type of illnesses is the leading cause of death in the United States. The success of this model's design and function could have many potential advantages and offer long-term possibilities in medical research.

6.5 Ethical Concerns

There are minimal ethical concerns in regards to the design and function of this system. Similar to other contemporary models, the development of this system uses *in vitro* testing methods. This allows for experimentation to be conducted outside of living organisms and will primarily involve chemical compounds before pursuing animal-based studies. By using a controlled release microsphere to achieve the local delivery to engineered tissue rings, a successful model will be able to mimic the IH lesions which occurs within human vascular tissue. Our approach has limited ethical concerns because animal models are not being used. However, this does not entirely eliminate the incorporation of animal subjects for future testing. Since the controlled-release microsphere will incorporate the natural polymer silk, there will be less ethical concerns regarding the testing procedure.

6.6 Health & Safety Issues

The overall design our controlled-release microsphere system has the potential to treat IH by investigating its initiation and progression. In the future, further studies can be performed to assess PDGF-BB's incorporation into tissue rings. Following FDA regulations, extensive animal and clinical studies will need to be performed using this design. Our model will be tested with potential treatment options to help identify what option is the most suitable. Silk is also a biodegradable material, minimizing concerns of producing adverse by-products.

6.7 Manufacturability

The production of a PDGF controlled-release silk microsphere consists of materials that are easily accessible and a design that is easy to manufacture. Materials such as silk are expensive, available online for approximately $200 for 50mg/mL. However, it can be purchased from many commercially available sources. The fabrication of silk microspheres takes approximately 6 hours. The microparticles can be stored in a 4℃ refrigerator for preservation in a microsphere suspension. Overall, there are minimal manufacturing difficulties for the final design of this sustained-release microparticle.

6.8 Sustainability

The components of the design comply with sustainability criteria by reducing the concern for waste and depletion of available resources. The fabrication of the microparticle does not require excessive materials or resources. Disposal of materials would not harm the environment as reagents such as silk, PVA, and Milli-Q water will be transferred to a chemical waste container once discarded. Silk is a natural polymer which allows for easy availability and renewability of the material.

7. Discussion

Based on the desires of the client, the team was tasked with proposing an efficient way to deliver growth factor from microspheres to a localized position of a TEBV in order to mimic IH for disease modeling. The team therefore focused on determining an appropriate design material for such microspheres, as a starting point for the endeavor. Based on review of literature, the team decided to test four promising materials for their aptitude with regard to meeting established constraints and objectives: gelatin, chitosan, PLGA and silk. After testing and comparing the different microsphere materials, the team concluded silk microspheres showed the most promise for the intended application and therefore recommends this material for further consideration as the client progresses towards the goal of constructing a TEBV model of IH.

Throughout fabrication and testing of the microspheres, silk met the team's design constraints. Because the microspheres are intended to be incorporated within toroids of SMCs, it is necessary that the design materials be capable of being sterilized to allow for proper incorporation without contamination. They also must be biocompatible to allow for the cells to maintain function and morphology needed for vessel integrity. All fabricated microspheres, including silk, were sterilized with ultraviolet radiation. Therefore all tested microspheres equally met this constraint. Once sterilized, the unloaded microspheres were tested for biocompatibility by conducting an MTT assay. Literature suggests all four materials are biocompatible with nearly all mammalian cell types. Silk, like the other three materials, showed significant decrease of smooth muscle cell viability in the assay. That said, the reductions in quantified metabolic activity decrease only slightly for each of the experimental groups, indicating that statistical significance likely arose from low variation among replicates of the same treatment. All materials affected cell viability in a very similar fashion. In all, the slight reduction in quantified cells in silk was not deemed drastic enough to consider the material incompatible with the SMCs.

The microsphere-based mechanism for achieving the desired lesion formation is contingent on the stimulation of cell proliferation from the release of growth factor. Because it is ultimately necessary to induce cell proliferation within the IH model, it is necessary that lysozyme, the enzyme used to model PDGF-BB, is active once released from the spheres. The release assay was conducted not only to assess the release profile of the fabricated particles but also to ensure that the loaded lysozyme remains active once released. Silk did show positive enzyme-substrate absorbance quantities relative to blanks, suggesting at least a proportion of the lysozyme that was encapsulated and released was shown to be active. Though the activity assay performed does prove some activity among the released protein, it cannot be determined for sure whether any observed lack of expected active lysozyme in the microsphere suspensions occurred as a result of inhibition of enzyme activity or release. Also, though active lysozyme was confirmed in the release suspension for the silk microspheres, it cannot be entirely confirmed that the same trends would be seen with loaded PDGF-BB, though there is no reason to believe, based on the literature review, that post-release activity would differ much depending on the protein used.

In addition to adhering to established design constraints, silk met the design objectives better than the other tested microsphere materials. One design objective was a consistent and uniform particle size distribution. To better understand physical properties, such as particle size of the fabricated microspheres,

the microspheres were imaged with SEM. The SEM images showed a very consistent diameter distribution, in relation to other materials with far greater observed size ranges. SEM also confirmed a consistent spherical morphology for the silk microspheres. It should be noted that the fabricated microspheres were smaller than he target size range determined by the team. Though their small size may reduce the amount of PDGF-BB they are capable of carrying, they are still far bigger than 24.9kDa PDGF-BB, which has a diameter on the order of nanometers. Therefore, silk being slightly beneath the target size range is not expected to hinder its function assuming it is still is able to achieve drug encapsulation.

Ideally, the microspheres can be fabricated with a high overall yield and high proportion of encapsulated drug. Silk showed a higher percent yield of loaded microsphere, relative to starting material, in contrast to chitosan, the other material still being considered in the protein-loading stages of experimentation. Of the fabrication yield measurements for silk microspheres, one showed a percent yield greater than the mass of the sphere components used during fabrication. Because this is not possible even under ideal conditions, it can be assumed that this peculiarity arose due to error, perhaps from weighing the microspheres before all of the liquid they were suspended in was dried off. An erroneous inflation of fabrication yield was also seen in one chitosan batch, and after removing these outliers, silk still showed higher encapsulation. The data therefore supports that silk provided better yield as there is no reason to believe silk was weighed less accurately than was chitosan. Analyzing results from the encapsulation assay, all materials showed low encapsulation efficiency of lysozyme of less than 13%. This is likely due to incomplete dissolving of the microspheres during preparatory stages of the assay, as they broke apart but remained visible in solution throughout the dissolving steps. This most likely occurred because the team sought out fabrication protocols yielding microspheres with minimal burst release of drug, which typically implies that they are resistant to quick degradation. Even though there was high likelihood of incomplete dissolution, encapsulation of active enzyme was confirmed through a statistically significant increase in active lysozyme in the silk samples compared to the blank negative control. Though not statistically significant, silk showed more lysozyme encapsulation than chitosan. All lysozyme-concentration data for silk were greater than those of chitosan, so absence of statistical significance likely came from the silk's high data variance.

Controlled release of growth factor from the microspheres was another important design objective which the team tested by conducting a lysozyme release assay. Minimal burst release and maximal release after ten days were the most important release-profile benchmarks, and were thus considered when comparing microsphere materials, Results of the 15-day assay showed increased active enzyme release from chitosan microspheres in comparison to silk, though these results were likely skewed due to unforeseen, improper loading of the tested silk batch as previously discussed. When the release assay was repeated, with properly loaded silk microspheres over a shorter time frame due to time restriction, an increase in total released lysozyme from silk was observed. These results are likely more indicative of the microspheres' ability to release a loaded protein like PDGF-BB, because greater active protein release from silk was seen in two successive 11-day release trials as well. Silk and chitosan microspheres presented a cumulative protein release plateau by as early as days 2 or 3 in the 7-day trial as well as in both 11-day trials. Because both microsphere types exhibited an early burst release of protein, it was difficult to compare the two microsphere types on the basis of a release profile.

To assure that the team's proposed design is realistic, cost of materials and associated equipment was also considered when comparing the different microspheres. Fabricating silk microspheres posed little, if any, cost concern because it was supplied directly from another lab. This associated lab, which produces silk and therefore has a steady supply, works closely with the lab of the client and may be a continued source for materials for future model development. In the event that this lab does not provide the materials, necessary for fabrication, silk-fibroin solution is available for online purchase at approximately $200 for 50mg/mL, making it one of the more expensive microsphere materials alongside PLGA. Consistency in results however, could reduce the amount of batches fabricated long-term, potentially offsetting the expense. The fabrication does not require any equipment that is not already available to the client.

Constraints and objectives related to microsphere interaction with the SMC toroids were not able to be tested due to limited time. Therefore, it is still important to perform tests to ensure that the silk microspheres can be incorporated within the toroids such that they remain long enough for growth factor release. They should also not disrupt the mechanical integrity or fusibility of the toroid, and growth factor release should stimulate cell proliferation in the toroid.

8. Conclusions and Recommendations

The main objective of this project was to design a microsphere capable of sustained release and local delivery of PDGF-BB into tissue rings composed of murine SMCs to mimic the initiation and progression of IH lesions within vascular tissue. After conducting extensive research and testing with various biomaterials which possessed unique properties, silk was chosen for the final design because it had demonstrated the most conclusive results and was determined to be the most suitable material for fulfilling the goal of the project. Silk microspheres were successfully produced within a consistent range that fulfilled the size range stated in the objectives. The high resolution SEM images of the biomaterial demonstrated that silk is capable of producing uniform microspheres. This can be achieved using a microfluidics device to alter the microparticle size to a desired range (Montoya, 2018)

Silk demonstrated the capability to encapsulate chicken lysozyme, a test protein to PDGF-BB, and release it in its active form. Additionally, silk's fabrication process was the least time consuming and resulted in the fewest difficulties when compared to the other tested materials. The integration of silk microspheres into tissue rings was not completed due to time constraints, but the material is biocompatible and should not adversely affect cells..

Future testing for this project should include mechanical strength testing of the toroids with the incorporated silk microspheres and the final TEBV with the lesion. Mechanical testing could be completed through the use of an Instron machine, which would determine whether the addition of the silk microspheres within the system significantly affects the mechanical strength when compared to the control.

In addition, histological testing should also be conducted on the toroids incorporated with the silk microspheres. Histological testing will evaluate the effects that the microspheres will have within the toroid, and whether the microspheres will cause any adverse effects in maintaining the toroid and TEBV. Histology will also allow for measuring the effect that the growth factor will have on the TEBV after release.

The release profile assay should also be performed again with PDGF-BB instead of the lysozyme used within this testing. The lysozyme was used as a model for the PDGF-BB at a cheaper cost. However, it is still unknown as to whether the release profile will vary with the loading of the growth factor.

Further research into potential adaptations to the fabrication design of the silk microspheres should also be considered. Specifically, changes to the protocol which will allow for a greater encapsulation efficiency and further delayed release of the growth factor should be reviewed and studied. While silk offered the best encapsulation and release profiles out of the different tested design materials, optimizing these parameters would improve silk's promise for use within the IH model.

References

Alagusundaram, M., Madhu Sudana Chetty, C., Umashankari, K., Badarinath, A. V., Lavanya, C., & Ramkanth, S. (2009). Microspheres as a novel drug delivery system - A review. *International Journal of ChemTech Research, 1*(3), 526-534

Anderson, J. M., & Shive, M. S. (1997). *Biodegradation and biocompatibility of PLA and PLGA microspheres* doi://doi.org/10.1016/S0169-409X(97)00048-3

Benjakul, S., & Kittiphattanabawon, P. (2018). *Gelatin* Elsevier. doi://doi.org/10.1016/B978-0-08-100596-5.21588-6

Berkland, C., Kipper, M. J., Narasimhan, B., Kim, K., & Pack, D. W. (2004). *Microsphere size, precipitation kinetics and drug distribution control drug release from biodegradable polyanhydride microspheres* doi://doi.org/10.1016/j.jconrel.2003.09.011

Blausen.com staff (2014). "Medical gallery of Blausen Medical 2014". *Wiki Journal of Medicine* 1 (2). doi:10.15347/wjm/2014.010. ISSN 2002-4436

Bravo-Osuna, I., Andrés-Guerrero, V., Arranz-Romera, A., Esteban-Pérez, S., Molina-Martínez, I. T., & Herrero-Vanrell, R. (2018). *Microspheres as intraocular therapeutic tools in chronic diseases of the optic nerve and retina* doi://doi.org/10.1016/j.addr.2018.01.007

Carpenter, D. P. (2002). Groups, the Media, Agency Waiting Costs, and FDA Drug Approval. *American Journal of Political Science,46*(3), 490-505. doi:10.2307/3088394

Cizek, S. M., Bedri, S., Talusan, P., Silva, N., Lee, H., & Stone, J. R. (2007). Risk factors for atherosclerosis and the development of preatherosclerotic intimal hyperplasia. *Cardiovascular Pathology,16*(6), 344-350. doi:10.1016/j.carpath.2007.05.007

Conzone, S. D., & Day, D. E. (2009). Preparation and properties of porous microspheres made from borate glass. *Journal of Biomedical Materials Research Part A: An Official Journal of the Society for Biomaterials, the Japanese Society for Biomaterials, and the Australian Society for Biomaterials and the Korean Society for Biomaterials, 88*(2), 531-542.

Collins, M. J., Li, X., Lv, W., Yang, C., Protack, C. D., Muto, A., . . . Dardik, A. (2012). Therapeutic strategies to combat neointimal hyperplasia in vascular grafts. *Expert Review of Cardiovascular Therapy,10*(5), 635-647. doi:10.1586/erc.12.33

Cortesi, R., Esposito, E., Osti, M., Menegatti, E., Squarzoni, G., Davis, S. S., & Nastruzzi, C. (1999). Dextran cross-linked gelatin microspheres as a drug delivery system. *European journal of pharmaceutics and biopharmaceutics*, *47*(2), 153-160.

Cortesi, R., Nastruzzi, C., & Davis, S. S. (1998). Sugar cross-linked gelatin for controlled release: Microspheres and disks. *Biomaterials, 19*(18), 1641-1649.

Dahl, S.L., Kypson, A.P., Lawson, J.H., Blum, J.L., Strader, J.T., Li, Y., Manson, R.J., Tente, W.E., DiBernardo, L., Hensley, M.T., Carter, R., Williams, T.P., Prichard, H.L., Dey, M.S., Begelman, K.G. and Niklason, L.E. (2011) Readily available tissue-engineered vascular grafts. *Sci Transl Med 3* (1), 68-69.

Danhier, F., Ansorena, E., Silva, J. M., Coco, R., Breton, A. L., & Préat, V. (2012). PLGA-based nanoparticles: An overview of biomedical applications. *Journal of Controlled Release,161*(2), 505-522. doi:10.1016/j.jconrel.2012.01.043

Dastidar, D.G., Saha, S., & Chowdhury, M. (2018). *Porous microspheres: Synthesis, characterisation and applications in pharmaceutical & medical fields* doi://doi.org/10.1016/j.ijpharm.2018.06.015

Day, D. E., & Ehrhardt, G. J. (1988). Glass microspheres. *Glass Microspheres,*

Del Gaudio, C., Crognale, V., Serino, G., Galloni, P., Audenino, A., Ribatti, D., & Morbiducci, U. (2017). *Natural polymeric microspheres for modulated drug delivery* doi://doi.org/10.1016/j.msec.2017.02.051

Delgado-Rivera, R., Rosario-Meléndez, R., Yu, W., & Uhrich, K. E. (2014). Biodegradable salicylate-based poly(anhydride-ester) microspheres for controlled insulin delivery. *Journal of Biomedical Materials Research. Part A, 102*(8), 2736-2742. doi:10.1002/jbm.a.34949

Deshmukh, S. S., & Sangawar, V. S. (2016). One-step synthesis of polyethylene microspheres using a modified chemical route for pulmonary drug delivery. *Journal of Taibah University for Science, 10*(4), 485-489.

Determan, A. S., Trewyn, B. G., Lin, V. S. -., Nilsen-Hamilton, M., & Narasimhan, B. (2004). *Encapsulation, stabilization, and release of BSA-FITC from polyanhydride microspheres* doi://doi.org/10.1016/j.jconrel.2004.08.006

Di Martino, A., Sittinger, M., & Risbud, M. V. (2005). *Chitosan: A versatile biopolymer for orthopaedic tissue-engineering* doi://doi.org/10.1016/j.biomaterials.2005.03.016

Fratzl, P. (2003). *Cellulose and collagen: From fibres to tissues* doi://doi.org/10.1016/S1359-0294(03)00011-6

Fredenberg, S., Wahlgren, M., Reslow, M., & Axelsson, A. (2011). *The mechanisms of drug release in poly(lactic-co-glycolic acid)-based drug delivery systems—A review* doi://doi.org/10.1016/j.ijpharm.2011.05.049

Fuchs, K., Duran, R., Denys, A., Bize, P. E., Borchard, G., & Jordan, O. (2017). *Drug-eluting embolic microspheres for local drug delivery – state of the art* doi://doi.org/10.1016/j.jconrel.2017.07.016

Galante, V., Corsi, C., Veronesi, F., Russo, V., Fattori, R., & Lamberti, C. (2007). Dynamic characterization of aorta morphology and function in presence of an aneurysm. *2007 Computers in Cardiology*. doi:10.1109/cic.2007.4745598

Geczy, R., Agnoletti, M., Hansen, M. F., Kutter, J. P., Saatchi, K., & Häfeli, U. O. (2018). *Microfluidic approaches for the production of monodisperse, superparamagnetic microspheres in the low micrometer size range* doi://doi.org/10.1016/j.jmmm.2018.09.091

Ghadi, R., Muntimadugu, E., Domb, A. J., Khan, W., & Zhang, X. (2017). In Zhang X. (Ed.), *5 - synthetic biodegradable medical polymer: Polyanhydrides* Woodhead Publishing. doi://doi.org/10.1016/B978-0-08-100372-5.00005-2

Glagov, S. (1994). Intimal hyperplasia, vascular modeling, and the restenosis problem. *Circulation,89*(6), 2888-2891. doi:10.1161/01.cir.89.6.2888

Göpferich, A. (1996). Mechanisms of polymer degradation and erosion. *Biomaterials, 17*(2), 103-114.

Göpferich, A., & Langer, R. (1993). The influence of microstructure and monomer properties on the erosion mechanism of a class of polyanhydrides. *Journal of Polymer Science Part A: Polymer Chemistry, 31*(10), 2445-2458.

Grainger, D. J., Metcalfe, J. C., Grace, A. A., Mosedale, D. E. (1998). Transforming growth factor-beta dynamically regulates vascular smooth muscle differentiation in vivo. Journal of Cell Science, 111(19), 2977-2988

Guggi, D., Krauland, A. H., & Bernkop-Schnürch, A. (2003). *Systemic peptide delivery via the stomach: In vivo evaluation of an oral dosage form for salmon calcitonin* doi://doi.org/10.1016/S0168-3659(03)00299-2

Guo, S., Yao, T., Wang, C., Zeng, C., & Zhang, L. (2015). *Preparation of monodispersed porous polyacrylamide microspheres via phase separation in microchannels* doi://doi.org/10.1016/j.reactfunctpolym.2015.04.006

Guo, X., Chen, S. (2012). Transforming growth factor-β and smooth muscle differentiation. *World Journal of Biological Chemistry, 3*(3), 41. doi:10.4331/wjbc.v3.i3.41

Han, F. Y., Thurecht, K. J., Whittaker, A. K., & Smith, M. T. (2016). Bioerodable PLGA-Based Microparticles for Producing Sustained-Release Drug Formulations and Strategies for Improving Drug Loading. *Frontiers in Pharmacology*. doi:10.3389/fphar.2016.00185

Hao, T., Wen, N., Cao, J., Wang, H., Lü, S., Liu, T., . . . Wang, C. (2010). The support of matrix accumulation and the promotion of sheep articular cartilage defects repair in vivo by chitosan hydrogels. *Osteoarthritis and Cartilage, 18*(2), 257-265.

Hashida, M., Takahashi, Y., Muranishi, S., & Sezaki, H. (1977). An application of water-in-oil and gelatin-microsphere-in-oil emulsions to specific delivery of anticancer agent into stomach lymphatics. *Journal of pharmacokinetics and biopharmaceutics*, *5*(3), 241-255.

He, M., Wang, H., Dou, W., Chou, G., Wei, X., & Wang, Z. (2016). *Preparation and drug release properties of norisoboldine-loaded chitosan microspheres* doi://doi.org/10.1016/j.ijbiomac.2016.06.076

He, Z., & Xiong, L. (2011). Drug Controlled Release and Biological Behavior of Poly(D,L-Lactide-Co-Glycolide) Microspheres. *Journal of Macromolecular Science, Part B,50*(6), 1154-1161. doi:10.1080/00222348.2010.503106

Heldin, C., & Westermark, B. (1999). Mechanism of Action and In Vivo Role of Platelet-Derived Growth Factor. *Physiological Reviews, 79*(4), 1283-1316. doi:10.1152/physrev.1999.79.4.1283

Hibino, N., McGillicuddy, E., Matsumura, G., Ichihara, Y., Naito, Y., Breuer, C., and Shinoka, T. (2010). Late-term results of tissue-engineered vascular grafts in humans. *J Thorac Cardiovasc Surg 139*(2), 431-436.

Hossain, K. M. Z., Patel, U., & Ahmed, I. (2015). Development of microspheres for biomedical applications: A review. *Progress in Biomaterials, 4*(1), 1-19.

Hu, X., Kaplan, D., & Cebe, P. (2006). Determining beta-sheet crystallinity in fibrous proteins by thermal analysis and infrared spectroscopy. *Macromolecules*, *39*(18), 6161-6170.

Huang, X., & Brazel, C. (2001). On the importance and mechanisms of burst release in matrix-controlled drug delivery systems. *Journal Of Controlled Release*, *73*(2-3), 121-136. doi: 10.1016/s0168-3659(01)00248-6

Huang, B., Dreyer, T., Heidt, M., Yu, J. C., Philipp, M., Hehrlein, F. W., Al-Fakhri, N. (2002). Insulin and local growth factor PDGF induce intimal hyperplasia in bypass graft culture models of saphenous vein and internal mammary artery. *European Journal of Cardio-Thoracic Surgery, 21*(6), 1002-1008. doi:10.1016/s1010-7940(02)00111-2

Hui, D. (2008). Intimal Hyperplasia in Murine Models. *Current Drug Targets,9*(3), 251-260. doi:10.2174/138945008783755601

Hudson, S. M., & Jenkins, D. W. (2002). Chitin and chitosan. *Encyclopedia of Polymer Science and Technology, 1*

Iwanaga, K., Yabuta, T., Kakemi, M., Morimoto, K., Tabata, Y., & Ikada, Y. (2003). Usefulness of microspheres composed of gelatin with various cross-linking density. *Journal of Microencapsulation, 20*(6), 767-776.

Jain, J. P., Modi, S., Domb, A. J., & Kumar, N. (2005). *Role of polyanhydrides as localized drug carriers* doi://doi.org/10.1016/j.jconrel.2004.12.021

Karnchanajindanun, J., Srisa-ard, M., & Baimark, Y. (2011). *Genipin-cross-linked chitosan microspheres prepared by a water-in-oil emulsion solvent diffusion method for protein delivery* doi://doi.org/10.1016/j.carbpol.2011.03.035

Kawadkar, J., & Chauhan, M. K. (2012). Intra-articular delivery of genipin cross-linked chitosan microspheres of flurbiprofen: Preparation, characterization, in vitro and in vivo studies. *European Journal of Pharmaceutics and Biopharmaceutics, 81*(3), 563-572.

Kawashita, M. (2005). Ceramic microspheres for biomedical applications. *International Journal of Applied Ceramic Technology, 2*(3), 173-183.

Khoshroo, K., Jafarzadeh Kashi, T. S., Moztarzadeh, F., Tahriri, M., Jazayeri, H. E., & Tayebi, L. (2017). *Development of 3D PCL microsphere/TiO2 nanotube composite scaffolds for bone tissue engineering* doi://doi.org/10.1016/j.msec.2016.08.081

Kim, I., Seo, S., Moon, H., Yoo, M., Park, I., Kim, B., & Cho, C. (2008). *Chitosan and its derivatives for tissue engineering applications* doi://doi.org/10.1016/j.biotechadv.2007.07.009

Kim, M. J., Kim, J., Yi, G., Lim, S., Hong, Y. S., & Chung, D. J. (2008). In vitro and in vivo application of PLGA nanofiber for artificial blood vessel. *Macromolecular Research,16*(4), 345-352. doi:10.1007/bf03218527

Koda, Sho, et al. "Development of Poly Lactic/Glycolic Acid (PLGA) Microspheres for Controlled Release of Rho-Associated Kinase Inhibitor." *Journal of Ophthalmology*, vol. 2017, 2017, pp. 1–9., doi:10.1155/2017/1598218.

Kumar, N., Langer, R. S., & Domb, A. J. (2002). *Polyanhydrides: An overview* doi://doi.org/10.1016/S0169-409X(02)00050-9

Lammel, A. S., Hu, X., Park, S. H., Kaplan, D. L., & Scheibel, T. R. (2010). Controlling silk fibroin particle features for drug delivery. *Biomaterials*, *31*(16), 4583-4591.

Li, L., Wang, Q., Li, H., Yuan, M., & Yuan, M. (2014). Preparation, Characterization, In Vitro Release and Degradation of Cathelicidin-BF-30-PLGA Microspheres. *PLoS ONE, 9*(6). doi:10.1371/journal.pone.0100809

Lin, K., Zhou, Y., Zhou, Y., Qu, H., Chen, F., Zhu, Y., & Chang, J. (2011). Biomimetic hydroxyapatite porous microspheres with co-substituted essential trace elements: Surfactant-free hydrothermal synthesis, enhanced degradation and drug release. *Journal of Materials Chemistry, 21*(41), 16558-16565.

Lochhead, J. J., & Thorne, R. G. (2012). Intranasal delivery of biologics to the central nervous system. *Advanced Drug Delivery Reviews, 64*(7), 614-628. doi:10.1016/j.addr.2011.11.002

Long, T., Guo, Y., Liu, Y., & Zhu, Z. (2013). Hierarchically nanostructured mesoporous carbonated hydroxyapatite microspheres for drug delivery systems with high drug-loading capacity. *RSC Advances, 3*(46), 24169-24176.

Lorenzo-Lamosa, M. L., Remunan-Lopez, C., Vila-Jato, J. L., & Alonso, M. J. (1998). Design of microencapsulated chitosan microspheres for colonic drug delivery. *Journal of Controlled Release*, *52*(1-2), 109-118.

Ma, Z., Guan, Y., Liu, H., & Liu, H. (2005). Preparation and surface modification of non-porous micron-sized magnetic poly (methyl acrylate) microspheres. *J.Polym.Sci.A, Polym.Chem, 43*, 3433-3439.

Makadia, H. K., & Siegel, S. J. (2011). Poly Lactic-co-Glycolic Acid (PLGA) as Biodegradable Controlled Drug Delivery Carrier. *Polymers,3*(3), 1377-1397. doi:10.3390/polym3031377

McCall, R. L., & Sirianni, R. W. (2013). PLGA nanoparticles formed by single-or double-emulsion with vitamin E-TPGS. *Journal of Visualized Experiments: JoVE,* (82)

Moran, E., Larkin, A., Doherty, G., Kelehan, P., Kennedy, S., & Clynes, M. (1997). A new mdr-1 encoded P-170 specific monoclonal antibody: (6/1 C) on paraffin wax embedded tissue without pretreatment of sections. *J Clin Pathol, 50,* 465–471. https://doi.org/10.1136/jcp.50.6.465

Mondal, M. (2007). The silk proteins, sericin and fibroin in silkworm, Bombyx mori Linn.,-a review. *Caspian Journal of Environmental Sciences*, *5*(2), 63-76.

Montaya N.V., (2018). *Novel silk micro-particle fabrication technique for cancer therapy*. Retrieved from WPI.

Mylonaki, I., Strano, F., Deglise, S., Allémann, E., Alonso, F., Corpataux, J., . . . Delie, F. (2016). Perivascular sustained release of atorvastatin from a hydrogel-microparticle delivery system decreases intimal hyperplasia. *Journal of Controlled Release,232*, 93-102. doi:10.1016/j.jconrel.2016.04.023

Nafissi Varcheh, N., Luginbuehl, V., Aboofazeli, R., & Peter Merkle, H. (2011). Preparing Poly (Lactic-co-Glycolic Acid) (PLGA) Microspheres Containing Lysozyme-Zinc Precipitate Using a Modified Double Emulsion Method. *Iranian journal of pharmaceutical research : IJPR*, *10*(2), 203-9

Nguyen, A. H., McKinney, J., Miller, T., Bongiorno, T., & McDevitt, T. C. (2015). *Gelatin methacrylate microspheres for controlled growth factor release* doi://doi.org/10.1016/j.actbio.2014.11.028

Olsen, D., Yang, C., Bodo, M., Chang, R., Leigh, S., Baez, J., . . . Polarek, J. (2003). *Recombinant collagen and gelatin for drug delivery* doi://doi.org/10.1016/j.addr.2003.08.008

Perrella, M. A., Jain, M. K., Lee, M. (1998). Role of TGF-β in Vascular Development and Vascular Reactivity. *Mineral and Electrolyte Metabolism, 24*(2-3), 136-143. doi:10.1159/000057361

Poursamar, S. A., Lehner, A. N., Azami, M., Ebrahimi-Barough, S., Samadikuchaksaraei, A., & Antunes, A. P. M. (2016). *The effects of crosslinkers on physical, mechanical, and cytotoxic properties of gelatin sponge prepared via in-situ gas foaming method as a tissue engineering scaffold* doi://doi.org/10.1016/j.msec.2016.02.034

Qi, C., Zhu, Y., Lu, B., Zhao, X., Zhao, J., & Chen, F. (2012). Hydroxyapatite nanosheet-assembled porous hollow microspheres: DNA-templated hydrothermal synthesis, drug delivery and protein adsorption. *Journal of Materials Chemistry, 22*(42), 22642-22650.

Qi, Y., Shen, J., Jiang, Q., Jin, B., Chen, J., & Zhang, X. (2015). *The morphology control of hydroxyapatite microsphere at high pH values by hydrothermal method* doi://doi.org/10.1016/j.apt.2015.04.008

Rahaman, M. N., Day, D. E., Bal, B. S., Fu, Q., Jung, S. B., Bonewald, L. F., & Tomsia, A. P. (2011). Bioactive glass in tissue engineering. *Acta Biomaterialia, 7*(6), 2355-2373.

Ratanavaraporn, J., Rangkupan, R., Jeeratawatchai, H., Kanokpanont, S., & Damrongsakkul, S. (2010). *Influences of physical and chemical crosslinking techniques on electrospun type A and B gelatin fiber mats* doi://doi.org/10.1016/j.ijbiomac.2010.06.008

Rinaudo, M. (2006). *Chitin and chitosan: Properties and applications* doi://doi.org/10.1016/j.progpolymsci.2006.06.001

Saddler, J. M., & Horsey, P. J. (1987). The new generation gelatins: A review of their history, manufacture and properties. *Anaesthesia, 42*(9), 998-1004.

Saralidze, K., Koole, L. H., & Knetsch, M. L. (2010). Polymeric microspheres for medical applications. *Materials*, *3*(6), 3537-3564.

Srihanam, P., Srisuwan, Y., Imsombut, T., & Baimark, Y. (2011). Silk fibroin microspheres prepared by the water-in-oil emulsion solvent diffusion method for protein delivery. *Korean Journal of Chemical Engineering*, *28*(1), 293-297.

Silva, D., Arancibia, R., Tapia, C., Acuña‐Rougier, C., Diaz‐Dosque, M., Cáceres, M., . . . Smith, P. C. (2013). Chitosan and platelet‐derived growth factor synergistically stimulate cell proliferation in gingival fibroblasts. *Journal of Periodontal Research, 48*(6), 677-686.

Sinha, V. R., & Trehan, A. (2003). *Biodegradable microspheres for protein delivery* doi://doi.org/10.1016/S0168-3659(03)00194-9

Strobel, H. A., Dikina, A. D., Levi, K., Solorio, L. D., Alsberg, E., & Rolle, M. W. (2017). Cellular Self-Assembly with Microsphere Incorporation for Growth Factor Delivery Within Engineered Vascular Tissue Rings. *Tissue Engineering Part A, 23*(3-4), 143-155. doi:10.1089/ten.tea.2016.0260

Strobel, H. A., Hookway, T. A., Piola, M., Fiore, G. B., Soncini, M., Alsberg, E., & Rolle, M. W. (2018). Assembly of Tissue-Engineered Blood Vessels with Spatially Controlled Heterogeneities. *Tissue Engineering Part A, 24*(19-20), 1492-1503. doi:10.1089/ten.tea.2017.0492

Szcześ, A., Hołysz, L., & Chibowski, E. (2017). *Synthesis of hydroxyapatite for biomedical applications* doi://doi.org/10.1016/j.cis.2017.04.007

Tabata, Y., Ikada, Y., Morimoto, K., Katsumata, H., Yabuta, T., Iwanaga, K., & Kakemi, M. (1999). Surfactant-free preparation of biodegradable hydrogel microspheres for protein release. *Journal of Bioactive and Compatible Polymers, 14*(5), 371-384.

Uhrich, K. E., Cannizzaro, S. M., Langer, R. S., & Shakesheff, K. M. (1999). Polymeric systems for controlled drug release. *Chemical Reviews, 99*(11), 3181-3198.

Upputuri, P. K., & Pramanik, M. (2017). *Microsphere-aided optical microscopy and its applications for super-resolution imaging* doi://doi.org/10.1016/j.optcom.2017.05.049

Venuti, J. M., Pepicelli, C., & Flowers, V. L. (2004). Analysis of Sea Urchin Embryo Gene Expression by Immunocytochemistry. Methods in Cell Biology, 74, 333–369. https://doi.org/10.1016/S0091-679X(04)74015-7

Wang, R., Zhang, Y., Guanghui, M., & Su, Z. (2006). Preparation of uniform poly(glycidyl methacrylate) porous microspheres by membrane emulsification-polymerization technology. *Journal of Applied Polymer Science, 102*(5), 5018-5027. doi:10.1002/app.25015

Wang, X., Wenk, E., Matsumoto, A., Meinel, L., Li, C., & Kaplan, D. L. (2007). Silk microspheres for encapsulation and controlled release. *Journal of Controlled Release*, *117*(3), 360-370.

Wang, X., Yucel, T., Lu, Q., Hu, X., & Kaplan, D. L. (2010). Silk nanospheres and microspheres from silk/pva blend films for drug delivery. *Biomaterials*, *31*(6), 1025-1035.

Wang, Y., Zhang, W., Yuan, J., & Shen, J. (2016 a). *Differences in cytocompatibility between collagen, gelatin and keratin* doi://doi.org/10.1016/j.msec.2015.09.093

Wang, Y., Zhao, Y., Sun, C., Hu, W., Zhao, J., Li, G., . . . Ding, F. (2016 b). Chitosan degradation products promote nerve regeneration by stimulating schwann cell proliferation via miR-27a/FOXO1 axis. *Molecular Neurobiology, 53*(1), 28-39.

Wen, X., Peng, X., Fu, H., Dong, Y., Han, K., Su, J., ... & Wu, C. (2011). Preparation and in vitro evaluation of silk fibroin microspheres produced by a novel ultra-fine particle processing system. *International journal of pharmaceutics*, *416*(1), 195-201.

Wenk, E., Meinel, A. J., Wildy, S., Merkle, H. P., & Meinel, L. (2009). Microporous silk fibroin scaffolds embedding PLGA microparticles for controlled growth factor delivery in tissue engineering. *Biomaterials*, *30*(13), 2571-2581.

What is the cost of genetic testing, and how long does it take to get the results? - Genetics Home Reference - NIH. (n.d.). Retrieved from https://ghr.nlm.nih.gov/primer/testing/costresults

Xiao, W., Bal, B. S., & Rahaman, M. N. (2016). Preparation of resorbable carbonate-substituted hollow hydroxyapatite microspheres and their evaluation in osseous defects in vivo. *Materials Science and Engineering: C, 60*, 324-332.

Yamamoto, M., Ikada, Y., & Tabata, Y. (2001). Controlled release of growth factors based on biodegradation of gelatin hydrogel. *Journal of Biomaterials Science, Polymer Edition, 12*(1), 77-88.

Yang, Y. Y., Chung, T. S., Bai, X. L., & Chan, W. K. (2000). Effect of preparation conditions on morphology and release profiles of biodegradable polymeric microspheres containing protein fabricated by double-emulsion method. *Chemical Engineering Science*, *55*(12), 2223-2236.

Yang, G., Xiao, Z., Long, H., Ma, K., Zhang, J., Ren, X., & Zhang, J. (2018). Assessment of the characteristics and biocompatibility of gelatin sponge scaffolds prepared by various crosslinking methods. *Scientific Reports, 8*(1), 1616.

Yau, J. W., Teoh, H., & Verma, S. (2015). Endothelial cell control of thrombosis. *BMC Cardiovascular Disorders,15*(1). doi:10.1186/s12872-015-0124-z

Young, S., Wong, M., Tabata, Y., & Mikos, A. G. (2005). Gelatin as a delivery vehicle for the controlled release of bioactive molecules. *Journal of Controlled Release, 109*(1-3), 256-274.

Yuan, W., Hong, X., Chen, Y., Ma, L., Liu, Z., & Wei, L. L. (2013). Novel preparation method for sustained-release PLGA microspheres using water-in-oil-in-hydrophilic-oil-in-water emulsion. *International Journal of Nanomedicine,*2433. doi:10.2147/ijn.s45186

Zeng, W., Huang, J., Hu, X., Xiao, W., Rong, M., Yuan, Z., & Luo, Z. (2011). *Ionically cross-linked chitosan microspheres for controlled release of bioactive nerve growth factor* doi://doi.org/10.1016/j.ijpharm.2011.10.005

Zhai, L., Bai, Z., Zhu, Y., Wang, B., & Luo, W. (2018). *Fabrication of chitosan microspheres for efficient adsorption of methyl orange* doi://doi.org/10.1016/j.cjche.2017.08.015

Zhang, H., Yang, Z., Wang, J., Wang, X., Zhao, Y., & Zhu, F. (2018). Wall shear stress promotes intimal hyperplasia through the paracrine H2O2-mediated NOX-AKT-SVV axis. *Life Sciences,207*, 61-71. doi:10.1016/j.lfs.2018.05.045

Zhou, X., Kong, M., Cheng, X. J., Feng, C., Li, J., Li, J. J., & Chen, X. G. (2014). *In vitro and in vivo evaluation of chitosan microspheres with different deacetylation degree as potential embolic agent* doi://doi.org/10.1016/j.carbpol.2014.06.080

Zhao, Y., Biswas, S. K., Mcnulty, P. H., Kozak, M., Jun, J. Y., & Segar, L. (2011). PDGF-induced vascular smooth muscle cell proliferation is associated with dysregulation of insulin receptor substrates. *American Journal of Physiology-Cell Physiology, 300*(6). doi:10.1152/ajpcell.00670.2008

Zhao, Y., Wang, Y., Gong, J., Yang, L., Niu, C., Ni, X., . . . Yang, Y. (2017). *Chitosan degradation products facilitate peripheral nerve regeneration by improving macrophage-constructed microenvironments* doi://doi.org/10.1016/j.biomaterials.2017.02.026

Appendices

Appendix A: Acronym Glossary

The following consists of a list of all acronyms used throughout the paper.

- American Society for Testing and Materials (ASTM)
- Encapsulation Efficiency (EE)
- Endothelial Cells (EC)
- Fetal Bovine Serum (FBS)
- International Standards Organization (ISO)
- Intimal Hyperplasia (IH)
- Phosphate Buffered Saline (PBS)
- Platelet-Derived Growth Factor-BB (PDGF-BB)
- Polyglycolic Acid (PGA)
- Polylactic Acid (PLA)
- Poly(lactic co-glycolic) Acid (PLGA)
- Polypropylene (PPE)
- Polyvinyl alcohol (PVA)
- Scanning Electron Microscopy (SEM)
- Smooth Muscle Cell (SMC)
- Sodium Hydroxide (NaOH)
- Three dimensional (3D)
- Tissue Engineered Blood Vessels (TEBV)
- Transforming Growth Factor Beta (TGF-β)

Appendix B: Gelatin Microsphere Fabrication Protocol

The following consists of the materials, expected yield percentage, and the procedure used for gelatin microsphere fabrication.

Materials:

- 4 mL 11.1 wt% acidic gelatin (Sigma Aldrich)
- 100 mL olive oil
- 100 mL chilled acetone
- 1 wt% genipin - .05 mL
- diH_2O - 5 mL
- Lysozyme ~ 80 ng/uL
- PBS ~ 40uL
- Stir plate and bar
- Filter

Procedure:

Adapted from: Tabata, Y. et al., 1999

1. 4 mL of 11.1 wt% acidic gelatin was added dropwise to 100 mL of olive oil and stirred at 45C
2. After 10 minutes, the temperature was lowered to 20C for thirty more minutes
3. Following the 30 minutes, 50 mL of chilled acetone is added to the solution and constantly stirred for 1 hour
4. Another 50 mL of acetone is added and the mixture is transferred from the stirrer and homogenized at 14,000 rpm for an additional 10 minutes
5. Microsphere solution is centrifuged at 7,000 for five minutes or until the formation of a pellet. The oil is aspirated from the tube and the microspheres are washed with acetone. The process is repeated three times, or until the entirety of the oil has been removed from the solution
6. The microspheres are air dried overnight to evaporate any residual liquid from the surface
7. Dry microspheres are added to aqueous solution of 2 mL 1 wt% genipin in diH_2O at varying times for varying levels of cross linking
8. Microspheres collected, washed three times with diH_2O and freeze dried
9. Microspheres are UV sterilized for 10 minutes
10. Sterile microspheres are then soaked in a solution of 80 ng/uL lysozyme/PDGF and PBS at a pH 7.4 for 2 hours at 37C. - Another protocol calls for vortexing of the solution without changing the pH and incubating at 4 C for 15 hours

Appendix C: Chitosan Microsphere Fabrication Protocol

The following consists of the materials, expected yield, and the procedure used for chitosan microsphere fabrication.

Materials:

- Chitosan (40 mg)
- Acetic Acid, 2% v/v (8 mL)
- Genipin (2 mg)
- Lysozyme (10 mg)
- Olive Oil (150 mL)
- Magnetic stir plate/rod
- Homogenizer
- Buchner funnel

Procedure:

Adapted from: Karnchanajindanun, J. et al., 2011

1. Dissolve 40 mg of chitosan into 8 mL of 2% v/v acetic acid.
2. Add 2 mg of genipin to the chitosan solution.
3. Let sit for 6 hr while gently stirring.

4. Dissolve 10 mg of lysozyme into the solution and stir for 10 min.
5. Add the chitosan/lysozyme solution dropwise into 150 mL of olive oil.
6. Stir the emulsion with a homogenizer at 1100 rpm for 1 hr.
7. Transfer the emulsion to 50mL conical tubes and centrifuge at 200G for 5 minutes
8. Remove as much of the supernatant oil as possible without disrupting the pellet.
9. Transfer the remainder of the tube's oil and chitosan pellet to a filter paper.
10. Let the contents sit over a funnel and beaker overnight at 4C until almost all of the oil has passed through the filter paper.
11. Use forceps to transfer the filter paper to a clean funnel.
12. Wash the filter paper with 5 mL of 70% isopropyl alcohol.

Appendix D: Silk Microsphere Fabrication Protocol

The following consists of the materials, expected yield, and the procedure used for silk microsphere fabrication.

Materials:

- 1 mL ~ 5 wt% silk fibroin solution
- 4 mL ~ 5 wt% Polyvinyl alcohol (PVA)
- Centrifuge device
- Stirring plate
- Vortex device
- 32 mL ~ milli-Q water
- 50 mL centrifuge tube
- 50 mL glass beaker
- 100 mm petri dish
- PBS
- 5 mg lysozyme

Procedure:

Adapted from: Wang X. et al., 2010

1. 5 mg of lysozyme in 1 mL of PBS (pH 7.4) was added to the silk solution.
2. 1 mL of 5 wt% silk solution and 4 mL of 5 wt% PVA solution were mixed together in a glass beaker at a ratio of 1:4 to obtain a blend solution.
3. The solution was transferred to an open 100 mm petri dish and mixed on a stirring plate at 150 rpm for 2 hours at room temperature.
4. The dish was then dried for 3 hours in a fume hood. (Can leave overnight if necessary)
5. The dried silk/PVA blend film was dissolved in 10 mL of milli-Q water by shaking the tube gently at room temperature for 10 minutes and transferred to a 15 mL centrifuge tube..
6. The tube was centrifuged at 2,000 rpm for 20 minutes.

7. Supernatant was carefully removed and the pellet was resuspended in 10 mL of milli-Q water and centrifuged once more.
8. The supernatant was removed again and the pellet was resuspended in 2 mL of milli-Q.
9. A vortex device was used to disperse the clustered silk microspheres for 15 seconds.
10. The dispersed microspheres were stored at 4℃ (if necessary).

Appendix E: PLGA Microsphere Fabrication Protocol

The following consists of the materials, expected yield, and the procedure used for PLGA microsphere fabrication.

Materials:

- Resomer® RG 858 S, Poly (D,L-lactide-*co*-glycolide) (85:15)
- Polyvinyl Alcohol (PVA)
- Dichloromethane
- PBS
- Chicken lysozyme
- DI water

Procedure:
Adapted from:
He, Z. et al., 2011. Koda, S. et al., 2017. Nafissi, N. et al., 2011. Li, L. et al., 2014

1. Insert 1 mg of lysozyme into 250 µl of PBS.
2. Invert mixture for ~2 min, and then mix at 1000 rpm for 5 min with stir bar.
3. 250 mg PLGA powder is then added to 2.5 mL dichloromethane to make 10% oil
4. Primary water phase from steps 1 and 2 and the above PLGA mix are then combined with sonication (6W, speed knob set to 3) for 30 sec to form W/O emulsion.
5. This emulsion is then mixed with 300 mL of 1.0% (w/v) PVA (already at between 4-10°C) with homogenizer (setting at 2 speed) and then at 500 rpm for 3 hours in fume hood to make a W/O/W.
6. The dichloromethane should evaporate from the reaction mixture and microspheres should form
7. Microspheres are then collected by running PVA solution through 60 mm filter paper in Buchner funnel.
8. Wash and collect microspheres by rolling up filter paper into 50 mL conical tube and washing with 70 % isopropanol several times. Microspheres will collect at the bottom of the tube.
9. Filter the microsphere-laden PVA solution through a filter and wash filter paper with isopropanol or water and collect runoff in a tube.
10. Repeat step 9 three times, with runoff from the previous iteration used being filtered with fresh filter paper.
11. Spin down microspheres at 5000 rpm for 30 minutes to collect a pellet.
12. Store at -20°C for short-term storage or freeze-dry for long-term storage.

Appendix F: MTT Assay Protocol

The following consists of the materials and procedure used for the MTT Assay for biocompatibility. The procedure was adapted from an excepted protocol from the *Cayman Chemical MTT Cell Proliferation Assay Kit Booklet.*

Materials:

- Cayman Chemicals MTT Cell Proliferation Assay Kit
    - MTT Reagent (25 mg)
    - Assay Buffer
    - Crystal Dissolving SDS (5 vials/1 g)
    - Crystal Dissolving (hydrochloride) (5 vials/10 mL)
- Adjustable pipette
- 96 well plate for cell culturing
- 96 well Colorimetric Microplate Reader
- DI water
- Shaker plate

Procedure:

1. Prepare the Assay Buffer by dissolving the cell-based assay buffer tablet provided with the kit in 100 mL of DI water
2. Prepare the MTT Reagent
    a. Dissolve 5 mg of MTT reagent in 1 mL of assay buffer through vortexing (This amount is applicable for one 96 well plate. If more or less is being tested change values accordingly)
    b. Remove any undissolved material through filtration or centrifugation if applicable
3. Prepare the Crystal Dissolving Solution
    a. Dissolve one vial of crystal dissolving SDS with one vial of crystal dissolving (hydrochloride). Both reagents are provided with the kit
    b. Mix well through vortexing
    c. Each vial is good for one 96 well plate
4. Add 3 mg of respective microspheres into 1 mL of SMC culture media. Incubate the media at 37 C and 5% CO_2 for 1 hour.
5. Seed 50,000 cells/well in a 96 well plate
6. After the hour incubation time, various amounts of the microsphere containing culture media will be added to the respective microsphere testing wells. The control and blank wells will contain normal SMC culture media. In total there should be 100 uL of volume per well
7. Place cells in an incubator at 37 C for 24-48 hours
8. Add 10 uL MTT reagent to each well
9. Mix on shaker plate for 1 minute

10. Incubate the cells for 3-4 hours
11. Add 100 uL of crystal dissolving solution to each well and incubate for 4-18 hours until the solution turns purple
12. Measure the absorbance of each sample with the Microplate Reader at 570 nm

Appendix G: Miscellaneous SEM Images

Gelatin (2520x):

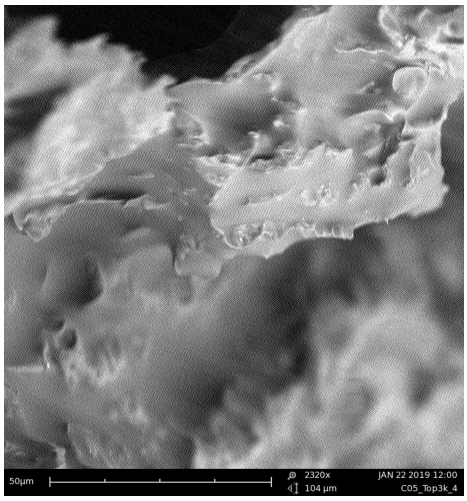

Silk microspheres (3150x):

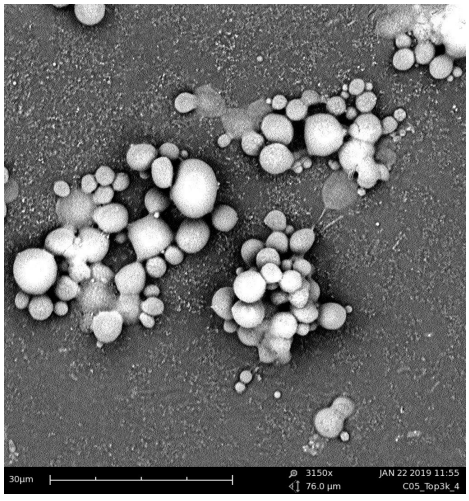

PLGA microsphere (2540x):

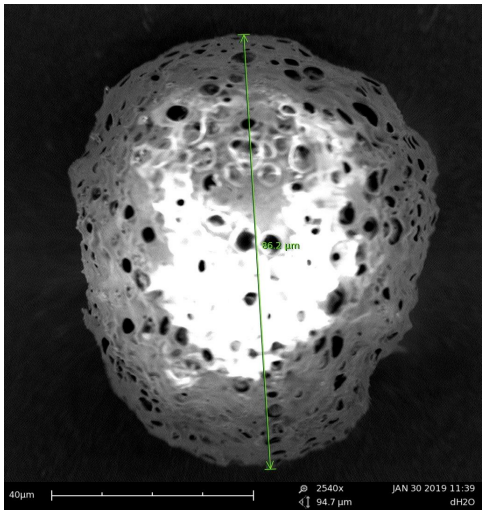

Chitosan microsphere (610x):

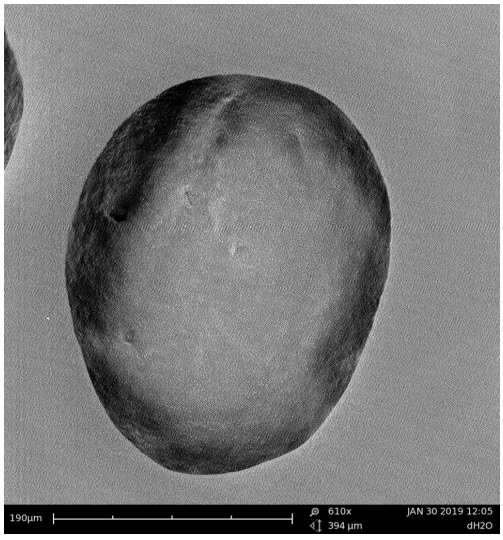

Chitosan fragment (7400x):

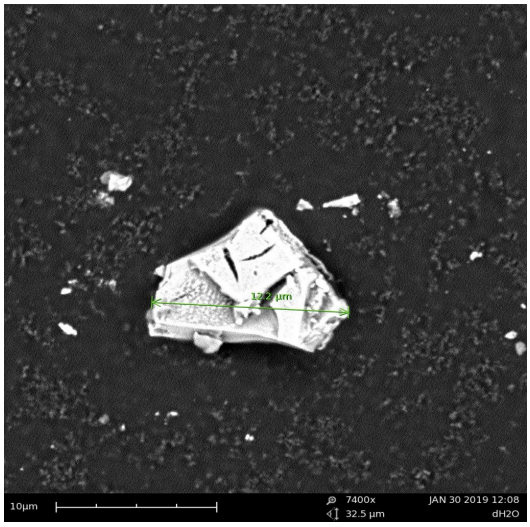

Gelatin with visible crosslinking (640x):

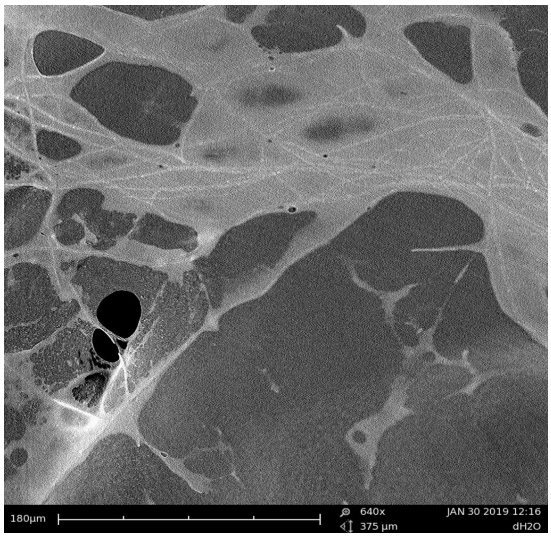

Two chitosan microspheres fused (620x):

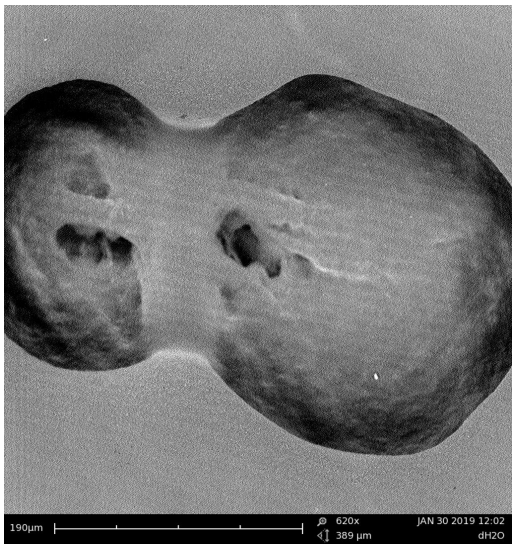

Chitosan surface (1100x):

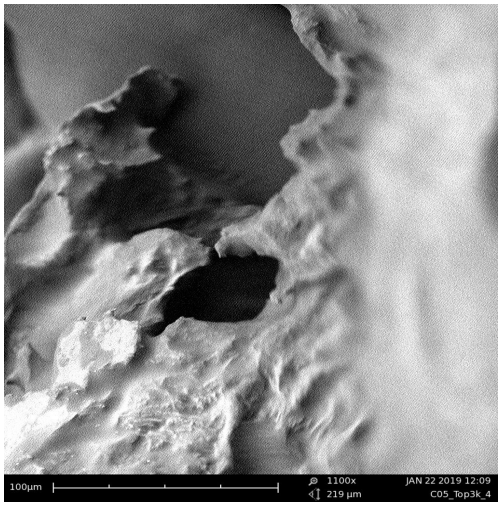

PLGA microsphere (635x):

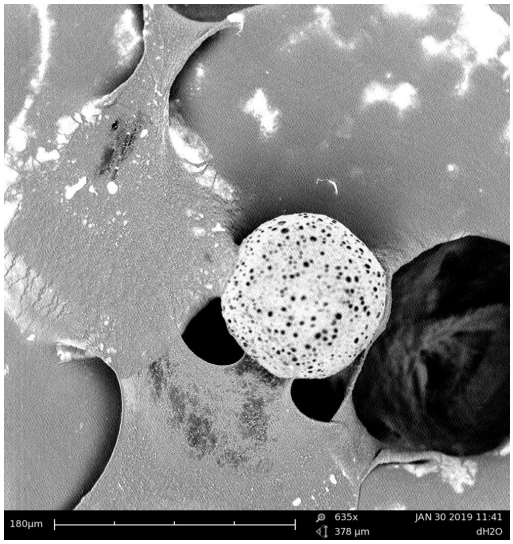

Appendix H: Encapsulation Efficiency Protocol

Gelatin Microsphere Encapsulation Efficiency

Materials:

- Distilled water (600 uL)
- Loaded gelatin microspheres (3 mg)

Procedure:

Adapted from: Cortesi, et al., 1999

1. Dissolve 3 mg of loaded gelatin microspheres in 600uL of distilled water and let sit for 72 hours.
2. Run a lysozyme activity assay to determine the quantity encapsulated.
3. Calculate encapsulation efficiency with the following equation:
   EE=[(quantified lysozyme)/(lysozyme initially loaded)]*100%

Chitosan Encapsulation Efficiency

Materials:

- 2% Acetic Acid (500 uL)
- Loaded chitosan microspheres (3 mg)

Procedure:

Adapted from: Zeng, et al., 2011

1. Dissolve 3 mg of dried, loaded microspheres in 500 uL of acetic acid.
2. Vortex the solution for 20 min at room temperature.
3. Centrifuge the solution at 1000 rpm for 10 min.
4. Add 60uL of 10x PBS to solution.
5. Add 80uL of 1M NaOH to solution.
6. Run a lysozyme activity assay to determine the quantity encapsulated.
7. Calculate encapsulation efficiency with the following equation:
   EE=[(quantified lysozyme)/(lysozyme initially loaded)]*100%

PLGA Encapsulation Efficiency

Materials:

- Dichloromethane (600 uL)
- Loaded PLGA microspheres (3 mg)

Procedure:

Adapted from: Yang, et al., 2000

1. Dissolve 3 mg of dried microspheres in 600uL dichloromethane into a glass container in the fume hood.
2. Vortex the solution for 2 min.
3. Run a lysozyme activity assay to determine the quantity encapsulated.
4. Calculate encapsulation efficiency with the following equation:
   EE=[(quantified lysozyme)/(lysozyme initially loaded)]*100%

Silk Encapsulation Efficiency

Materials:

- Deionized water (600 uL)
- Loaded silk microspheres (3 mg)

Procedure:

Adapted from: Wen et al., 2011

1. Dissolve 3 mg of loaded silk microspheres in 600 mL of deionized water.
2. Vortex the solution for 2 min.
3. Centrifuge at 4,000 rpm for 10 minutes.
4. Run a lysozyme activity assay to determine the quantity encapsulated.
5. Calculate encapsulation efficiency with the following equation:
   EE=[(quantified lysozyme)/(lysozyme initially loaded)]*100%

Appendix I: EnzChek Lysozyme Assay Protocol

The following consists of the materials and protocol used for the EnzChek Lysozyme Assay. The procedure was adapted from the *EnzChek Lysozyme Assay Kit Manuals & Protocols* from Thermo Fisher Scientific.

Materials:

- EnzChek Lysozyme Activity Assay Kit (E-22013)
    - DQ Lysozyme Substrate (Component A) (1 mg *Micrococcus lysodeikticus*)
    - 1X Reaction Buffer (Component B) (50 mL buffer)
    - Chicken Egg White Lysozyme (Component C) (1000 U)
- DI water
- Microplate Reader
- 96 well plate
- Adjustable pipette
- Aluminum Foil

Procedure:

1. Prepare lysozyme substrate stock suspension
    a. Suspend the contents of the Component A vial in 1 mL DI water and mix
    b. This stock can be stored at 4 C for one month
    c. For six month storage add 2 mM sodium azide in single use aliquots of the solution and freeze in -20 C freezer
2. Prepare 1000 U/mL lysozyme stock solution
    a. Dissolve the contents of the Component C vial in 1 mL of DI water
    b. Lysozyme can be frozen in single use aliquots for six months to avoid freeze-thaw cycles
3. Calculate standard curve
    a. Fill 8 wells with 50 ul of 1X reaction buffer (Component B)
    b. Add 50 uL of 1000 U/mL lysozyme stock solution to the first well and mix through pipetting
    c. Transfer 50 uL solution from first well to the second well
    d. Repeat this process until you reach the seventh well. Remove 50 uL from the seventh well and discard, adding nothing to the eighth well creating a range from 500 U/mL to 0 U/mL
4. Dilute lysozyme samples in 1X reaction buffer and add 50 uL sample into each well. Dilution will only be necessary if the activity is greater than the microplate readers ability and will therefore need to be optimized based on tests
5. Dilute 1 mg/mL lysozyme substrate stock suspension 20-fold in 1X reaction buffer to prepare a 50 ug/mL suspension. The amount of substrate stock suspension and reaction buffer used will vary based off of number of assays being run
6. Add 50 uL of the 50 ug/mL lysozyme substrate solution to each well containing a sample for a total well volume of 100 uL

7. Incubate the plate for at least thirty minutes. Cover the plate in aluminum foil to eliminate exposure to light
8. Measure fluorescence using the microplate reader
    a. Lysozyme substrate has an absorption maxima of 494 nm and a fluorescence emission maxima of 518 nm

Appendix J: Lysozyme Release Assay Protocol

A Lysozyme assay was chosen as the method for quantifying lysozyme released into solution over time for similar reasons as with encapsulation efficiency.

Materials:

- EnzChek Lysozyme Activity Assay Kit (E-22013)
    - DQ Lysozyme Substrate (Component A)
    - 1X Reaction Buffer (Component B)
    - Chicken Egg White Lysozyme (Component C)
- DI water
- Rat smooth muscle cell complete media
- 96 well plate
- Adjustable pipette
- Vortex
- Colorimetric Microplate Reader

Procedure:
Adapted from:
Zeng et al., 2011

1. Dissolve 3 mg of dried, loaded microspheres into 6 mL of culture media (pH 7.4).
2. Collect a 300 µl sample of the media and freeze at -20°C for later use in quantification. This will act as the sample from the 0 day time point.
3. Place samples in an incubator at 37°C.
4. 24 hours later, centrifuge the sample at 1,500 rpm.
5. Withdraw 300 µL from this supernatant and similarly freeze in -20°C. This will act as the sample from the 1 day time point.
6. Replace the removed media by adding 100 µl of fresh media.
7. Redisperse the microspheres in the media solution and return to the incubator.
8. Repeat the centrifuging, extracting, freezing, replacing process on predetermined collection days.
9. Thaw the frozen samples.
10. Perform a lysozyme activity assay exactly.

Appendix K: Encapsulation Assay Raw Data

Test 1:

- Using loaded batches fabricated at different time points
- Most concentrated wells for standards (top row of plate map) contained 12.5% sample (either lysozyme stock), 37.5% reaction buffer, 50% substrate
- Most concentrated wells for microspheres (first row) contained 12.5% sample, 37.5% reaction buffer, 50% substrate
- Decreased concentrations were included by performing a 1:2 serial dilution from first row
- Negative controls contain 25% solvent, 25% reaction buffer, and 50% substrate (should have no lysozyme)
- Last row of standards acted as negative control blanks which lacked lysozyme, containing 50% reaction buffer, and 50% substrate
- Plate map:

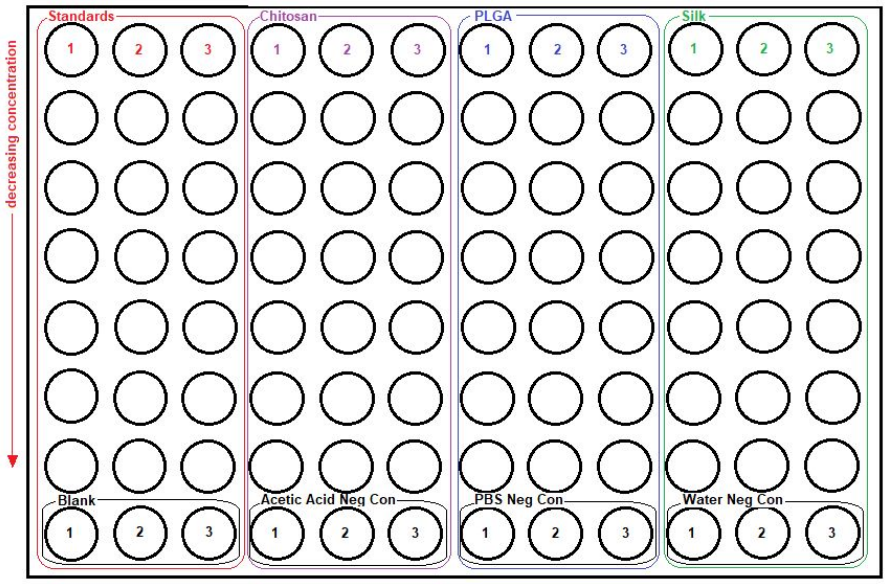

- Raw absorbance data (yellow=high concentration, green=low concentration):

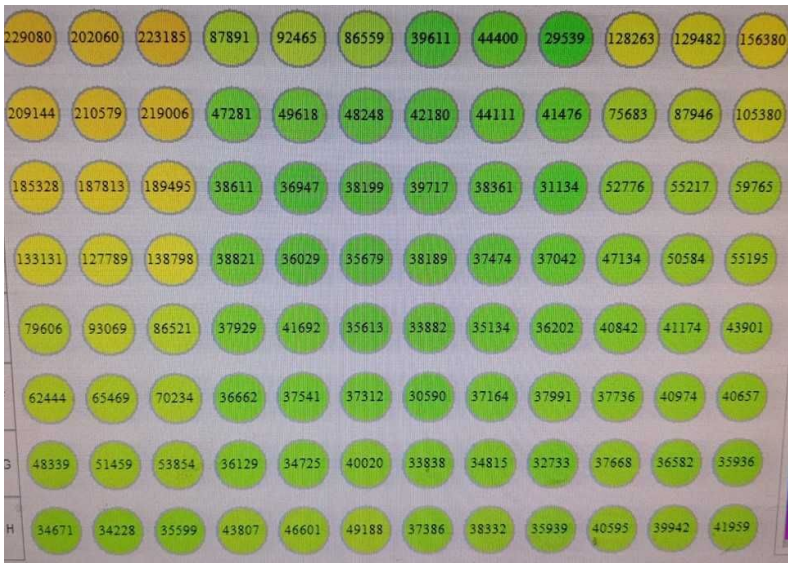

Test 2:

- Using new dissolved samples from same batches assayed in Test 1
- Most concentrated wells for microspheres (first row for PLGA and silk and fifth row for chitosan) contained 25% sample, 25% reaction buffer, 50% substrate
- Chitosan dilutions begin on columns 4-6 of row 5, continue to row 6, then continue to columns 7-9 of row 5, then culminate at row 6
- Positive controls contain 12.5% lysozyme stock, 25% solvent, 12.5% reaction buffer, and 50% substrate
- Otherwise same conditions as specified in Test 1
- Plate map:

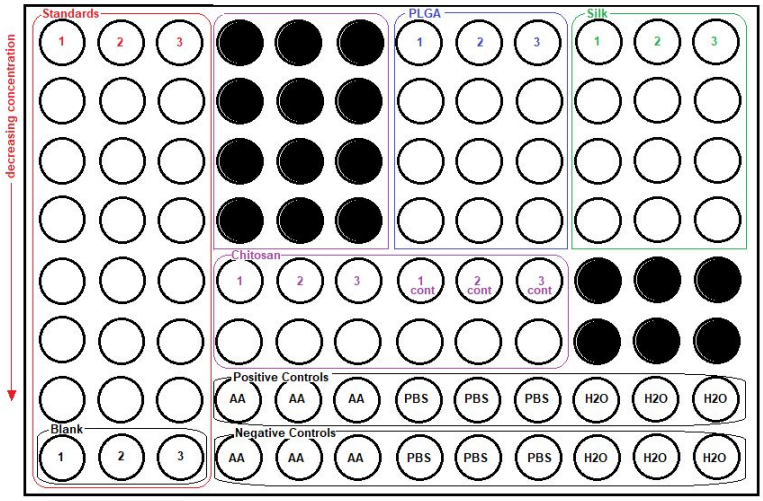

- Raw absorbance data (yellow=high concentration, green=low concentration):

309965	300095	283216				46126	45661	46311	187416	168416	170202
294057	271471	291757				46498	51239	39448	121002	119853	123541
266065	244653	257453				46249	57070	49390	90133	88955	100825
167527	186200	197733				38450	43385	46376	68653	66863	68665
100289	115078	122239	36948	40680	38999	49824	49916	48770			
67676	86017	92462	50119	45383	44339	46817	53987	48074			
51259	63813	68673	54544	54930	52307	289838	292197	291193	283050	301056	311445
41787	46381	45854	38561	39995	40916	35621	36425	39127	43731	37306	39991

Test 3:

- Using newly fabricated batches of loaded microspheres that were made just before the assay
- Most concentrated wells for microspheres (first row for PLGA and silk and fifth row for chitosan) contained 25% sample, 25% reaction buffer, 50% substrate
- 10x PBS and NaOH were added to the chitosan sample including the solvents of the positive and negative controls for chitosan
- Otherwise same conditions as specified in Test 2
- Plate map:

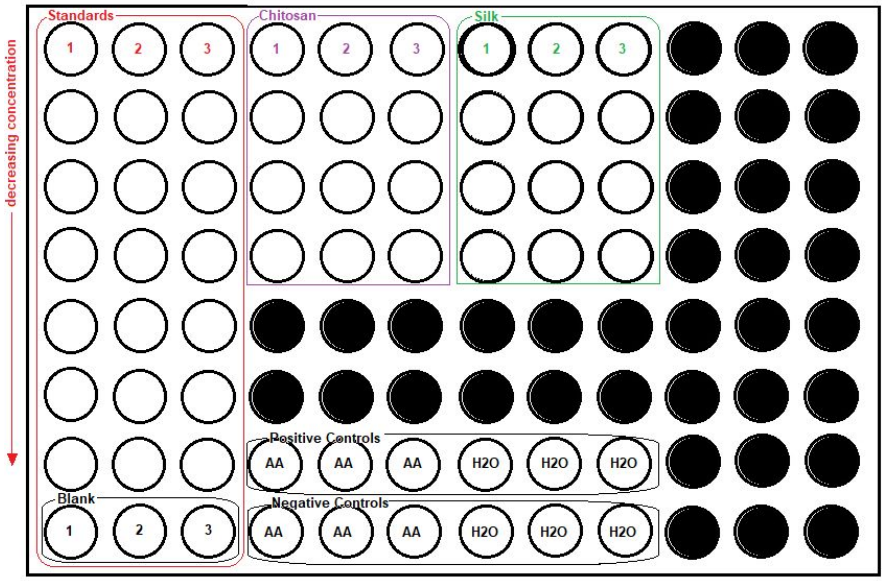

- Raw absorbance data (yellow=high concentration, green=low concentration):

375989	353231	371803	67662	66734	68793	48595	56702	50520			
398304	360105	351104	123632	138121	118528	45461	49901	46611			
322116	310195	293810	148175	132952	128348	42230	42557	43334			
239168	244455	224656	116553	109816	109442	41935	46288	46002			
181163	157708	185004									
131079	120553	134965									
117464	101953	105368	373538	317872	328485	433321	521925	550934			
41726	44254	44656	44733	45741	46507	52821	45481	49641			

Test 4:

- Using new dissolved samples from same batches assayed in Test 3
- Otherwise same conditions as specified in Test 3

- Plate map:

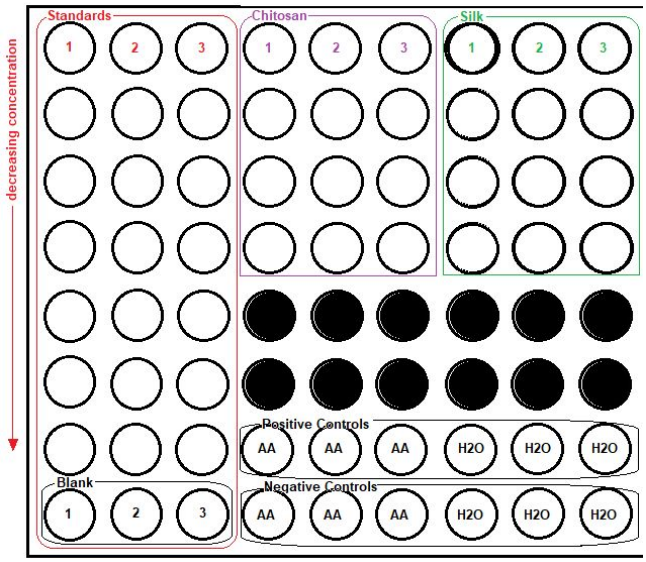

- Raw absorbance data (yellow=high concentration, green=low concentration):

476876	458163	486971	73117	73187	62388	70291	57578	78092
473695	484727	465824	132420	126957	134822	51347	51508	72567
415439	430489	388429	170203	183109	181106	56664	47512	58380
279368	305785	291220	202619	155266	176542	51131	52758	48730
232024	170091	141016						
93575	97179	93030						
75959	81413	69079	318101	333450	337602	525638	543370	533356
49867	46155	50685	53923	48387	76976	49857	67985	68131

Test 4:

- Using newly fabricated batches of loaded microspheres that were made just before the assay
- Otherwise same conditions as specified in Test 4
- Plate map:

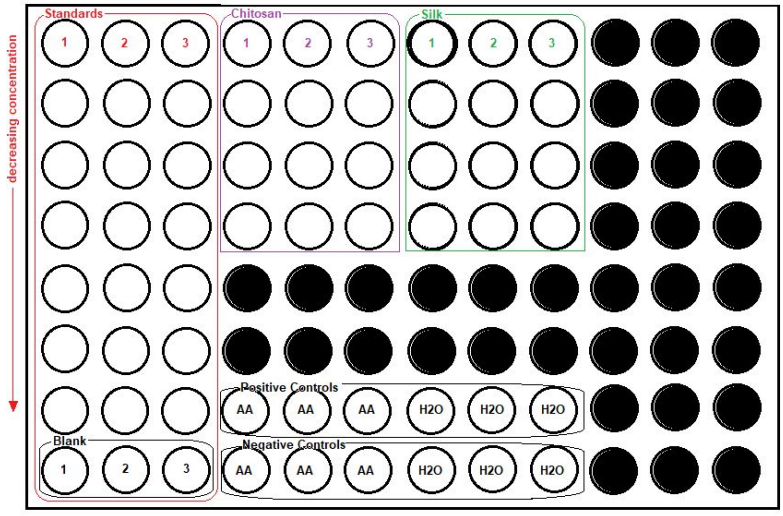

- Raw absorbance data (yellow=high concentration, green=low concentration):

764752	856093	944811	141404	138324	155213	349760	432179	837774			
807547	848623	852716	170948	172015	185995	168177	185967	371723			
713695	628987	676616	152276	152789	168424	229055	139337	205575			
547648	481722	468537	122685	132292	140744	211480	144553	283258			
356233	333201	235193									
218442	242076	152953									
153007	210567	115839	585696	528461	479589	844074	790482	1265588			
75783	81642	95673	77224	93366	93400	136217	140571	21129			

Test 5:

- Using samples from newly fabricated batches assayed
- Tested new solvents (5% acetic acid and NaOH) for the microspheres (chitosan and silk, respectively) alongside the previously used solvents (2% acetic acid and DI water)
- Increased dissolving time to 1 day
- Otherwise same conditions as specified in Test 4
- Plate map:

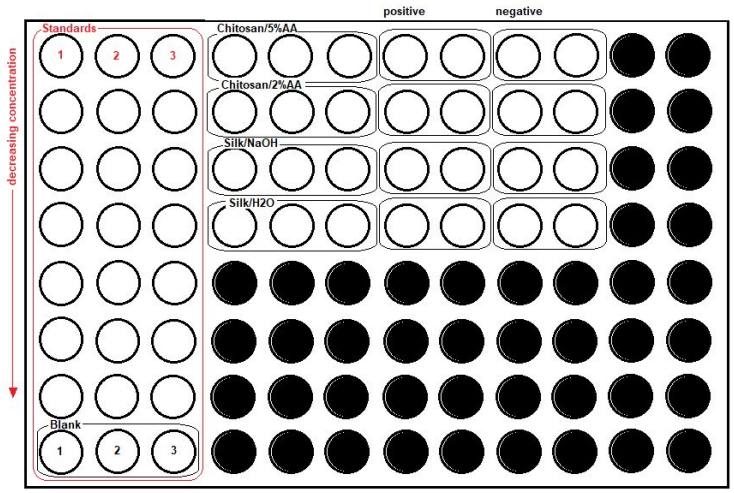

- Raw absorbance data (yellow=high concentration, green=low concentration):

578324	611263	610621	74036	76976	74057	98073	103039	70133	70536		
626767	604212	609318	104684	100909	109024	363471	345734	62661	61555		
500402	496386	479828	57951	59327	51969	467493	468622	49976	51618		
323848	341581	315060	569117	538843	559357	601478	606671	56461	59657		
168541	193784	172823									
104964	121574	109507									
80963	91987	82135									
51854	61125	51015									

Test 6:

- Using sample of silk microspheres from the same batch assayed in Test 5
- Using a sample from a newly fabricated batch of chitosan
- Reduced dissolving time back to that of the original protocol
- Otherwise same conditions as specified in Test 4
- Plate map:

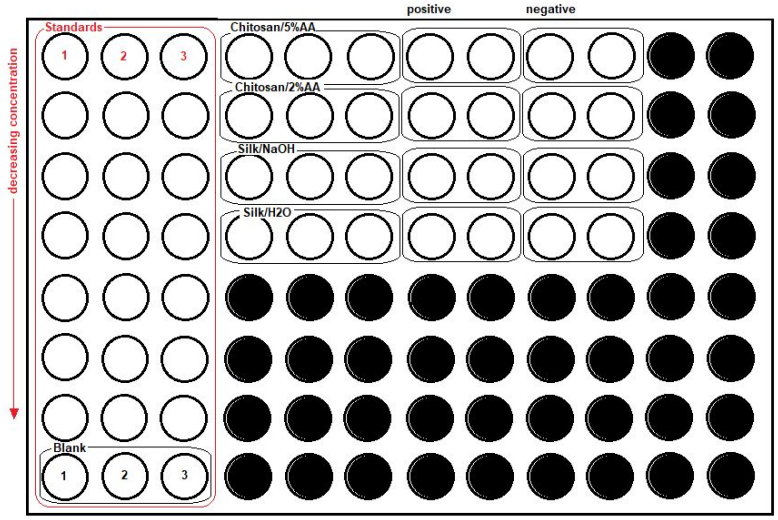

- Raw absorbance data (yellow=high concentration, green=low concentration):

1164428	972890	778656	86390	123256	93915	681790	632837	113733	103172		
833920	806256	735916	135523	161447	129554	729381	653842	132540	123747		
645564	670374	525544	154310	181894	168761	613997	631411	152423	140765		
369774	445384	359877	706141	736775	765132	707733	782939	147234	211099		
285960	266359	223229									
155426	162240	153350									
123593	160989	135041									
122070	152064	139814									

Appendix L: MTT Assay Raw Data

Standard Curve

Prior to experimentation with the unloaded microspheres, a standard curve was calculated with different cell densities to optimize the procedure based on the cell type. A 96 well plate was established with cellular conditions as follows:

- 0 cells/mL
- 2500 cells/mL
- 5000 cells/mL
- 10,000 cells/mL
- 25,000 cells/mL
- 50,000 cells/mL
- 100,000 cells/mL
- 150,000 cells/mL

This range was chosen based on recommended cell densities from the *Cayman Chemical* procedure. Three trials were set up for each condition and the MTT Assay Protocol was followed. The absorbance was measured through the use of a spectrophotometer plate reader at 570 nm. A standard curve was established given the average measurements at each of the conditions and error bars were created with standard deviation calculations.

- Standard curve graph given cell density conditions

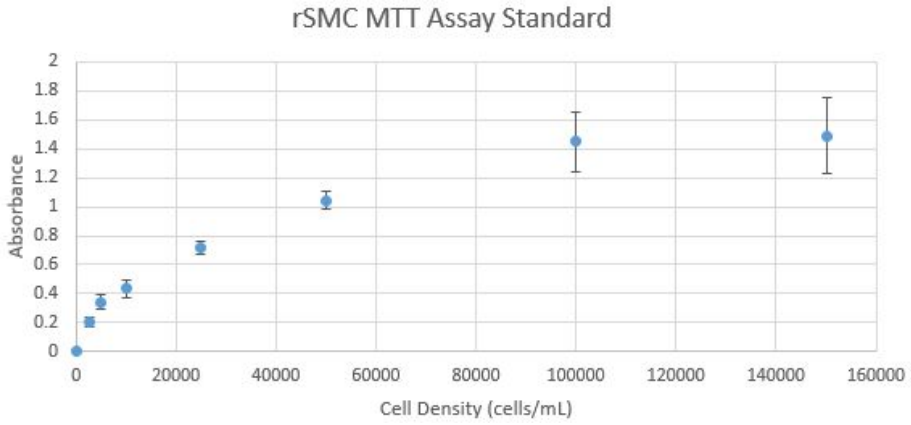

As seen in the figure above, the assay reached a saturation point beginning with the 100,000 cells/mL density. This was shown through the larger standard deviation values starting at this and increasing conditions. For that reason, a value prior to the saturation threshold was chosen. Therefore, 50,000 cells/mL was the cell density which was used for further experimentation.

Using the established cell density condition, an MTT assay with the unloaded microspheres was performed for each of the four different microspheres. The protocol used followed the one found in Appendix F. The results from the assay can be seen below.

- 96 well plate setup following incubation and prior to absorbance measurements. The conditions are blank, control, gelatin, chitosan, PLGA, and silk.

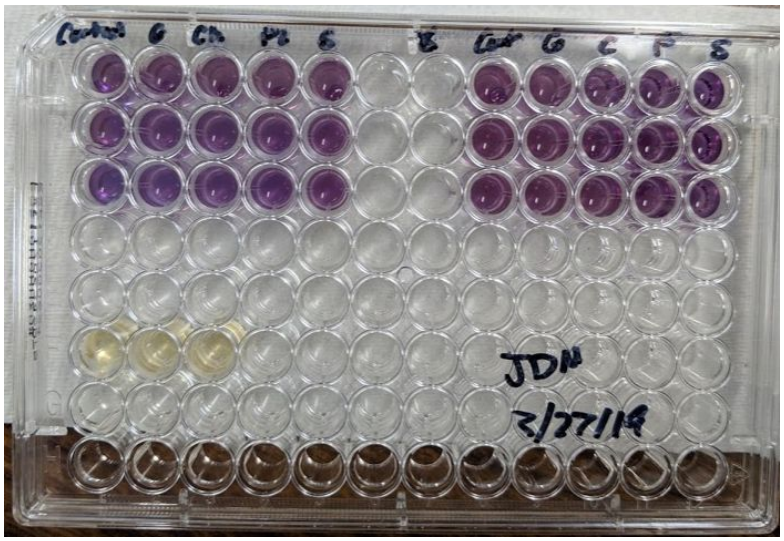

Qualitatively, the expected color change within the assay from yellow to purple was seen in each of the different conditions with cells present.

- Absorbance Measurements

Test 1:

Condition	570nm			Average (570nm)	Standard Deviation
Control	1.005	0.967	1.004	0.992	0.022
Gelatin	0.816	0.771	0.817	0.801	0.026
Chitosan	0.910	0.919	0.937	0.922	0.014
PLGA	0.848	0.851	0.896	0.865	0.027
Silk	0.824	0.807	0.855	0.829	0.024

Test 2:

Condition	570nm			Average (570nm)	Standard Deviation
Control	0.896	0.927	0.979	0.934	0.0419
Gelatin	0.884	0.908	0.861	0.884	0.0235
Chitosan	0.847	0.886	0.857	0.863	0.0203
PLGA	0.806	0.823	0.811	0.813	0.0087
Silk	0.805	0.819	0.827	0.817	0.0111

Test 3:

Condition	570nm			Average (570nm)	Standard Deviation
Control	0.948	0.976	0.968	0.964	0.0144
Gelatin	0.896	0.875	0.857	0.876	0.0195
Chitosan	0.887	0.871	0.838	0.865	0.0250
PLGA	0.818	0.837	0.859	0.838	0.0205
Silk	0.828	0.799	0.786	0.804	0.0215

Average Absorbance per Material:

Condtion	Average Absorbance (570nm)	Standard Deviation
Control	0.963	0.035
Gelatin	0.854	0.044
Chitosan	0.884	0.034
PLGA	0.839	0.028
Silk	0.817	0.020

Appendix M: Release Assay Raw Data

Test 1:

- Using samples from loaded batches of chitosan and silk (both properly loaded)
- 7-day duration of suspension
- Dilutions (1:5) of two latest time points also included for each material
- Positive controls contain media, lysozyme stock, and reaction buffer
- Negative controls contain media and reaction buffer
- Based on release profile analysis and review of the procedure, it was discovered that substrate was unintentionally forgotten
- Plate map:

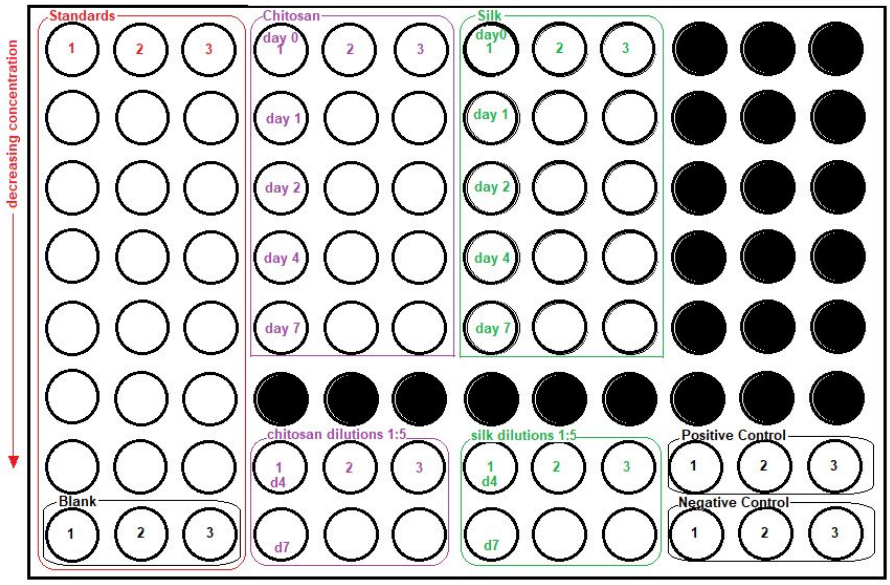

- Raw Data:

579949	569061	522060	74563	83844	72120	144066	147743	120823			
462516	514704	485014	134467	142301	123693	578677	591239	402181			
346819	381269	368112	169491	163050	129888	895782	686969	682755			
154051	222378	271963	168130	159133	144660	677517	446823	469805			
136592	146610	133493	159346	148508	162023	518444	498240	516879			
57399	88137	84620									
55713	71741	67027	87914	82805	90165	288540	350234	324667	842752	1201732	1679103
43179	49444	51693	73450	85513	87160	301138	282151	275123	81588	64722	86580

- Standard Curve:

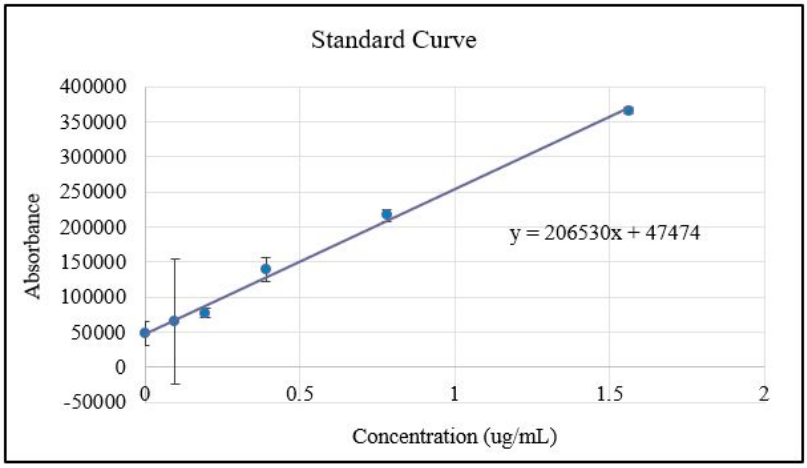

Test 2:

- 15-day assay and redo of 7-day assay where all samples are diluted 1:5.
- Fewer standard concentrations were used.

- Based on release profile analysis of the 15-day assay and review of the encapsulation assessment of microspheres from the same batches used, it was discovered that the silk microspheres tested were not loaded properly. This error did not apply to the 7-day batch which used different microsphere batches.
- Plate map:

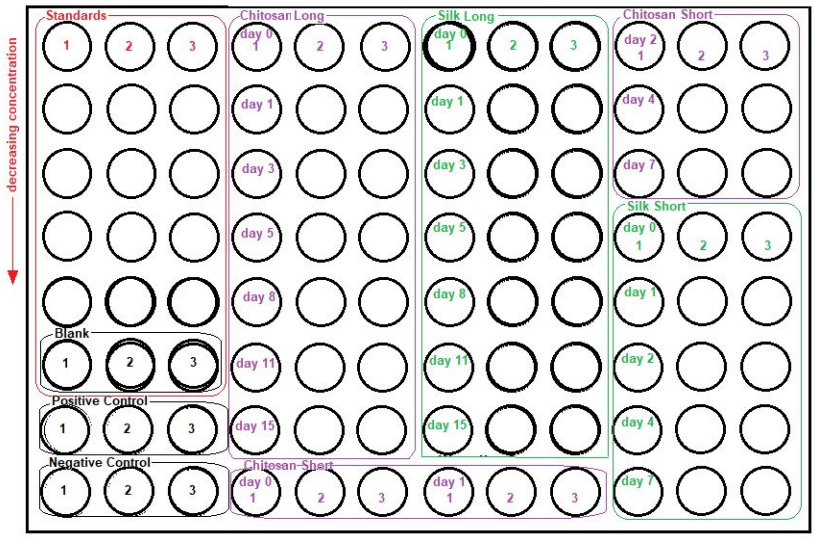

- Raw Data:

615049	661552	690506	57203	68556	61133	62562	69568	83352	95569	113111	122589
367613	287116	396544	103583	105039	197159	73446	79979	81607	115254	125018	145943
179909	118374	175584	123211	123825	82566	175335	92344	81175	131115	144797	129354
112717	93023	112806	157643	240643	167726	83223	88162	89452	120764	131681	103562
89644	91830	86725	132924	198261	182808	88575	79952	87004	424071	452890	456761
73297	72990	3793	183489	113526	145032	74569	103165	86687	430109	434229	459639
722678	706449	689989	120997	188011	144426	80957	80200	92770	432741	565464	461277
86633	79387	84377	80166	73840	79822	99053	125332	139668	462805	465815	513865

- Standard Curve:

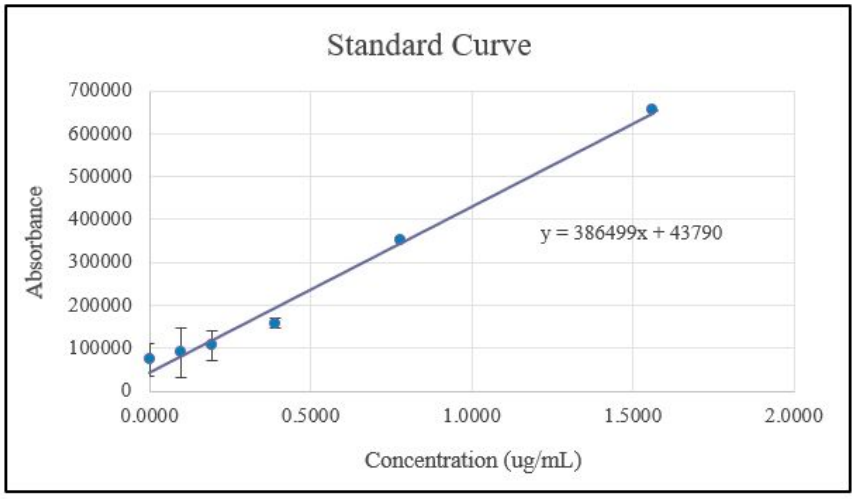

Test 3:

- Newly prepared batches of chitosan and silk microspheres used
- 11-day assay where all samples are diluted 1:5.
- Otherwise the same as Test 2.
- Plate map:

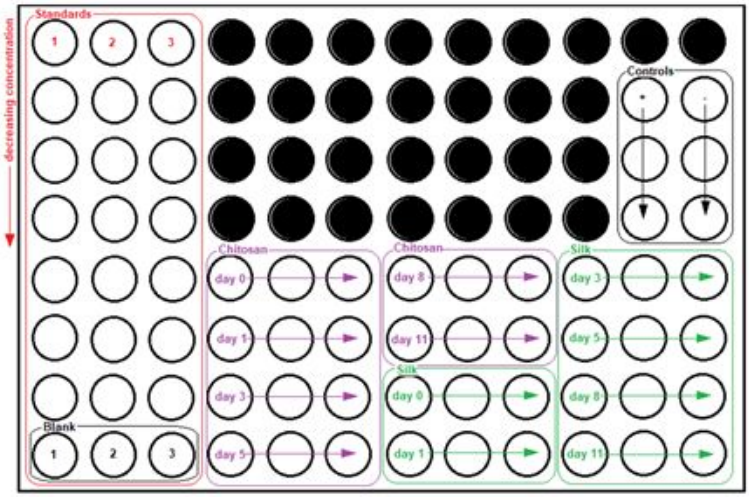

- Raw Data:

1164428	972890	778656									
833920	806256	735916								701690	89194
645564	670374	525544								692830	117277
369774	445384	359877								686931	188271
285960	266359	223229	112495	115812	112145	125690	134004	145266	867786	493810	447614
155426	162240	153350	182960	134093	146697	135301	127697	169035	450358	383236	417333
123593	160989	135041	169686	121832	237049	172126	181004	229987	463058	469494	349163
122070	152064	139814	147308	143474	131975	415506	470751	457255	411217	389481	302604

- Standard Curve:

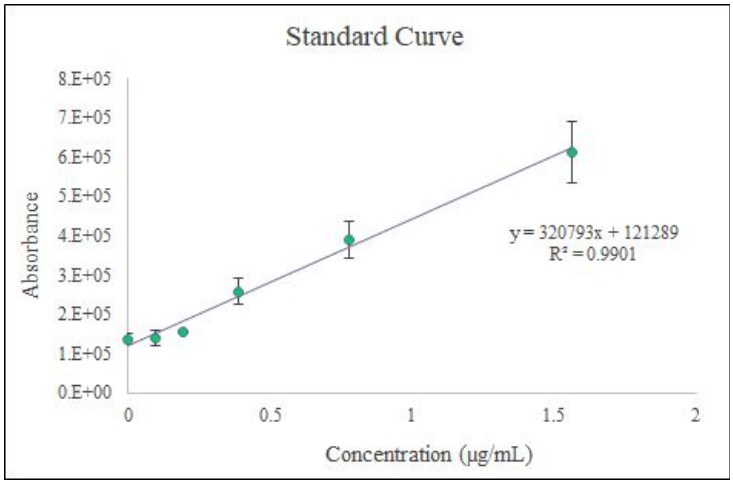

Test 4:

- Microsphere samples taken from the same batches used in Test 3
- 11-day assay where all samples are diluted 1:5.
- Repeat of Test 3, ran concurrently.
- Plate map:

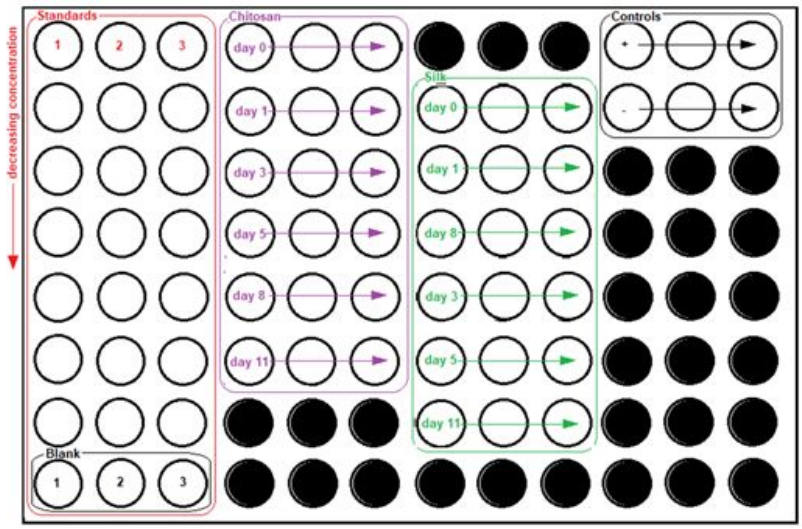

- Raw Data:

893588	875219	767310	123926	123748	110448				759612	898471	741059
845640	941125	820220	139361	141616	145140	211257	231067	249268	127803	188307	123672
679580	707322	660686	144485	156775	154480	490582	467832	454089			
484190	489400	442770	156940	160741	152369	505854	587804	485409			
294816	304743	272325	164458	145086	144272	566306	515220	643358			
271765	212623	194024	160523	154638	151396	492682	481574	473355			
143650	155351	198431				462662	553668	507659			
108441	116406	133150									

- Standard Curve: